MICROPROCESSOR BASED VOLTAGE CONTROL OF STAND-ALONE INDUCTION GENERATOR

A DISSERTATION

*Submitted in partial fulfillment of the requirements
for the award of the degree*

of

MASTER OF TECHNOLOGY

in

Alternate Hydro Energy Systems

By

RISHI RAJ MEENA

ALTERNATE HYDRO ENERGY CENTRE
INDIAN INSTITUTE OF TECHNOLOGY, ROORKEE
ROORKEE – 247 667 (INDIA)
May, 2007.

CANDIDATE'S DECLARATION

I hereby declare that the work which has been presented in the dissertation entitled "**MICROPROCESSOR BASED VOLTAGE CONTROL OF STAND-ALONE INDUCTION GENERATOR**" in partial fulfillment of the requirements for the award of the degree of **Master Of Technology In Alternate Hydro Energy Systems**, submitted in Alternate Hydro Energy Centre, Indian Institute of Technology, Roorkee, is an authentic record of my own work carried out during the period from July 2006 to May , 2007 under the supervision of **Shri S. N. Singh, Senior Scientific Officer, Alternate Hydro Energy Centre, Indian Institute of Technology, Roorkee.**

The matter embodied in the dissertation has/not been submitted by me for the award of any other degree or diploma.
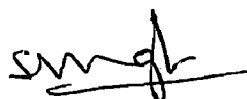
Place: Roorkee

Date: May 22, 2007   (RISHI RAJ MEENA)

CERTIFICATE

This is to certify that the above statement made by the candidate is correct to the best of my knowledge and belief.

(S. N. SINGH)
Senior scientific officer,
Alternate Hydro Energy Centre,
Indian Institute of Technology
Roorkee,
Roorkee-247 667, (India)

i

ACKNOWLEDGEMENT

ABSTRACT

This thesis covers the analysis, modelling and simulation of an isolated self excited induction generator (SEIG). A microprocessor-based closed-loop system has been developed for wind-driven stand-alone induction generators using a controlled rectifier to maintain a constant dc load voltage with varying rotor speeds. The configuration and implementation of the control scheme have been fully described. Results on a stand-alone induction generator demonstrate the satisfactory performance on software. A similar voltage build up is obtained when the isolated induction generator is excited using an inverter/rectifier system with a single DC capacitor on the DC link of the converter. In this type of excitation the voltage build up starts from a small DC voltage in the DC link and is implemented using vector control. The dynamic voltage, current, power and frequency developed by the induction generator have been analysed, simulated. To model the self excited induction generator accurate values of the parameters of the induction machine are required. The use of the variation in magnetizing inductance with voltage leads to an accurate prediction of whether or not self-excitation will occur in a SEIG for various capacitance values and speeds in both the loaded and unloaded cases.

The characteristics of magnetizing inductance, Lm, with respect to the rms induced stator voltage or magnetizing current determines the regions of stable operation as well as the minimum generated voltage without loss of self-excitation. In the SEIG, the frequency of the generated voltage depends on the speed of the prime mover as well as the condition of the load. With the speed of the prime mover of an isolated SEIG constant, an increased load causes the magnitude of the generated voltage and frequency to decrease. This is due to a drop in the speed of the rotating magnetic field. When the speed of the prime mover drops with load then the decrease in voltage and frequency will be greater than for the case where the speed is held constant. Dynamic simulation studies shows that increasing the capacitance value can compensate for the voltage drop due to loading, but the drop in frequency can be compensated only by increasing the speed of the rotor. In vector control of the SEIG, the reference flux linkage varies according to the variation in rotor speed. The problems associated with the estimation of stator flux

linkage using integration are investigated and an improved estimation of flux linkage is developed that compensates for the integration error

TABLE OF CONTENTS

LIST OF FIGURES

LIST OF SYMBOLS

Generally symbols are defined locally. The list of principal symbols is given below

v_a, v_b and v_c	phase voltages in three axes system (stationary reference frame), V
i_a, i_b and i_c	phase currents in three axes system (stationary reference frame), A
v_q^s and v_d^s	phase voltages in two axes system (stationary reference frame), V
i_q^s and i_q^s	phase currents in two axes system (stationary reference frame), A
i_q^s and i_q^s	phase currents in two axes system (excitation reference frame), A
d^s-q^s	stationary dq axes
d^e-q^e	dq axes in rotating reference frame (rotating at excitation frequency)
v_{ds}	d-axis stator voltage, V
v_{qs}	q-axis stator voltage, V
v_{dr}	d-axis rotor voltage, V
v_{qr}	q-axis rotor voltage, V
i_{ds}	d-axis stator current, A
i_{qs}	q-axis stator current, A
i_{dr}	d-axis rotor current, A
i_{qr}	q-axis rotor current, A
i_{md}	d-axis magnetising current, A
i_{mq}	q-axis magnetising current, A
Ψ_{ds}	d-axis stator flux linkage, Web-turn
Ψ_{qs}	q-axis stator flux linkage, Web-turn
Ψ_{dr}	d-axis rotor flux linkage, Web-turn
Ψ_{qr}	q-axis rotor flux linkage, Web-turn
Ψ_{dm}	d-axis air gap flux linkage, Web-turn

Ψ_{qm}	q-axis air gap flux linkage, Web-turn
V_m	peak phase voltage, V
I_m	Peak Phase Current, A
V_{rms}	Rms Phase Voltage, V
I_{rms}	Rms Phase Current, A
V_{dq}	Phase Voltage Space Vector, V
I_{dq}	Phase Current Space Vector, A
T_s	Sampling Time(Period), Seconds
θ	Angle Between The Two Axes And Three Axes, Rad
ω	Angular Speed Of The Space Vector, Speed Of The General Reference Frame, Rad/S
ω_e	Angular Speed Of The Excitation Reference Frame, Synchronous Speed, Rad/S
ω_r	Electrical Rotor Angular Speed, Rad/Sec
ω_m	Mechanical Rotor (Shaft) Angular Speed, Rad/Sec
s	The Slip Of The Rotor With Respect To The Stator Magnetic Field
P_p	Number Of Pole Pairs Of The Induction Machine
N_e	Synchronous Speed In Revolutions Per Minute (Rpm)
I_r	Rms Rotor Current, A
R_s	Stator Winding Resistance
R_r	Rotor Winding Resistance
R_m	Equivalent Resistance Representing Iron Loss Or Core Loss
L_{ls}	Stator Leakage Inductance, H
L_{lr}	Rotor Leakage Inductance, H
L_m	Magnetising Inductance, H
L_s	Stator Leakage Inductance (L_{ls}) + Magnetising Inductance (L_m) , H
L_r	Rotor Leakage Inductance (L_{lr}) + Magnetising Inductance (L_m), H
E_s	Rms Induced Emf In The Stator Winding Due To The Rotating Magnetic Field
E_r	Rms Induced Voltage In The Rotor When The Rotor Is Stationary, V
T_e	Electromagnetic Torque, Nm
T_m	Mechanical Torque
V_d	DC voltage
V_p	Generator terminal voltage
β	Extinction angle
Φ	Phase angle of the fundamental component of current

Superscript

* Commanded variables

ABBREVIATIONS

ADC   Analog to digital converter

DSP   Digital Signal Processor (Processing)

DVC   Direct vector control

emf   Electromotive force

IGBT   Insulated Gate Bipolar Transistor

IVC   Indirect vector control

PI   Proportional and integral (PI controller)

PWM   Pulse Width Modulation

RMS   Root mean square

SEIG   Stand-alone Induction Generator

VAR   Volt ampere reactive

VSI   Voltage source inverter

INTRODUCTION

1.1 GENERAL

Today, most of the electricity generated comes from fossil fuels (coal, oil, and natural gas). These fossil fuels have finite reserves and will run out in the future. The negative effect of these fossil fuels is that they produce pollutant gases when they are burned in the process to generate electricity. Fossil fuels are a non-renewable energy source. However, renewable energy resources (solar, wind, hydro, biomass, geothermal and ocean) are constantly replaced, hence will not run out, and are usually less polluting. Due to an increase in greenhouse gas emissions more attention is being given to renewable energy. As wind is a renewable energy it is a clean and abundant resource that can produce electricity with virtually no pollutant gas emission. Induction generators are widely used for wind and hydro powered as shown in Fig 1.1 electric generation, especially in remote and isolated areas, because they do not need an external power supply to produce the excitation magnetic field. Furthermore, induction generators have more advantages such as cost, reduced maintenance, rugged and simple construction, brushless rotor (squirrel cage) and so on.

Electronic equipment has become an indispensable part of everyday life. An important feature of the equipment used is the low power consumption, in a range of a few watts to a few hundreds of watts. Far less familiar is the electronic equipment, which operates at power levels of interest to the industry. Such equipment, its study, design, manufactures, and utilization is known under the general heading of power electronics. There are numerous reasons for the importance of power electronics, of which the most important is controllability. Power electronic equipment is highly controllable. The speed of operation of these devices and the comparatively low losses are the main reason for the large range of applications of power electronics. From the history of development of power electronics, it is evident that there are a large number of switching converter topologies and composite switching converters are possible. These possibilities are expanded in terms of the realization of all the switching functions possible with the

semiconductor switching devices available at present. This adds up to a very vast array of possible solutions in applying switching power converters to AC drive problems.

Induction generators are used extensively in the industry due to the low cost, and brushless commutator. However, the application of induction generators used to be minimal due to the lack of voltage control and stability of the generator. Therefore, the synchronous generator had taken precedence for a large period of time. With the advent of nonconventional sources of energy, such as wind, hydro etc. the applications of induction generators has greatly increased. Apart from the low cost and advantageous structure, the main feature of an induction generator that has led to the increase in its application in these areas is the ability for the generator to self-excite. With the connection of capacitors across the stator terminals of the machine, the build up of the air-gap flux takes place which in turn causes the voltage buildup. Other machines such as the synchronous generator require an independent source to enable excitation. The process of self-excitation can be achieved in numerous ways, one of which is primarily used in this thesis.
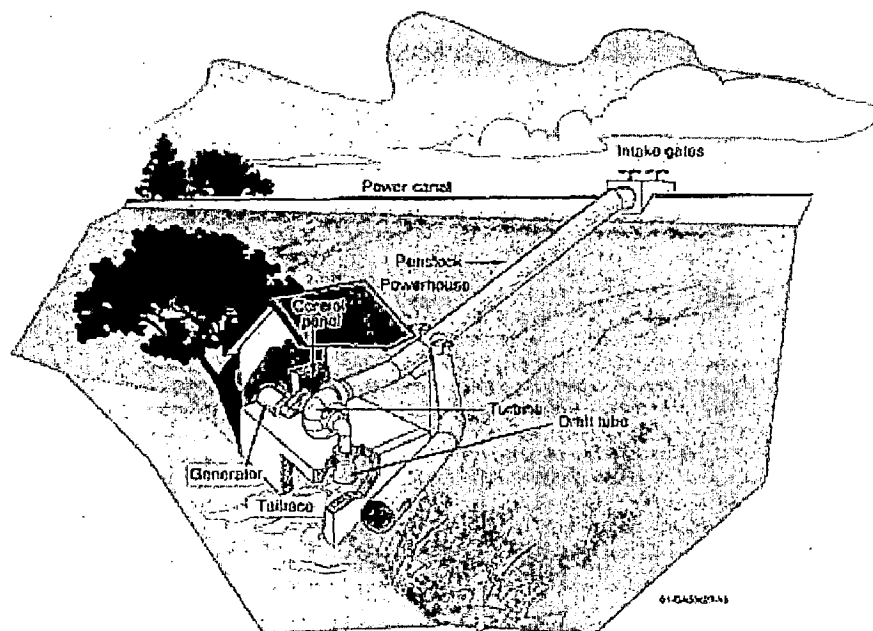

Fig 1.1: Hydro power plant [microhydro.com]

1.2 ORGANIZATION OF DISSERTATION

There are eight chapters in this Dissertation. The Dissertation presents the modelling of the dynamic characteristics of an isolated stand-alone induction generator. Analysis of an induction generator is discussed using modelling and the theory of induction machines.

The organization of the Dissertation is as follows.

(i.)   Chapter 2 conducts a detailed literature survey on the previous work done in induction generator systems; both dynamic and steady-state operation. The chapter also includes sections on the past work done in inverter.

(ii.)   Chapter 3 details the system model of the induction generator used in the system under consideration. Steady state analysis of VSI assisted induction generator and equivalent circuit is presented in this chapter.

(iii.)   Chapter 4 presented different control strategies of induction generator mainly scalar control and vector control. in vector control direct vector control and indirect vector control is described. Reference frames are also described in this chapter.

(iv.)   In Chapter 5 the modelling of an induction machine using the conventional or steady state model and the D-Q or dynamic model are explained. The voltage, current and flux linkage in the rotating reference frame and their phase relationships in the motoring region and generating region are presented. Chapter 5 gives the fundamentals of induction machine modelling and characteristics as a preparation of the modelling and analysis of an isolated induction generator. The induction machine model in D-Q axes has been improved to include the equivalent iron loss resistance, Rm. This improved model is presented in a simple and understandable way. Using this model the dynamic current, torque and power can be calculated more accurately.

(v.)   Chapter 6 proposes simulation of self excited induction generator model of a voltage source inverter assisted induction generator for the generation of AC voltages. The dynamic simulation has been carried out using the control scheme for the induction generator-inverter system using direct stator flux vector control.

(vi.)   The microprocessor application is presented in chapter 7. Program flowchart and control strategies proposed in this chapter.

(vii.)   In chapter 8 many important and interesting aspects of an isolated stand-alone induction generator have been discussed and presented. The study comprises theoretical analysis, simulation and experimental results related to induction generators. The result of simulation of induction machines in general has also been presented to provide an overall perspective of induction generators.

LITERATURE REVIEW

This chapter presents a review on the various works previously done on induction machines. The review includes the vast amount of work done in the area of inverter and the self-excitation methods of induction generators. It deals primarily with the self-excitation studies on induction generators. The vast amount of work done is discussed and the method of study of the process of self-excitation developed in this Dissertation is briefly put forth in contrast. Also, the different methods of control used in the dc voltage regulation of induction generators are discussed. Implementation of loss minimization in induction machines as well as application of induction generators in wind and hydro power generation is studied. The stability of an induction machine under different operating slips is also presented.

The study of the operation of induction machines as generators is well known. There has been an exhaustive amount of work done with regard to the steady-state and dynamic response of an induction generator. The details of the use of an induction machine operating as a stand-alone generator, both analytically and experimentally determined are illustrated in [1]. The operation of the generator with resistive and reactive loads is studied at steady state, operating at a constant terminal voltage. A given range of power ratings quantifies the amount of power that can be extracted from low-power motors for different operating loads. It is well known that a three-phase induction machine can be made to work as a stand-alone induction generator. There are different modes of operation. Each mode is discussed in [2]. The possible modes are listed below

(i) Polyphase AC Supply

(ii) Voltage Source Inverter with DC Supply

(iii) Current Source Inverter with DC Supply

(iv) Capacitive Self-Excitation

(v) Voltage Source Inverter Self-Excitation

(vi) Current Source Inverter Self-Excitation.

The study of the different modes as carried out in [3] is by the representation of each mode of excitation using an equivalent circuit. To study the systems, per-unit representation is used. The effect of the change in the magnetizing flux is considered. It is shown that the effect of saturation in the system is of secondary importance in the case of the regenerative modes of operation; however for the self-excitation modes of operation, saturation plays a significant role in the nature of response. The nature of response of the system to varying operating slips and stator voltage frequency is studied. In the case of capacitive self-excitation, for a fixed load and capacitance, the self excitation at a specific flux level can occur either at two frequencies, one frequency, or not at all depending on the load parameters and the operating speed. The different possible regions of operation are illustrated for varying operating conditions. For all three cases of self excitation, constraining equations are derived to determine the possible operating conditions and self-excitation regions. Similarly, a large amount of work has been done on the capacitance requirements as well as the air gap flux linkage requirements for self-excitation [4, 5, 6, and 7]. In the case of [5] detailed analysis has been carried out with regard to two different operating conditions, loaded and no-load. Predominantly, most of the work previously done on the steady-state analysis of induction generators involves study using the conventional equivalent circuit. The effect of changing load, slip, and magnetizing flux on the system performance in terms of the possible regions of operation as well as the effect of the rotor speed on the operation of the generator is discussed. In [5], expressions for the possible regions of operating slip that the system can self-excite are obtained.

The minimum and maximum values of the operating slip are determined. Using these expressions, the actual region of self-excitation can be determined. In all the abovementioned references, an equivalent resistance has represented the model of the inverter. In [8] and [3] the effect of the operating conditions of the induction generator on the air-gap flux requirements is studied for single as well as three-phase induction generators. The variation of the air-gap flux with the load resistance is studied for fixed capacitance values. Also the variation of the capacitance requirements of the generator with the load resistance for the minimum air-gap flux required is illustrated. Another approach to the steady-state analysis of a stand-alone induction generator involves the

study of the effect of the parameters of the machine on the terminal voltage of the generator [9]. In this case, the effect of the core-loss is neglected. The influence of the stator resistance, rotor resistance, leakage reactance, and magnetizing reactance on the terminal voltage of the generator is studied and illustrated. The method employed is a Newton-Raphson method as the solution is complicated due to the effect of magnetic saturation being considered. The nature of response of the system to changing rotor speed and capacitance is also studied. Similarly, the steady-state analysis of the stand-alone induction generator by a single capacitor is dealt with in [10]. The operation of the system with star and delta connected stator windings is studied, with a single capacitor connected between any two phases (in this case, phase b and c). The influence on the value of the capacitor used as well as the effect of the load on the machine currents and voltages are studied for both the star as well as delta connected stator windings The effect of the load on a stand-alone induction generator is of importance, as shown in [11]. The stand-alone induction generator is studied under free-running and loaded conditions. The effect of variable speed on the machine and the region of variable speed for which the induction generator can operate without loss in self-excitation are studied. The control of induction generators has also been studied.

The operation of induction generators driven by wind turbines is vastly important. Although the application of an induction generator in wind power is popular due to the ability of an induction generator to self-excite, the drawback of using an induction generator is the inability of the generator to maintain a controlled voltage. Therefore, a large number of control schemes have been proposed to overcome this drawback. The specific interest in induction generators for wind power applications is due to the fact that because the machine can self-excite, an independent source of power is not required for excitation. Also the relative cost of an induction machine is less. [8,21, 22,], deal with the operation of an induction generator driven by a wind turbine. This would therefore mean the system is studied under conditions of varying rotor speeds. Also effect of the operating slip on the generated voltage and frequency is studied. The importance of magnetic saturation in stand-alone induction generators, discussed earlier is also included in [12]. An important aspect of the self excitation process and voltage buildup with respect to the variation of the magnetizing inductance and phase voltage is detailed in

[13]. The stability of the system during this process is highlighted as in the initial buildup of flux in the generator; a small drop in the phase voltage would further decrease the phase voltage. This continual decrease in both could lead to no buildup of voltage in the system. In [14], the induction generator system driven by a wind turbine is controlled for constant voltage at the stator terminals of the machine. The system uses a PWM inverter for control of the excitation current to thereby enable control of the generated voltage. The control methodology is verified by simulation results for operation of the system under varying rotor speeds and loads. In [15], the system configuration used is similar; however, the analysis carried out shows the effect of the dc side capacitor value on the time of voltage buildup in the system.

Also the dc voltage ripple is determined by the capacitor value used. Another method of control proposed utilizes a current controlled voltage source converter [16]. The type of controller used is a hystersis current controller. Just like in the previous reference cited, the effectiveness of the control scheme is illustrated using varying operating conditions of load and rotor speed. A stator flux-oriented vector control of an induction generator system is proposed in [17]. In this case the control scheme proposed uses stator flux as a control variable to regulate the voltage. Similar operating conditions as [18] are applied. The system is specifically studied for varying rotor speeds as the proposed scheme is aimed at a wind turbine driven generator. Some other control schemes proposed are in [19, 20] where the control scheme is different from the ones described earlier; however, the operating conditions for which the system is studied under are similar. Finally some work has been done in the area of stability of an induction machine. The system transfer function is obtained and the poles and zeros of the system are studied under pole and zero migration, where the movement of the poles under varying current command is studied. The system is shown to be unstable for high values of rotor speed.

INDUCTION GENERATOR

3.1 Introduction

The induction machine offers advantages for hydro and wind power plants because of its easy operation as either motor or a generator, its robust construction, its natural protection against short circuits, and its low cost compared to other generators. Many commercial power plants in developed countries were designed to operate in parallel with large power systems, usually supplying the maximum amount of available primary energy for conversion in their surroundings (hydro, wind and solar). The induction generator accepts constants and variable loads, starts either loaded or without load, is capable of continuous or intermittent operation, its natural protection against short circuits. That is, when the load current goes above certain limits, the residual magnetism falls to zero and the machine is de-excited. When this happens, there are three methods available for it's re magnetization:

(i) Maintain a spare capacitor always charged and, when necessary, discharge it across one of the generator phases;

(ii) Use a charged battery; or

(iii) Use an inverter fed by the distribution network.

An induction generator with a squirrel cage rotor can be specifically designed to work with hydro and wind turbine, in other words, with a larger slip factor, with more convenient deformation in the torque curve, winding sized to support higher saturation current, increased number of poles, and so on. The SEIG can provide reliable and relatively cheaper means to generate electricity compared to synchronous generator for the application where small frequency variation are allowed.SEIG can be used to generate power from hydro turbine or wind turbine. Induction generator can be used as an isolated or stand alone power source driven by either constant speed prime movers such as diesel engines, hydro turbines or variable speed wind turbines. The variable speed

prime mover need not to be governed, although generator must be able to sustain over speed up to 2-3 p.u. A distinct advantage of such generators is much lower unit cost as compared to the conventional synchronous generator. Cross section shown in Fig. 3.1.
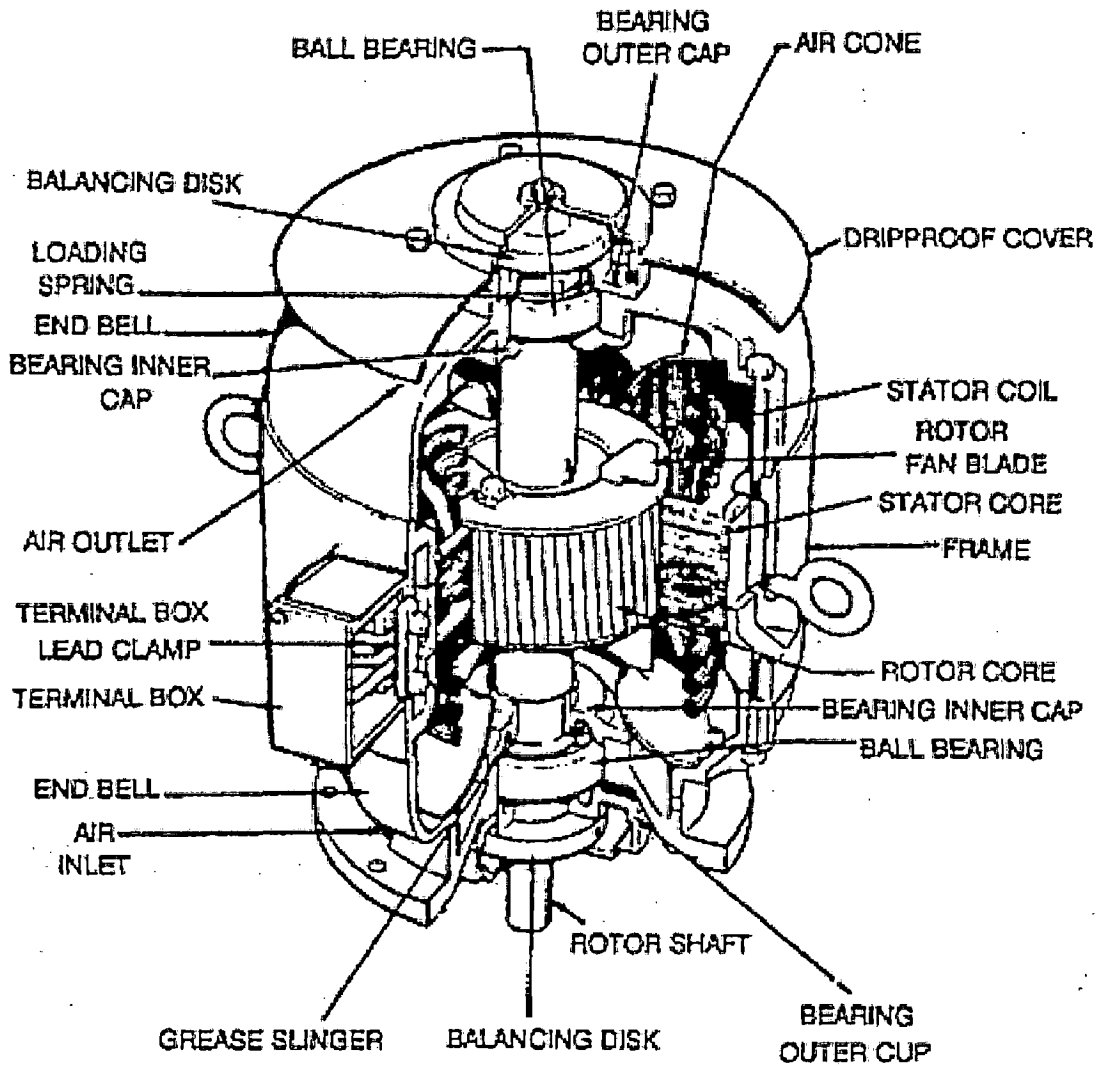

Fig. 3.1: Cross-sectional view of Induction Machine[30].

3.2 Characteristics of induction generator

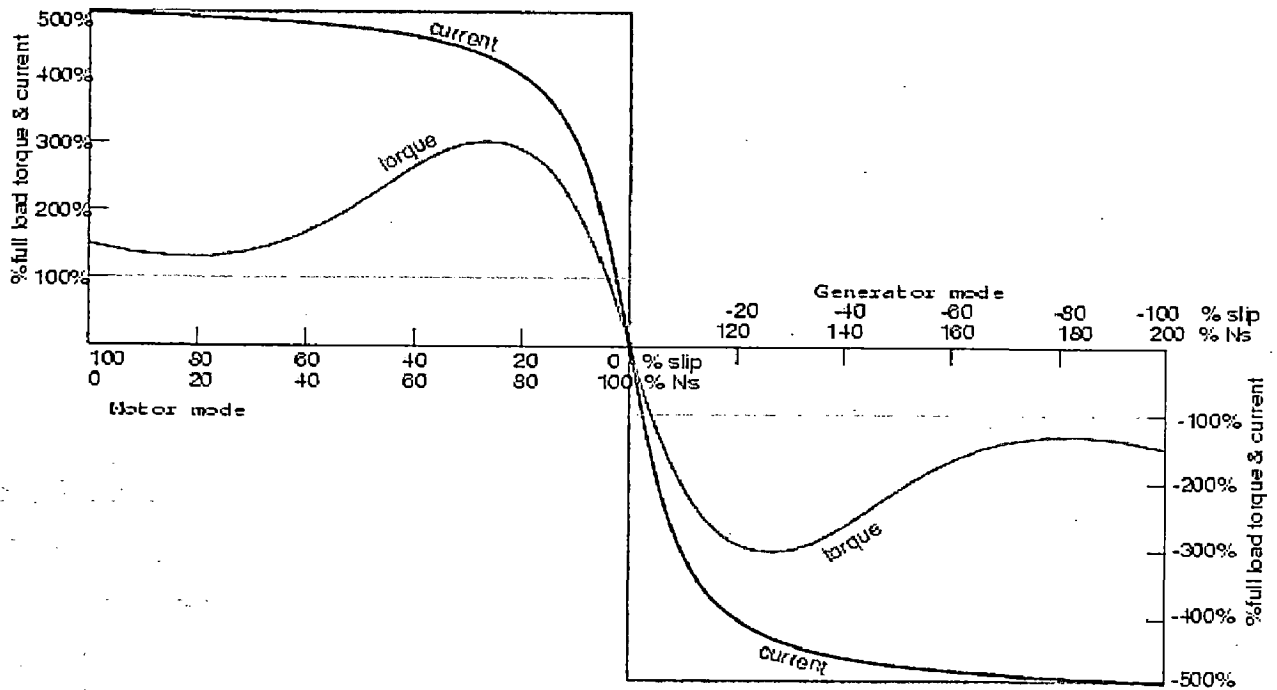Torque speed characteristics of induction machine

Fig. 3.2: Torque-speed characteristic of the induction machine [31].

Figure can be used to determine the torque-speed characteristic of the induction generator by neglecting the magnetizing loss resistance R_m.

3.3 STEADY-STATE ANALYSIS OF VSI-ASSISTED INDUCTION GENERATOR

The system proposed is an induction generator connected to a boost inverter, which uses the dc side capacitor of the boost inverter for self-excitation. Further analysis on the proposed model will be discussed in the later chapters. The scheme studied in this Chapter is a .voltage-source inverter assisted induction generator. The converter is connected to a battery to enable bi-directional flow of power. The direction of flow would be dependant on the load condition. The type of power generated in this scheme. This chapter proposes a model, which has three-phase capacitors, connected across the stator windings of the machine. The capacitors are used to maintain a consistent load voltage. Steady-state analysis of is studied for the different conditions of the system to illustrate the bi-directional flow of power.

3.4 System Model

The system model used in the analysis is as shown in Figure 3.4. The system includes a boost inverter. The main feature of the boost inverter in the operation of this model is the bi-directional power flow capability of the inverter. The operation of the system is such that the capacitors connected at the terminals of the generator are used for marinating a constant voltage across the load, and the generator is stand-alone by the voltage-source converter connected to the stator windings through a three-phase transformer. Depending on the load condition, the system can either absorb power or supply power for charging of the battery.
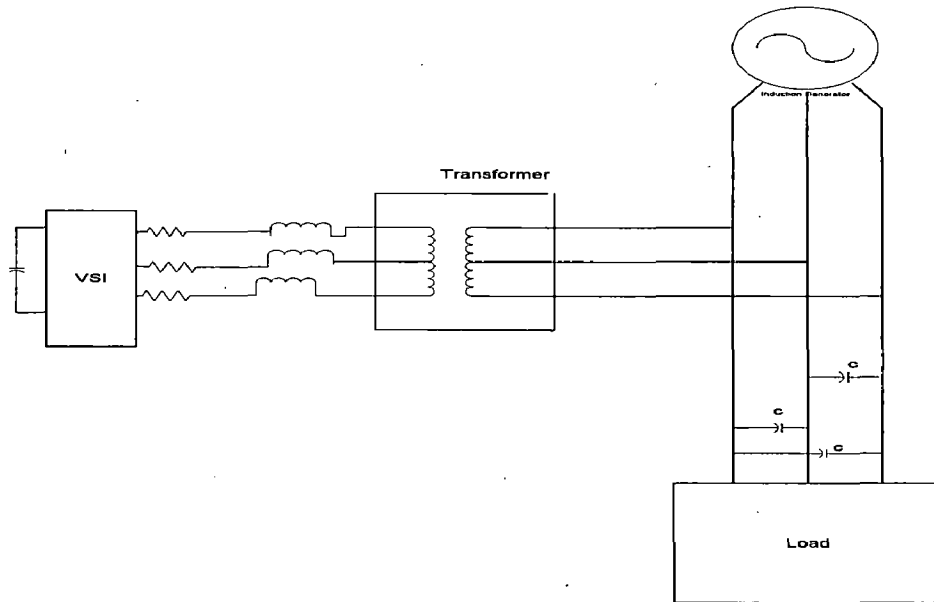
Figure 3.3: The system model [31].

During the process of self-excitation, the voltage-source inverter provides the required reactive power. This is provided by the capacitor on the dc-side of the converter. However, it has been shown that the voltage stability of the induction generator is poor when the rotor speed and load conditions vary. Therefore there have been some schemes proposed whereby the required active power by the load, if in excess of the input rotor mechanical power is supplied by a battery connected to the dc side of a three-phase inverter. One such scheme has been proposed for a dual-winding generator. When the generated power is in excess, the power flow is towards the capacitor, thereby the charging of the capacitor takes place.

12

CONTROL STRATEGIES OF INDUCTION GENERATOR

4.1 INTRODUCTION

Basically two types of controls are need in induction generator as listed below.

    (i) Scalar control

    (ii) Vector control

4.2 SCALAR CONTROL

Scalar control of Generators means control of the magnitude of voltage and frequency so as to achieve suitable torque and speed with an impressed slip. Scalar control can be easily understood based on the fundamental principles of induction machine steady state modeling. A power electronic system is used either for a series connection of inverters. When induction generator used in stand-alone operation, reactive power must be supplied for proper excitation, and the use of power electronics allows for variable impedances, series and shunt regulators. The overall scheme is based on fig 4.1. Capacitor bank is source of reactive current. The static VAR compensator is an inverter providing a controlled source of reactive current. The inverter uses a scalar control approach.

Machine torque and flux input would be used in this application to regulate both DC-link voltage at the capacitance Cp and generator voltage supplied for the ac load. These regulators have to reject the disturbances produced by load and speed variations. A dc-link voltage regulator has been implemented to achieve a high-enough DC-link voltage for proper current controlled inverter operation. The regulator input is the difference between the DC link voltage reference and the measured value.

At the generator side terminal current and voltages are measured to calculate the magnetizing current needed for the generator, and the instantaneous peak voltage is compared to a stator voltage reference, which generates a set point for flux through the feedback loops on the inverter side. This system requires a charged battery for startup. That can be recharged with an auxiliary circuit after the system is operational. Since stator voltage is kept constant, the frequency can be stabilized at about 50 Hz for ac load, but some slight frequency variation is still observed, and the range of turbine shaft

variation should be within the critical slip in order to avoid instability. Therefore, AC loads should not be too sensitive for frequency variation in this stand-alone operation. In order to optimize the efficiency of the generator, a look-up table reads the torque command and programs the optimum flux reference for the system. A start-up sequence initially boosts the DC-link voltage to a higher voltage than the peak value; in order for the PWM modulation to work properly, the overall system is very robust due to the current control in the inverters, the DC-Link capacitor, the online estimation of generator torque and flux. The system may be implemented with the last generation of microcontrollers since internal computations are not so mathematically intensive. All scalar based control schemes can also incorporate speed governor systems on the mechanical shaft in order to control the incoming power for small hydro and wind application.

The voltage will be set to control the flux and the frequency in order to control the torque. However, flux and torque are also functions of frequency and voltage, respectively. Scalar control is different from vector control in that both magnitude and phase alignment of the vector variables are controlled. Scalar control drives give somewhat inferior performance, but they are easy to implement and are very popular for pumping and industrial applications. The importance of scalar control has diminished recently because of the superior performance of the vector-controlled drives and the introduction of high performance inverters.

The main constraint on the use of a scalar control method for induction generators is related to the transient response. If shaft torque and speed are bandwidth-limited and torque varies slowly, tracking required speed variation, scalar control may work appropriately. Hydropower and wind power application have slower mechanical dynamics that. Therefore, it seems that scalar control is still good approach for renewable energy applications
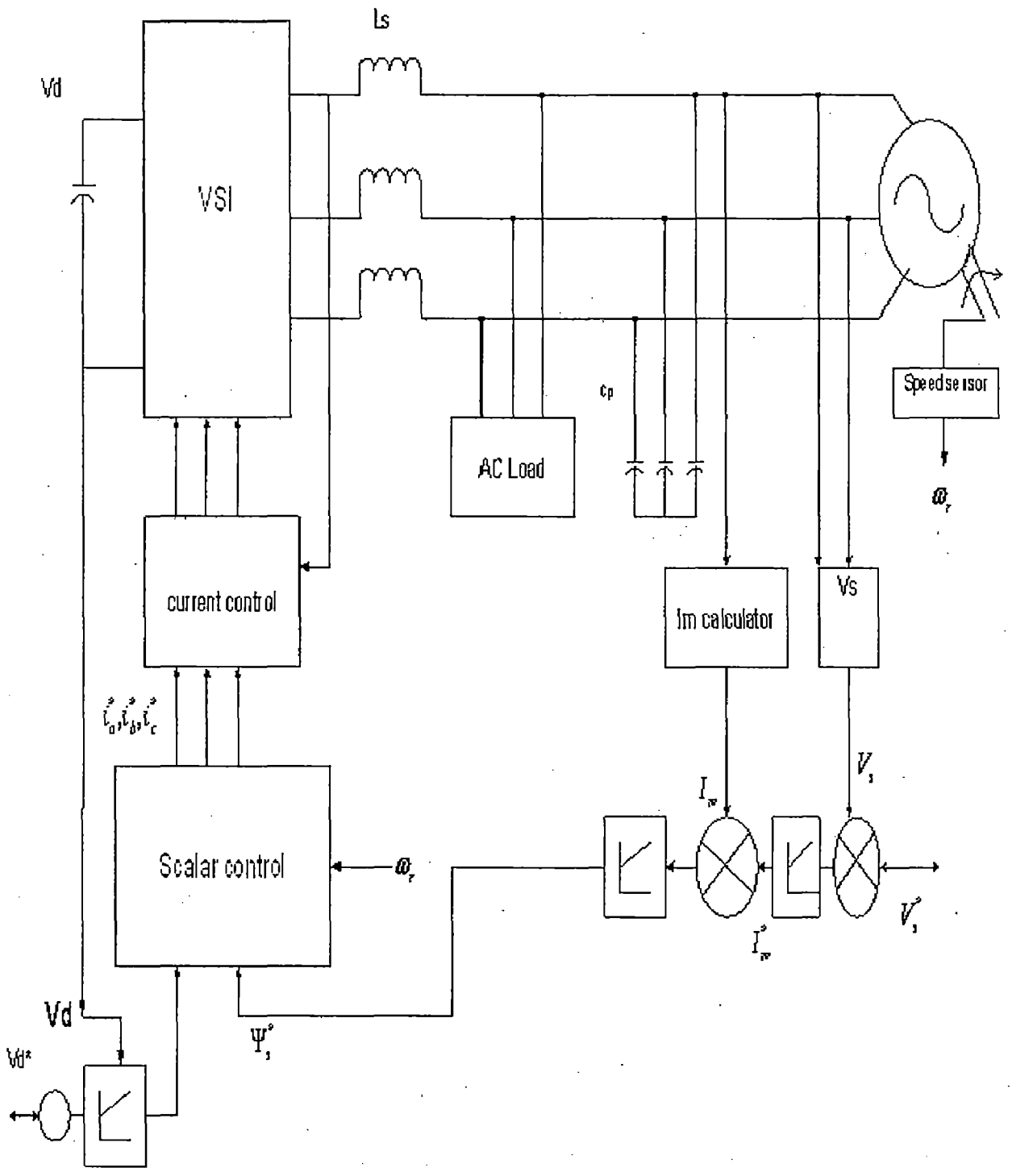
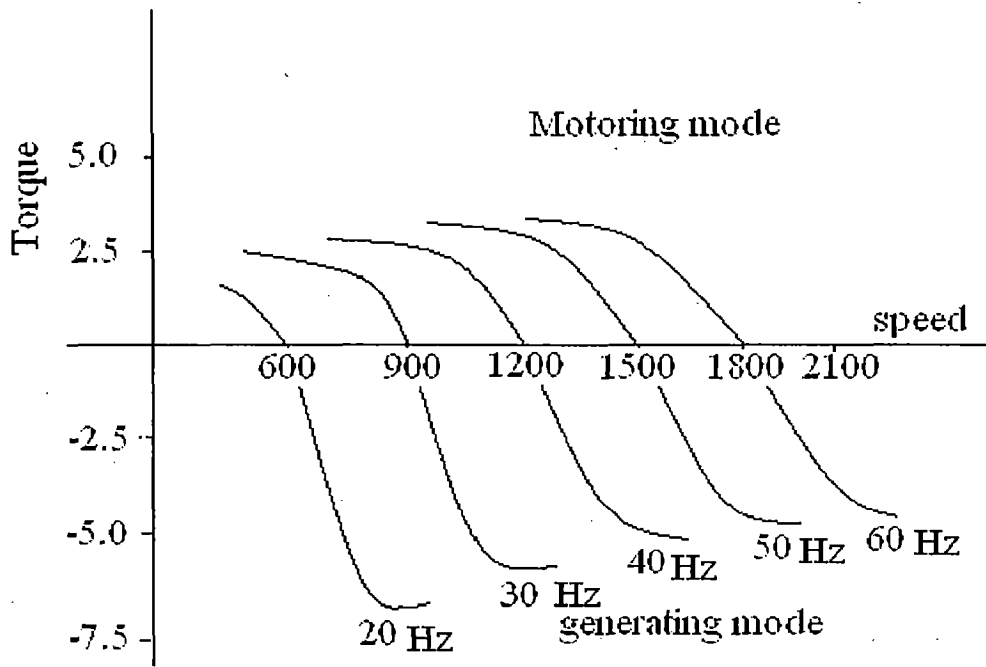**Fig. 4.1:** Static VAR compensator scalar-based control with voltage regulation [31].

Fig. 4.2: Torque/speed performance for constant V/Hz. [31].

Torque is given by

$$T_e = 3\frac{p}{2}\frac{1}{r_1}\Psi_m^2\omega_{sl}$$

Above equation shows that for a fixed V/Hz ratio one characteristics curve is locked, and the torque crossover operating point changes in accordance with the impressed stator frequency as shown in fig 4.2. Therefore depending on the shaft speed, one point along the torque speed curve will be developed. For negative slip the machine will develop negative torque, and the operation will be as generator. If variable speed is required, the V/Hz ratio must be maintained to keep rated air-gap flux. The stator voltage is reserved, resulting in an increased back-emf with increased air gap flux. In that case the torque initially increases with speed reduction, but saturation of the magnetizing inductances offsets such an increase.

4.3 VECTOR CONTROL

Vector control is the basic of high performance machines. Vector control technique can be classified according to their method of finding the instantaneous position of the machine flux, which can be either

(i)   Feed forward method or indirect control

(ii)   Feedback or direct method

Induction machines are difficult to control because being polyphase electromagnetic systems they have a non-linear and highly interactive multivariable control structure. The technique of field oriented or vector control permits an algebraic transformation that converts the dynamic structure of the AC machine into that of a separately excited decoupled control structure with independent control of flux and torque.

Two major classes of vector control are

(i) Direct control

(ii) Indirect control

4.4 FRAMES OF REFERENCE

Figure 4.2 shows the predicted start-up characteristics against no load; using each one of the above three reference frames. The electrical torque exhibits the familiar initial 50 Hz oscillations and full speed is reached within 0.2 s. Without any soft-start control being used, and considering the worst case, the motor starting current reaches 9.5 p.u. Despite the fact that the behavior of the physical variables as predicted by each reference frame is identical, the d, q variables in the respective frames of reference are different; this difference can be exploited by careful matching of the reference frame to the problem being solved, as illustrated in the following sections.

4.4.1 Stationary reference frame

In this reference frame the d-axis is fixed to and thus coincident with the axis of the stator phase A winding. This means that the mmf wave of the stator moves over this frame at the same speed as it does over the stator phase A windings. This reference frame's stator d-axis variables therefore behave in exactly the same way as do the physical stator phase A variables of the motor itself. Figures 4.3(a) and (b) show the identical nature of the stator phase A current and the stator d-axis current. It is therefore

17

not necessary to go through the inverse of Park's transform to compute the phase A current, thus saving in valuable computer time. The calculated rotor d-axis variables of this reference frame are, however, also transformed at 50 Hz frequencies and are therefore not the same as the actual rotor phase A variables, which are at slip frequency. Figure 4.3(c) and (d) show this difference between the rotor phases A current and the rotor DR current. It would therefore be an advantage when studying transient occurrences involving the stator variables to use this reference frame.

4.4.2 Rotor reference frame

Since in this reference frame the d-axis of the reference frame is moving at the same relative speed as the rotor phase A winding and coincident with its axis, it should be expected from the considerations 2 that the behaviors of the d-axis current and the phase A current would be identical. Figures 4.4(c) and (d) show how the rotor phase A current and the rotor d-axis current are initially at 50 Hz, when the rotor is at standstill, but gradually change to slip frequency at normal running speed. If this reference frame is used for the study of rotor variables, it is therefore not necessary to go through the inverse Park's transform to compute the actual rotor phase A current. Since the rotor d-axis variables are at slip frequency, this reference frame is useful in studying transient phenomena in the rotor. The transformation of the stator variables at slip frequency in this frame clearly shows its unsuitability for studying stator variables, which are at 50 Hz frequencies. Synchronously rotating reference frame when the reference frame is rotating at synchronous speed, both the stator and rotor are rotating at different speeds relative to it. However, with the reference frame rotating at the same speed as the stator and rotor space field mmf waves, the stator and rotor d, q variables are constant quantities, whereas the actual variables are at 50 Hz and slip frequencies respectively. Figure 4.5(b) shows how the stator d-axis current gradually reduces from 50 Hz frequencies at the instant of switching to the equivalent of a steady DC when at rated speed. The steady nature of this stator d-axis current makes this reference frame useful when an analog computer is used in Simulation [25].
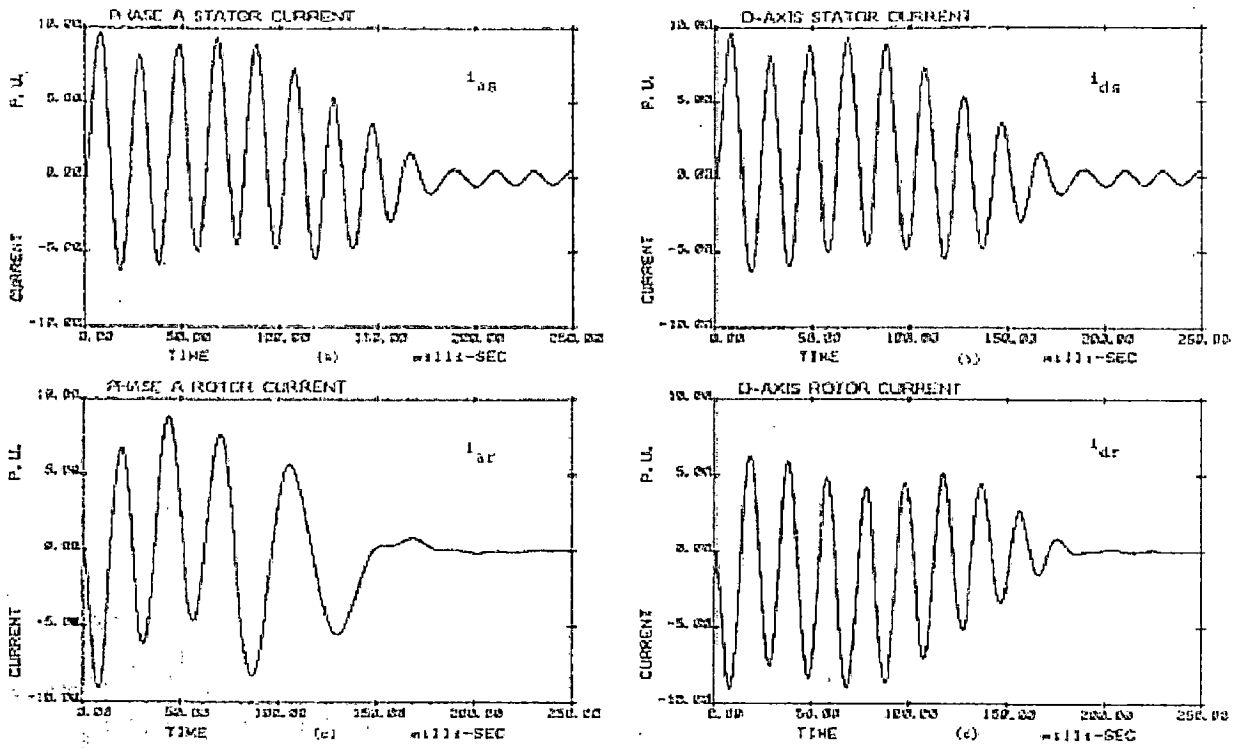
18

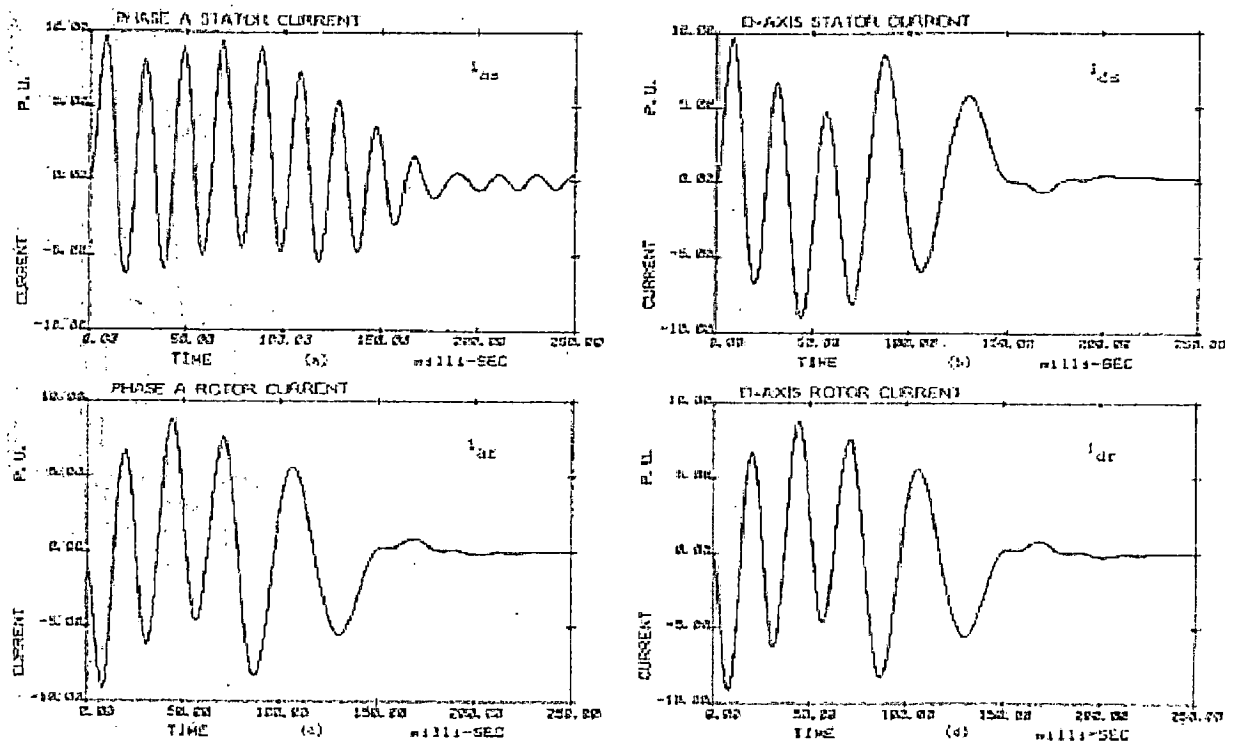**Fig 4.3** Predicted starting up current using the stationary reference frame[25]

Fig 4.4: Predicted starting up current using the rotor reference frame[25]
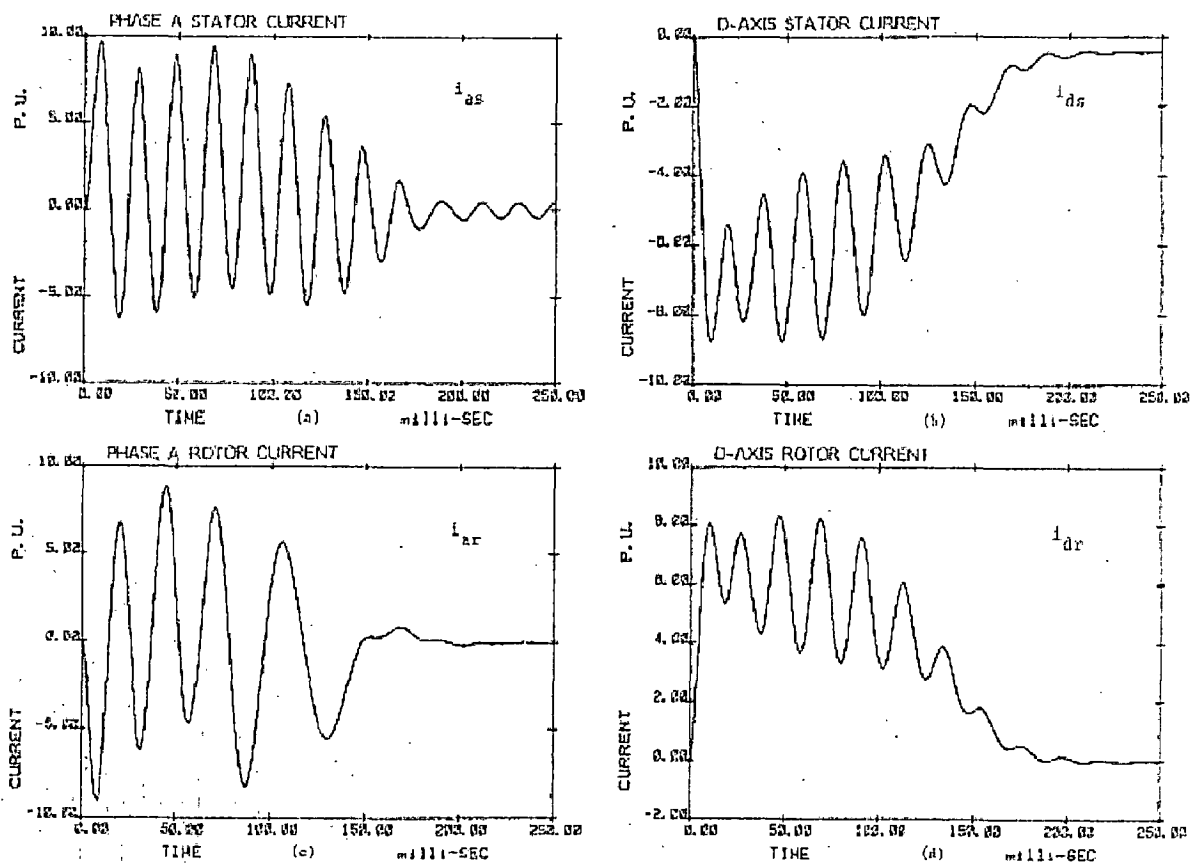
19

Fig 4.5: Predicted starting up current using the synchronously rotating reference frame[25]

4.5 INDIRECT VECTOR CONTROL

In Indirect vector control (IVC), the unit vector, $\sin\theta_e$, and $\cos\theta_e$, used for vector rotation of the terminal variables is calculated in a feed forward manner through the use of internal signals ω_r (rotor speed) and i_{qs}^* quadrature stator current component proportional to torque).

4.6 DIRECT VECTOR CONTROL

The basic block diagram of the direct vector control method for a PWM voltage-fed inverter drive is shown in figure 4.6. The principle vector control parameters, i_{ds}^* and i_{qs}^* which are dc values in synchronously rotating frame, are converted to stationary frame with the help of a unit vector ($\cos\theta_e$ and $\sin\theta_e$) generated from flux vector signal Ψ_{dr}^* and Ψ_{qr}^*. The resulting stationary frame signals are then converted to phase current

command for inverter. The flux signal Ψ_{dr} and Ψ_{qr} are generated from the machine terminal voltage and current with the help of the voltage model estimator.

A flux control loop has been added for precision control of flux. The torque component of current i_{qs}^* is generated from the speed control loop through a bipolar limiter. The torque, proportional to i_{qs} with constant flux can be bipolar. It is negative with negative i_{qs}^*, and correspondingly, the phase position of i_{qs} becomes negative in figure 4.6. An additional torque control loop can be added within the speed loop, if desired. Figure 4.6 is extended to field-weakening mode by programming the flux command as a function of speed so that the inverter remains in PWM mode. Vector control by current regulation is lost if the inverter attains the square-wave mode of operation.

The correct alignment of current i_{ds}^* in the direction of flux Ψ_{dr} and the current i_{qs} perpendicular to it are crucial in vector control. This alignment, with the help of stationary frame rotor flux vector Ψ_{dr}^s and Ψ_{qr}^s . The d^e-q^e frame is rotating at synchronous speed we with respect to stationary frame d^e-q^e, and at any instant, the angular position of the d^e-axis with respect to the d^s axis is θ_e, where $\theta_e = \omega_e t$.

Where vector Ψ_{dr} is represented by magnitude Ψ_{dr} Signal ($\cos\theta_e$ and $\sin\theta_e$) have been plotted in correct phase position. These unit vector signals, when used for vector rotation in figure 4.6, give a ride of current i_{ds} on the d^e-axis
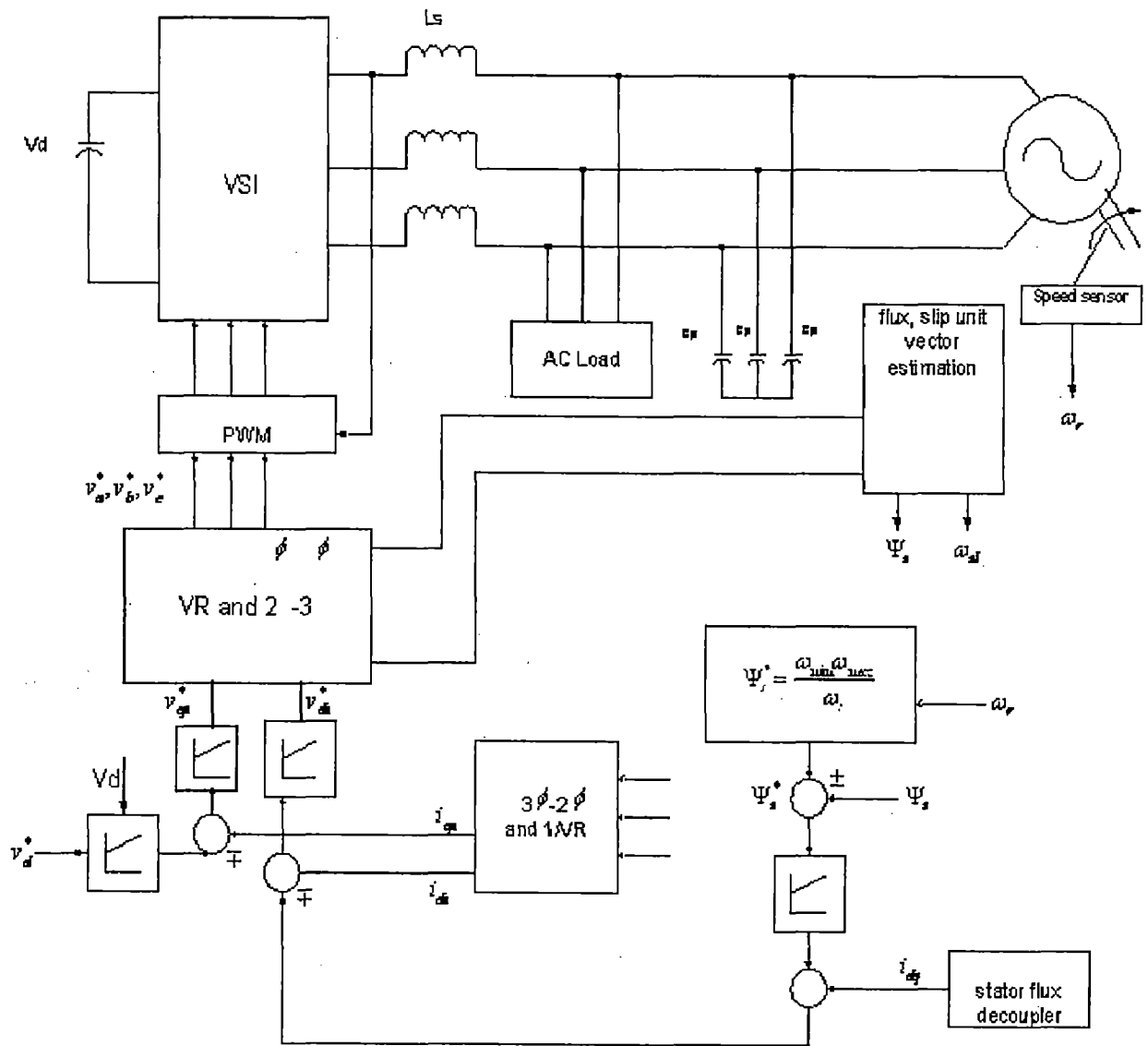
Fig 4.6: Stand alone DVC stator flux based induction generator control [31].

MODELING OF INDUCTION GENERATOR

5.1 INTRODUCTION

For the two phase machine need to represent both d^s-q^s and d^r-q^r circuits and their variables in a synchronously rotating d^e-q^e frame. We can write the following stator equations from Fig 5.2[29]:

$$v_{qs}^s = R_s i_{qs}^s + \frac{d}{dt}\Psi_{qs}^s \tag{1}$$

$$v_{ds}^s = R_s i_{ds}^s + \frac{d}{dt}\Psi_{ds}^s \tag{2}$$

Where Ψ_{ds}^s and Ψ_{qs}^s are q- axis and d-axis stator flux linkages, respectively. When these equations are converted to $d^e - q^e$ frame, the following equations can be written:

$$v_{qs} = R_s i_{qs} + \frac{d}{dt}\Psi_{qs} + \omega_e \Psi_{ds} \tag{3}$$

$$v_{ds} = R_s i_{ds} + \frac{d}{dt}\Psi_{ds} - \omega_e \Psi_{qs} \tag{4}$$

Where all the variables are in rotating form. The last term in equations 5 and 6 can be defined as speed emf due to rotation of the axes, that is, when $\omega_e = 0$, the equations revert to stationary form. The flux linkage in the $d^e - q^e$ axes induces emf in the q^e and d^e axes, respectively, with $\pi/2$ lead angle. For $\omega_r = 0$ the rotor equations are

$$v_{qr} = R_r i_{qr} + \frac{d}{dt}\Psi_{qr} + \omega_e \Psi_{dr} \tag{5}$$

$$v_{dr} = R_s i_{dr} + \frac{d}{dt}\Psi_{dr} - \omega_e \Psi_{qr} \qquad (6)$$

Where all the variables and parameters are referred to the stator. Since the rotor actually moves at speed ω_r, the d-q axes fixed on the rotor move at a speed $\omega_e - \omega_r$ relative to the synchronously rotating frame. Therefore, in $d^e - q^e$ frame, the rotor equations should be modified as

$$v_{qr} = R_r i_{qr} + \frac{d}{dt}\Psi_{qr} + (\omega_e - \omega_r)\Psi_{dr} \qquad (7)$$

$$v_{dr} = R_s i_{dr} + \frac{d}{dt}\Psi_{dr} - (\omega_e - \omega_r)\Psi_{qr} \qquad (8)$$

Figure 5.3 shows the $d^e - q^e$ dynamic model equivalent circuits that satisfy equations (3-4) and (7-8). A special advantage of the $d^e - q^e$ dynamic model of the machine is that all the sinusoidal variables in stationary frame appear as dc quantities in synchronous frame. The flux linkage expressions in terms of currents can be written from figure 3 as follows:

$$\Psi_{qs} = L_{ls} i_{qs} + L_m (i_{qs} + i_{qr}) \qquad (9)$$

$$\Psi_{qr} = L_{lr} i_{qr} + L_m (i_{qs} + i_{qr}) \qquad (10)$$

$$\Psi_{qm} = L_m (i_{qs} + i_{qr}) \qquad (11)$$

$$\Psi_{ds} = L_{ls} i_{ds} + L_m (i_{ds} + i_{dr}) \qquad (12)$$

$$\Psi_{dr} = L_{lr} i_{dr} + L_m (i_{ds} + i_{dr}) \qquad (13)$$

$$\Psi_{dm} = L_m (i_{ds} + i_{dr}) \qquad (14)$$

Combining the above expressions with equations (3–5), (7-8) the electrical transient model in terms of voltage and currents can be given in matrix form as

24

$$
\begin{bmatrix} v_{qs} \\ v_{ds} \\ v_{qr} \\ v_{dr} \end{bmatrix} =
\begin{bmatrix}
R_s + sL_s & \omega_e L_s & sL_m & \omega_e L_m \\
-\omega_e L_s & R_s + sL_s & -\omega_e L_m & sL_m \\
sL_m & (\omega_e - \omega_r) L_m & R_r + sL_r & (\omega_e - \omega_r) L_r \\
-(\omega_e - \omega_r) L_m & sL_m & -(\omega_e - \omega_r) L_r & R_r + sL_r
\end{bmatrix}
\begin{bmatrix} i_{qs} \\ i_{ds} \\ i_{qr} \\ i_{dr} \end{bmatrix}
\tag{15}
$$

Where s is the Laplace operator. For a singly-fed machine $v_{qr} = v_{dr} = 0$.

If the speed ω_r is considered constant (infinite inertia load), the electrical dynamics of the machine are given by fourth order linear system. Then knowing the inputs v_{qs} v_{ds} and ω_e, the currents i_{qs}, i_{ds}, i_{qr} and i_{dr} can be solved from equation (15). If the machine is fed by current source, i_{qs}, i_{ds} and ω_e are independent. Then different variables v_{qs}, v_{ds}, i_{qr} and i_{dr} can be solved from (15).

The speed ω_r in equation (15) cannot normally be treated as a constant. It can be related to the torques as

$$
T_e = T_L + J \frac{d\omega_m}{dt} = T_L + \frac{2}{P} J \frac{d\omega}{dt}
\tag{16}
$$

Where $T_l =$ load torque, J = rotor inertia, and $\omega_m =$ mechanical speed.

Often, for compact representation, the machine model and equivalent circuits are expressed in complex form, multiplying equation (4) by -j and adding with (3) gives

$$
v_{qs} - jv_{ds} = R_s(i_{qs} - ji_{ds}) + \frac{d}{dt}(\Psi_{qs} - j\Psi_{ds}) + j\omega_e(\Psi_{qs} - j\Psi_{ds})
\tag{17}
$$

Or

$$
v_{qds} = R_s i_{qds} + \frac{d}{dt}\Psi_{qds} + j\omega_e \Psi_{qds}
\tag{18}
$$

Where v_{qds}, i_{qds} are complex vectors. Similarly the rotor equations can be combined to represent

$$v_{qdr} = R_r i_{qdr} + \frac{d}{dt}\Psi_{qdr} + j\omega_e \Psi_{qdr} \qquad (19)$$

Figure 4 shows the complex equivalent circuit in rotating frame V_{qdr}=0. The steady state equation can always be derived by substituting the time derivative components to zero. Therefore from equations (17)-(18), the steady state equations can be derived as

$$v_s = R_s i_s + j\omega_e \Psi_s \qquad (20)$$

$$0 = \frac{R_r}{S} I_r + j\omega_e \Psi_r \qquad (21)$$

Where the complex vectors have been substituted by the corresponding rms phasors. These equations satisfy the steady state equivalent circuit if the parameter R_m is neglected. The torque can be generally expressed in the vector form as

$$T_e = \frac{3}{2}\left(\frac{P}{2}\right)\Psi_m \times I_r \qquad (22)$$

Resolving the variables into $d^e - q^e$ components, as shown in figure 5,

$$T_e = \frac{3}{2}\left(\frac{P}{2}\right)\left(\Psi_{dm} i_{qr} - \Psi_{qm} i_{dr}\right) \qquad (23)$$

Several other torque expressions can be derived easily as follows:

$$T_e = \frac{3}{2}\left(\frac{P}{2}\right)\left(\Psi_{dm} i_{qs} - \Psi_{qm} i_{ds}\right) \qquad (24)$$

$$T_e = \frac{3}{2}\left(\frac{P}{2}\right)L_m\left(i_{dr} i_{qs} - i_{ds} i_{qr}\right) \qquad (25)$$

Equation (14),(15) and (24) give the complete model of the electromechanical dynamics of an induction machine synchronous frame. The composite system is of the fifth order and nonlinearity of the model is evident. Figure 5.1 shows the block diagram of the machine model along with input voltage and output current transformations.
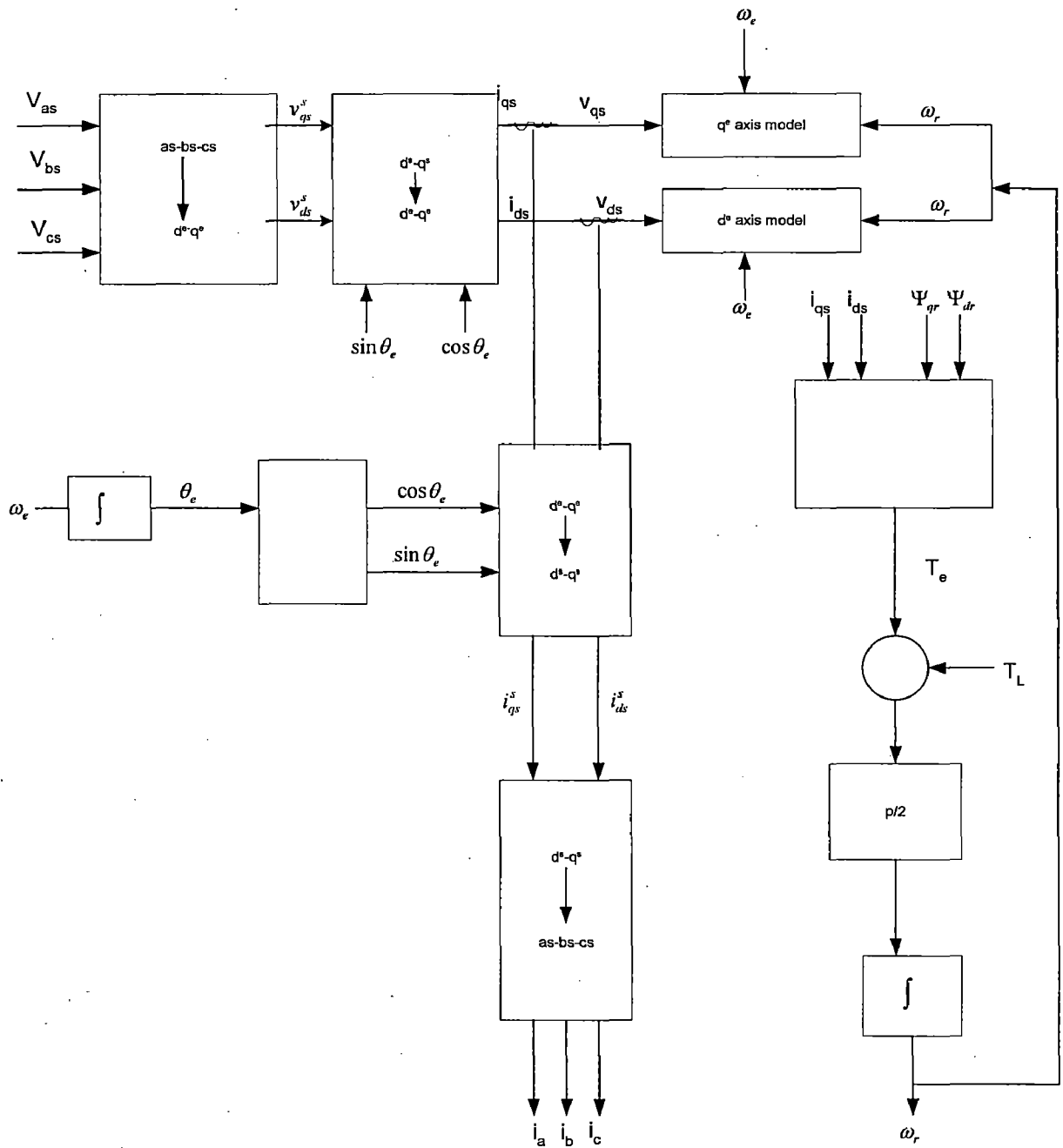
Fig 5.1: Synchronously rotating frame machine model with input voltage and output current transformations [29].
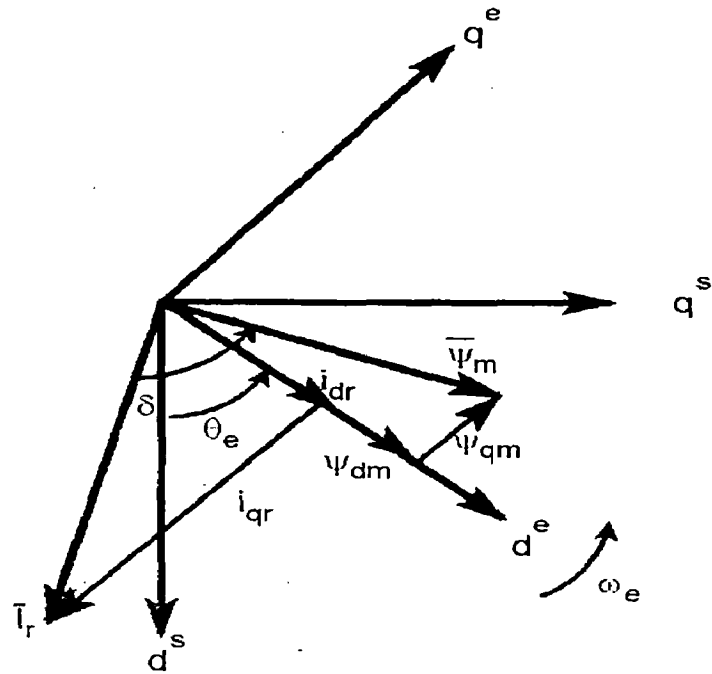
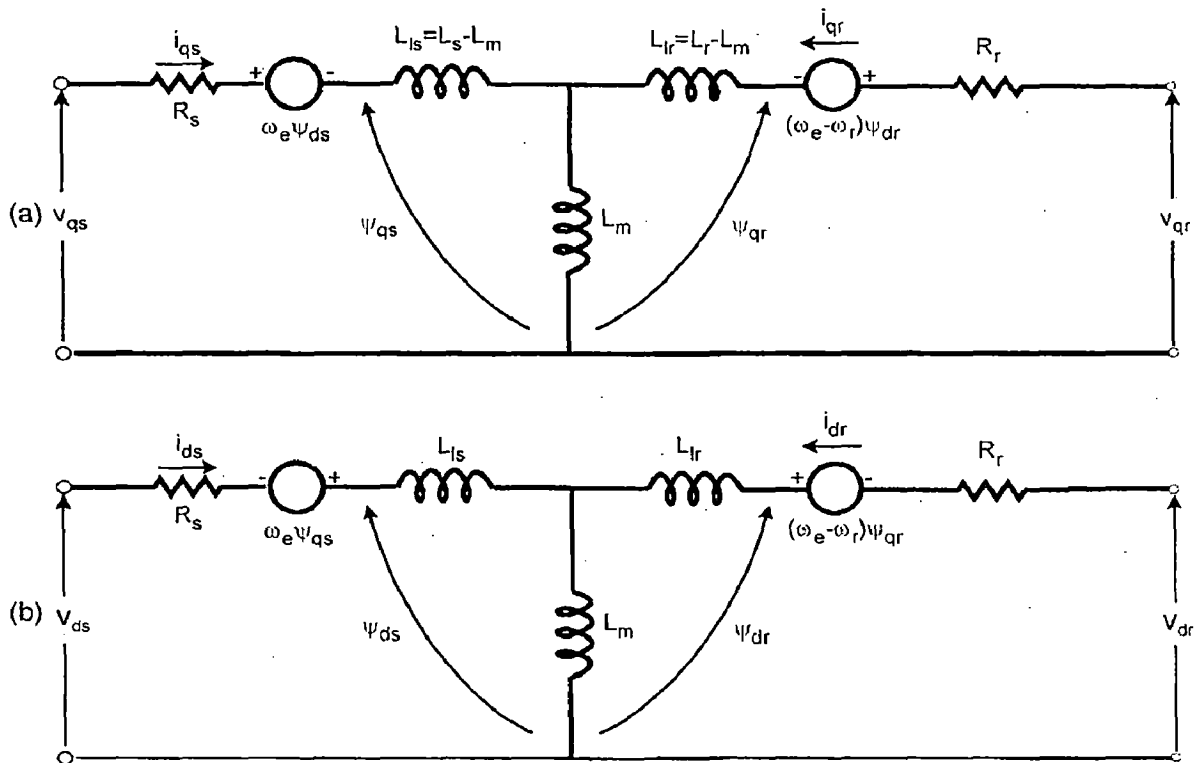**Fig 5.2:** Flux and current vectors in d^e-q^e frame [29].

Fig 5.3: Dynamic de-qe equivalent circuits of machine q^e axis circuit and d^e axis circuit [29].
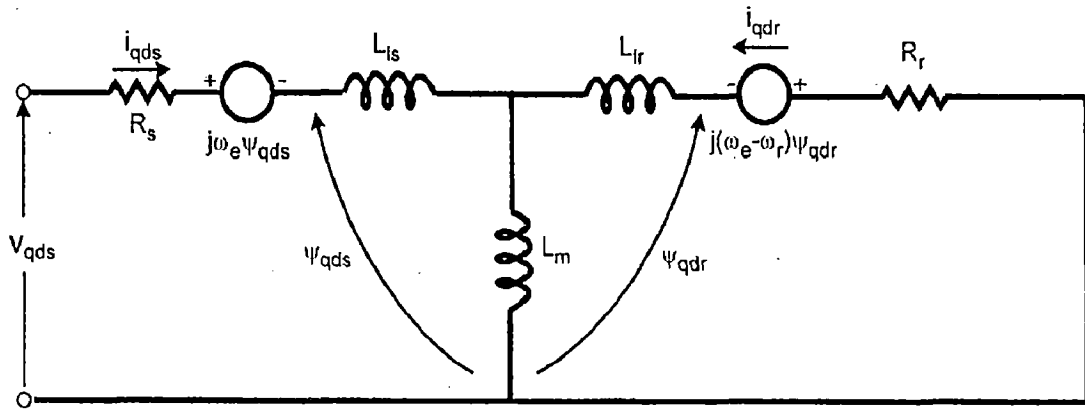
Fig 5.4: Complex synchronous frame dq^s equivalent circuit[29].
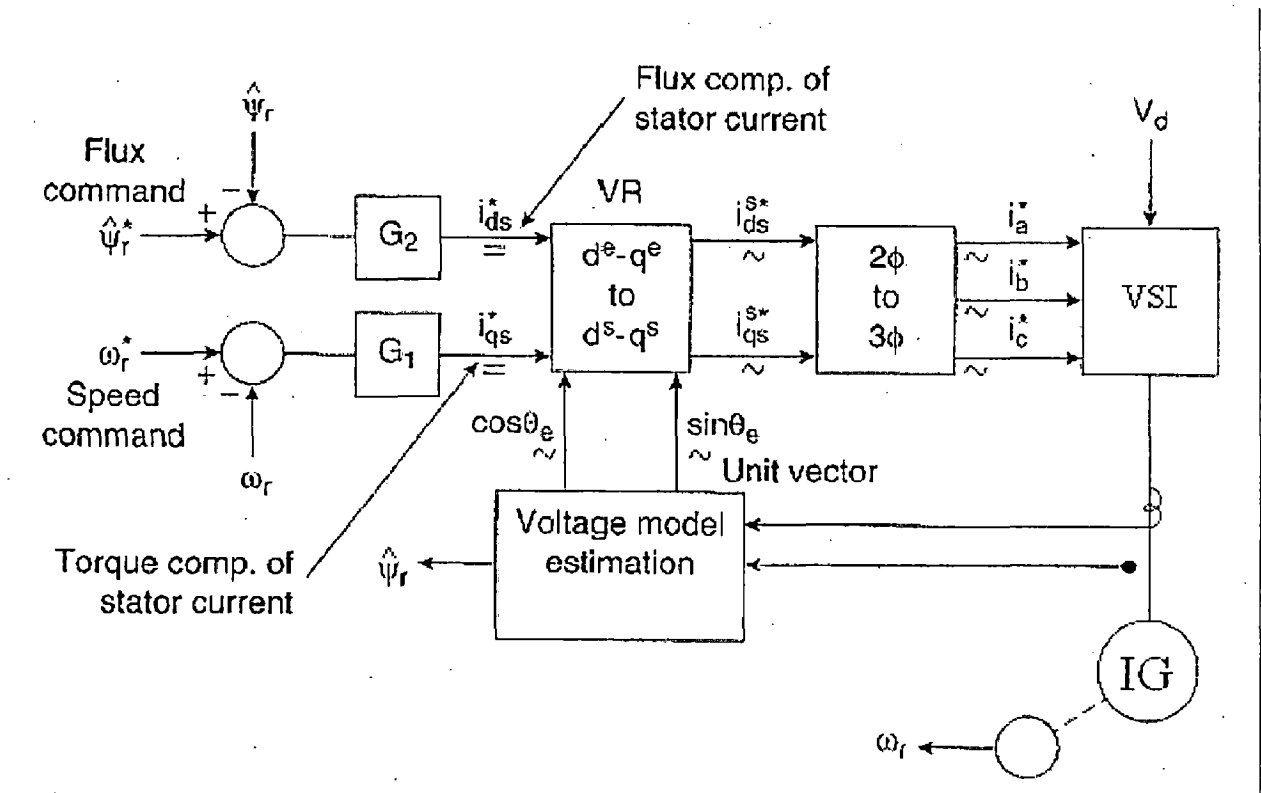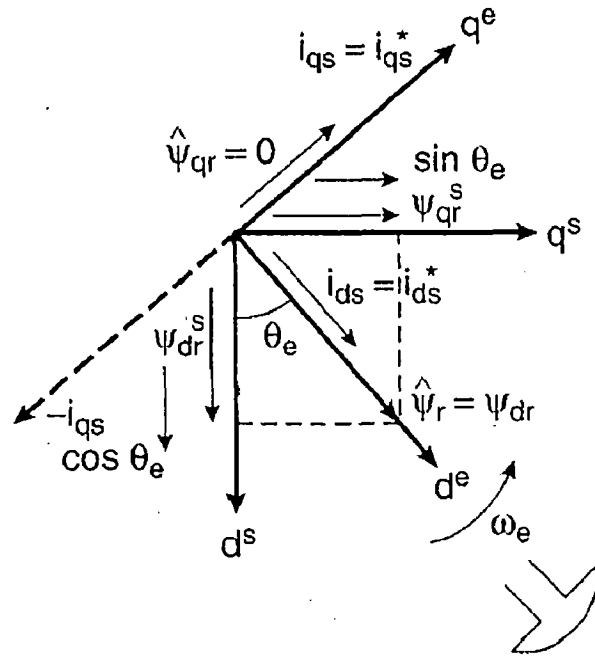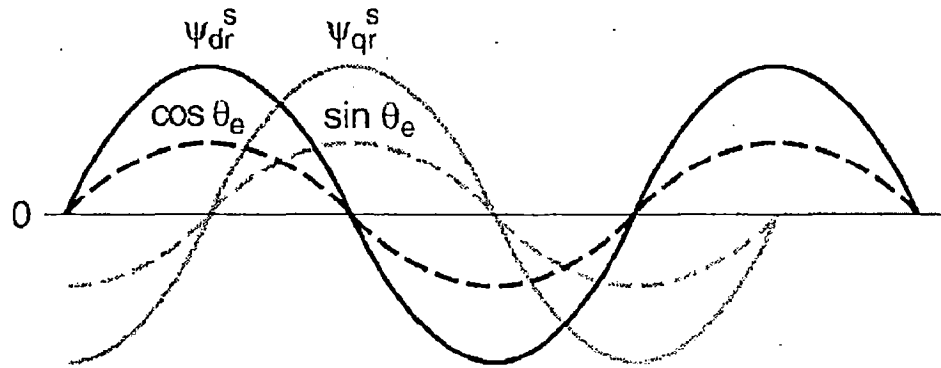

Fig 5.5: Direct vector control block diagram with rotor flux orientation [29].

Fig 5.6: (a) d^s-q^s and d^e-q^e phasors showing correct rotor flux orientation (b) plot of unit vector signals correct phase position [29].
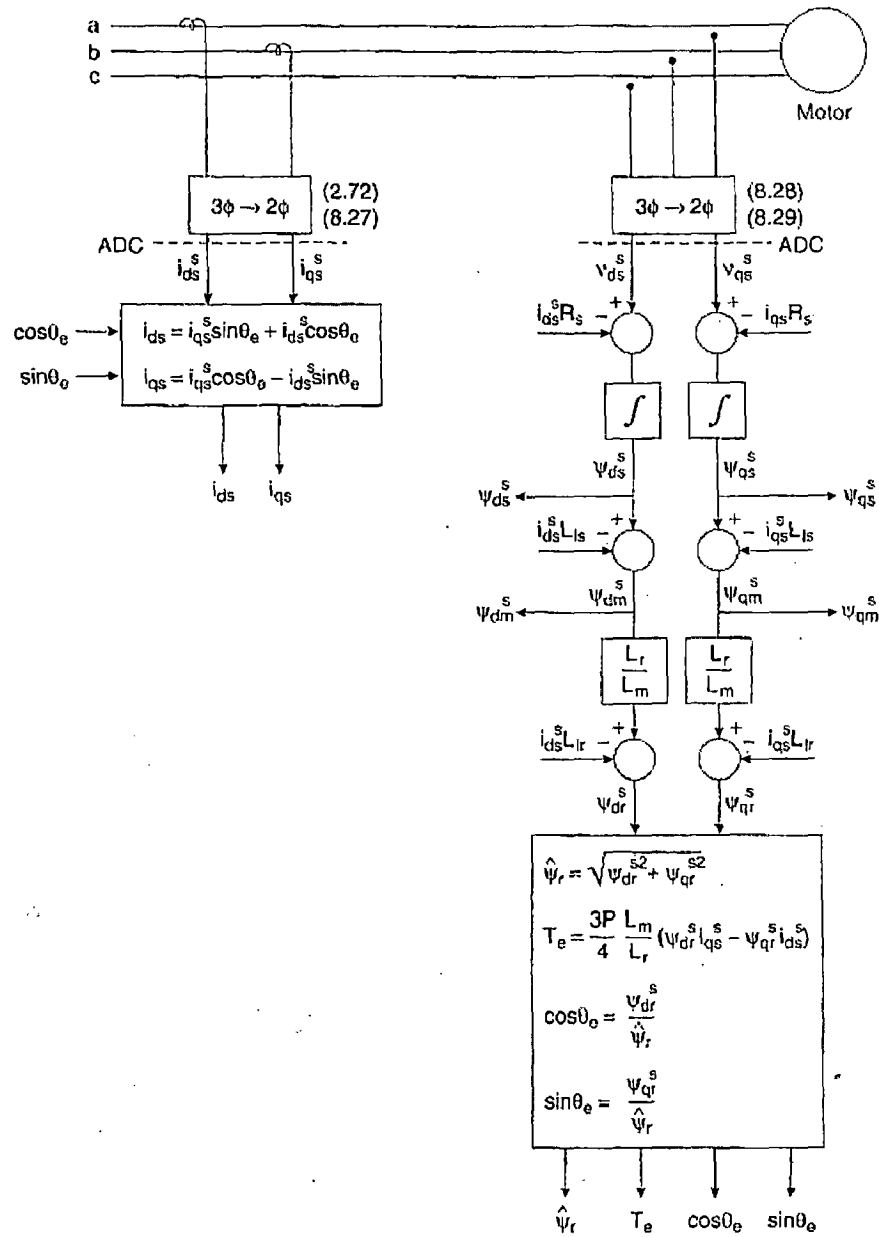
Fig 5.7: Voltage model feedback signal estimation block diagram [29].
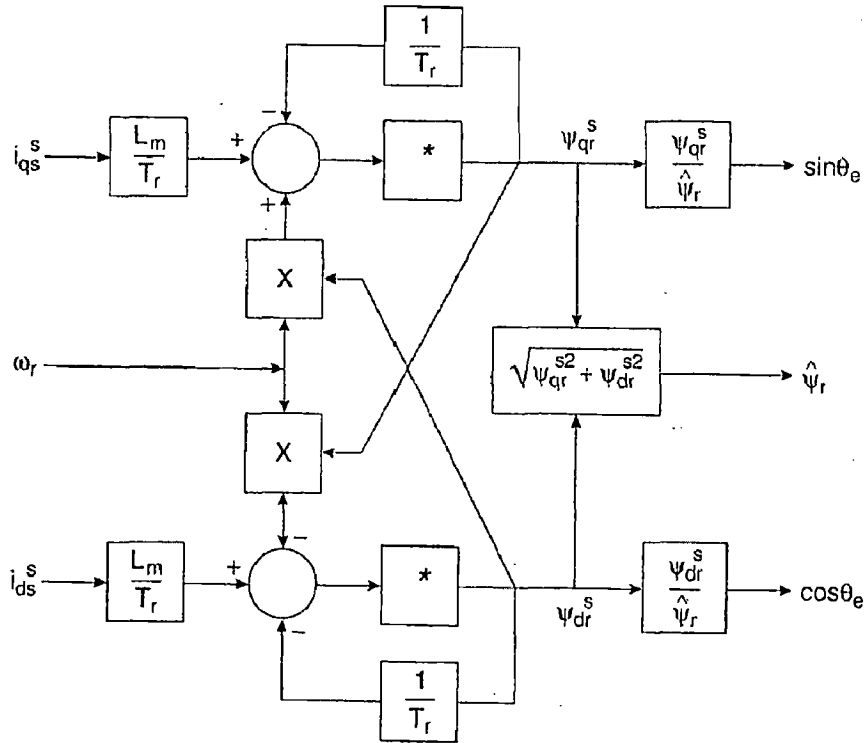
Fig 5.8: Current model flux estimation [29].

5.2 FLUX VECTOR ESTIMATION

In the direct vector control method, it is necessary to estimate the rotor flux components Ψ_{drs}^{s} and Ψ_{qrs}^{s} so that the unit vector and rotor flux can be calculated by equations

$$\cos\theta_e = \frac{\Psi_{dr}^s}{\Psi_r} \tag{a}$$

$$\sin\theta_e = \frac{\Psi_{qr}^s}{\Psi_r} \tag{b}$$

$$\Psi_r = \sqrt{\Psi_{dr}^{s^2} + \Psi_{qr}^{s^2}} \tag{c}$$

Two commonly method of flux estimation is

5.3 VOLTAGE MODEL

In this model, the machine terminal voltages and currents are sensed and the fluxes are computed from the stationary frame (d^s-q^s) equivalent circuit shown in figure 5.3. These equations are:

$$i_{qs}^{s} = \frac{2}{3}i_a - \frac{1}{3}i_b - \frac{1}{3}i_c = i_a \tag{26}$$

$$i_{ds}^{s} = -\frac{1}{\sqrt{3}}i_b + \frac{1}{\sqrt{3}}i_c \tag{27}$$

$$= -\frac{1}{\sqrt{3}}(i_a + 2i_b) \tag{28}$$

Since $i_c = -(i_a + i_b)$ for isolated neutral load.

$$i_{qs}^{s} = \frac{2}{3}v_a - \frac{1}{3}v_b - \frac{1}{3}v_c \tag{29}$$

$$= -\frac{1}{3}(v_{ab} + v_{ac}) \tag{30}$$

$$v_{ds}^{s} = -\frac{1}{\sqrt{3}}v_b + \frac{1}{\sqrt{3}}v_c \tag{31}$$

$$= -\frac{1}{\sqrt{3}}v_{bc} \tag{32}$$

$$\Psi_{ds}^{s} = \int (v_{ds}^{s} - R_s i_{ds}^{s})dt \tag{33}$$

$$\Psi_{qs}^{s} = \int (v_{qs}^{s} - R_s i_{qs}^{s})dt \tag{34}$$

$$\Psi = \sqrt{\Psi_{ds}^{s^2} + \Psi_{qs}^{s^2}} \tag{35}$$

$$\Psi_{dm}^{s} = \Psi_{ds}^{s} - L_{ls}i_{ds}^{s} = L_m(i_{ds}^{s} + i_{dr}^{s}) \tag{36}$$

$$\Psi_{qm}^s = \Psi_{qs}^s - L_{ls}i_{qs}^s = L_m(i_{qs}^s + i_{qr}^s) \tag{37}$$

$$\Psi_{dr}^s = L_m i_{ds}^s + L_r i_{dr}^s \tag{38}$$

$$\Psi_{qr}^s = L_m i_{qs}^s + L_r i_{qr}^s \tag{39}$$

Eliminating i_{dr}^s and i_{qr}^s from equation (37)-(38) with the help of equation (35)-(36), respectively, gives the following

$$\Psi_{dr}^s = \frac{L_r}{Lm} \Psi_{dm}^s - L_{lr}i_{ds}^s \tag{40}$$

$$\Psi_{qr}^s = \frac{L_r}{Lm} \Psi_{qm}^s - L_{lr}i_{qs}^s \tag{41}$$

This can also be written in the following form with the help of equation 35-36

$$\Psi_{dr}^s = \frac{L_r}{Lm}(\Psi_{ds}^s - \sigma L_s i_{ds}^s) \tag{42}$$

$$\Psi_{qr}^s = \frac{L_r}{Lm}(\Psi_{qs}^s - \sigma L_s i_{qs}^s) \tag{43}$$

Where $\sigma = 1 - L_m^2 / L_r L_s$

Substituting equation (39)-(40) in the torque equation (23), in stationary frame and simplifying, we get

$$T_e = \frac{3}{2}\frac{P}{2}\frac{L_m}{L_r}(\Psi_{dr}^s i_{qs}^s - \Psi_{qr}^s i_{ds}^s) \tag{44}$$

Figure 5.9 shows the block diagram for feedback signal estimation with the help of a microprocessor, where the estimation of additional signal, such as stator fluxes, air gap fluxes, and torque, are also shown. In the front end, there is some hardware low-pass filtering and 3 to 2 phase conversion with the help of operational amplifier before conversion by the A/D converter, which is not shown in detail. Machines are normally isolated neutral load, and therefore, only two current sensors are needed. The vector drive uses a current controlled PWM inverter. The current control is logical, because both the flux torque is directly related to currents. The inverter can have hysteresis-band current control, or some type of voltage control within the current control loop. The current estimation equation for ids and iqs are also included in figure 5.9. Any error in the unit vector or distortion associated with the feedback signals will affect the performance of drive.

5.4 CURRENT CONTROL

$$\frac{d\Psi_{dr}^s}{dt} + R_r i_{dr}^s + \omega_r \Psi_{qr}^s = 0 \tag{45}$$

$$\frac{d\Psi_{qr}^s}{dt} + R_r i_{qr}^s + \omega_r \Psi_{dr}^s = 0 \tag{46}$$

Adding terms $(L_m R_r / L_r) i_{ds}^s$ and $(L_m R_r / L_r) i_{qs}^s$, respectively, on both sides of the above equation, we get

$$\frac{d\Psi_{dr}^s}{dt} + \frac{R_r}{L_r}(L_m i_{ds}^s + L_r i_{dr}^s) + \omega_r \Psi_{qr}^s = \frac{L_m}{L_r} R_r i_{ds}^s \tag{47}$$

$$\frac{d\Psi_{qr}^s}{dt} + \frac{R_r}{L_r}(L_m i_{qs}^s + L_r i_{qr}^s) - \omega_r \Psi_{dr}^s = \frac{L_m}{L_r} R_r i_{qs}^s \tag{48}$$

a

b

c

IG

$3\phi \rightarrow 2\phi$

$3\phi \rightarrow 2\phi$

ADC

i_{ds}^{s} i_{qs}^{s}

ADC

v_{ds}^{s} v_{qs}^{s}

$\cos\theta_e \longrightarrow$

$\sin\theta_e \longrightarrow$

$i_{ds} = i_{qs}^{s}\sin\theta_e + i_{ds}^{s}\cos\theta_e$

$i_{qs} = i_{qs}^{s}\cos\theta_e - i_{ds}^{s}\sin\theta_e$

$i_{ds}^{s}R_s \; - \quad + \; i_{qs}R_s$

$\int$ $\int$

i_{ds} i_{qs}

ψ_{ds}^{s} ψ_{qs}^{s}

$\psi_{ds}^{s} \longleftarrow$ $\longrightarrow \psi_{qs}^{s}$

$i_{ds}^{s}L_{ls} \; - \quad + \; i_{qs}^{s}L_{ls}$

$\psi_{dm}^{s} \longleftarrow$ ψ_{dm}^{s} ψ_{qm}^{s} $\longrightarrow \psi_{qm}^{s}$

$\dfrac{L_r}{L_m}$ $\dfrac{L_r}{L_m}$

$i_{ds}^{s}L_{lr} \; - \quad + \; i_{qs}^{s}L_{lr}$

ψ_{dr}^{s} ψ_{qr}^{s}

$\hat{\psi}_r = \sqrt{\psi_{dr}^{s2} + \psi_{qr}^{s2}}$

$T_e = \dfrac{3P}{4}\dfrac{L_m}{L_r}(\psi_{dr}^{s}i_{qs}^{s} - \psi_{qr}^{s}i_{ds}^{s})$

$\cos\theta_e = \dfrac{\psi_{dr}^{s}}{\hat{\psi}_r}$

$\sin\theta_e = \dfrac{\psi_{qr}^{s}}{\hat{\psi}_r}$

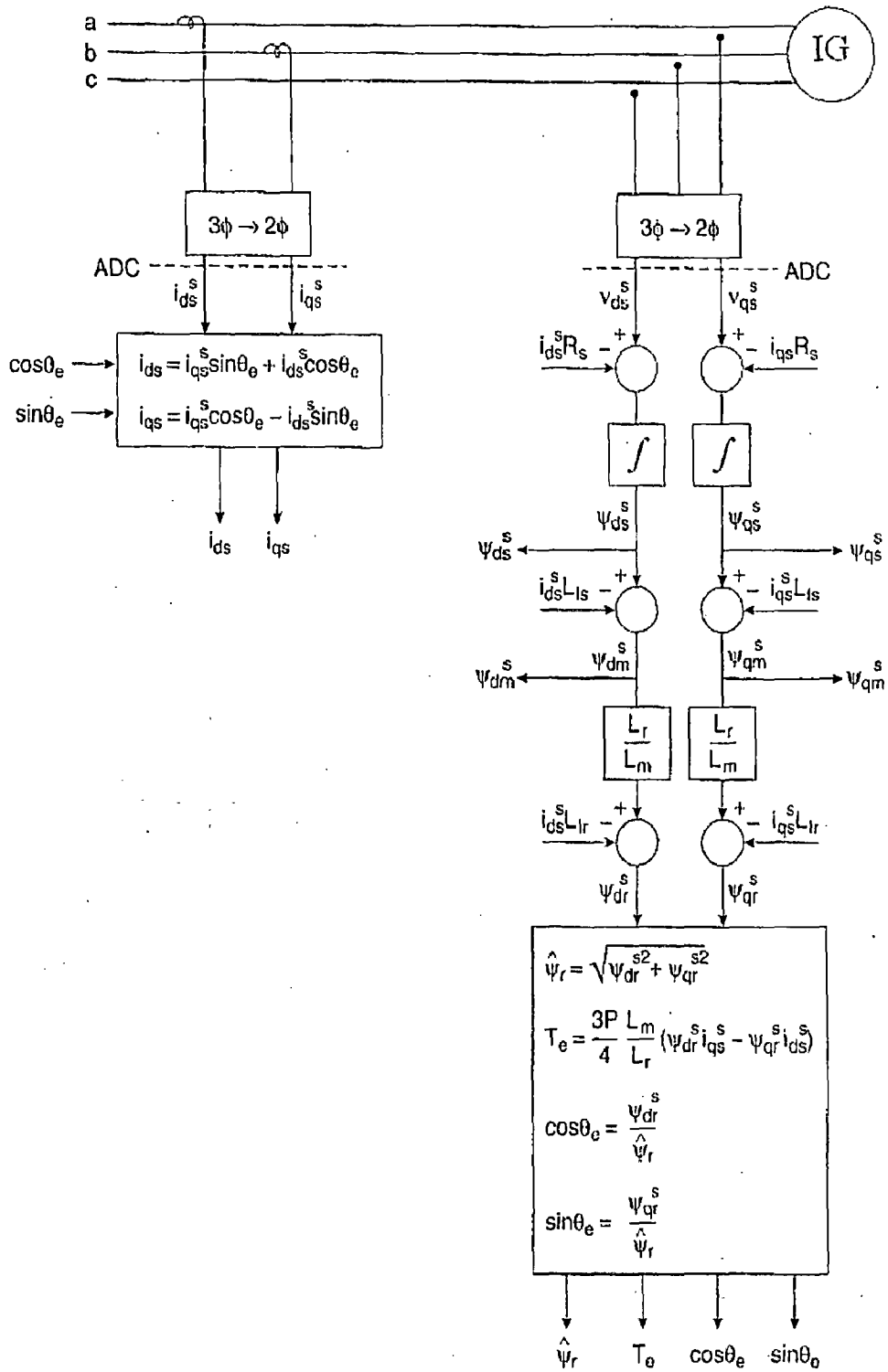$\hat{\psi}_r$ T_e $\cos\theta_e$ $\sin\theta_e$

Fig. 5.9: Voltage model feedback signal estimation block diagram [29].

Substituting 37-38, respectively, and simplifying we get

$$\frac{d\Psi^s_{dr}}{dt} = \frac{L_m}{T_r} i^s_{ds} - \omega_r \Psi^s_{qr} - \frac{1}{T_r} \Psi^s_{dr} \qquad (49)$$

$$\frac{d\Psi^s_{qr}}{dt} = \frac{L_m}{T_r} i^s_{qs} - \omega_r \Psi^s_{dr} - \frac{1}{T_r} \Psi^s_{qr} \qquad (50)$$

Where $T_r = L_r / R_r$ is the rotor circuit time constant. Equation (48)-(49) give rotor fluxes as functions of stator currents and speed. Therefore, knowing these signals, the fluxes and corresponding unit vector signal can be estimated. These equations are defined as the current model for flux estimation, which was originally formulated by blaschke. It is shown in fig 5.8, where the estimation of the cos θ_e and sin θ_e signal shown on the right. Flux estimation by this model requires a speed encoder, but the advantage is that the drive operation can be extended down to zero speed [29].

MICROPROCESSOR BASED VOLTAGE CONTROL

6.1 INTRODUCTION

From last decade, machine tool industry-both in the country and all over the world- is proving great request for high quality control parameters electric drives with high level reliability and maintainability. Above-mentioned requirements are accomplishing drive systems involving ac machines and frequency converters with field orientation control system. Vector or field orientation control theory came into being in Germany many years ago but it has not been using regarding high level of complexity. Nowadays, it is assumed that the theory has two authors Hasse and Blaschke. Field orientation control takes the analogy between ac and dc machines. The fundamental goal of this control is elimination of coupling influence through the coordinate's transformation then in consequence ac machine behaves like separately excited dc motor. Then stability problem of ac machine is on the decline and by fixed flux torque equation become linear. The response of the system becomes as quickly as in dc machine. The price of the solution is complicated coordinates transformation, phases converting and difficult transformation of feedback signal. Practical realization of this high complexity system is taken place together with dissemination of the microcomputers and VLSI technology. In world engineering vector control of ac motors acquired popularity and it can be taken as standard method. The field orientation method is realized in various practical versions.

Figure 6.1 shows block diagram of microprocessor based voltage control of self excited induction generator. Fig 6.1 shows all the equipment required control of SEIG. International inverter 2130 is used as a gate driver. Flowchart show the controlling scheme which is simulated. MATLAB can compute on symbolic variables just as on constants. This exempts one from the tedious job of manual manipulation of the complex equations to obtain the final equations. It can also solve several simultaneous equations hence the user does not need to use numerical methods to solve the complex equations obtained after the manipulation [34].

6.2 Extinction Angle Control Scheme

The extinction angle control scheme follows formulas listed below[34].

Case-a: $\beta < 60°$

$$V_d = 3\sqrt{6}\frac{V_p}{2\pi}\left(\frac{1}{2} - \cos\left(\beta + \frac{\pi}{3}\right)\right) \tag{51}$$

$$I_{s1} = \frac{\sqrt{6}}{\pi}I_d \sin(\beta/2) \tag{52}$$

$$\phi_1 = \frac{\pi}{6} - \frac{\beta}{2} \tag{53}$$

$$I_s = I_d\sqrt{\frac{\beta}{\pi}} \tag{54}$$

$$PF = \frac{\sqrt{6}}{\pi\beta}\sin(\beta/2)\cos\left(\frac{\pi}{6} - \frac{\beta}{2}\right) \tag{55}$$

Case-b: $\beta > 60°$

$$V_d = 3\sqrt{6}\frac{V_p}{2\pi}\left(\frac{3}{2} - \cos\beta\right) \tag{56}$$

$$I_{s1} = \sqrt{\frac{3}{2}}\frac{I_d}{\pi}\left[4 - \sqrt{3}\sin\beta - 3\cos\beta\right]^{\frac{1}{2}} \tag{57}$$

$$\phi_1 = \tan^{-1}\left(\frac{\sin\beta - \sqrt{3}/2}{3/2 - \cos\beta}\right) \tag{58}$$

$$I_s = I_d\sqrt{\frac{\beta}{\pi}} \tag{59}$$

$$PF = \left(\frac{3}{2\pi\beta}\left(4 - \sqrt{3}\sin\beta - 3\cos\beta\right)\right)^{\frac{1}{2}}\cos\phi_1 \tag{60}$$
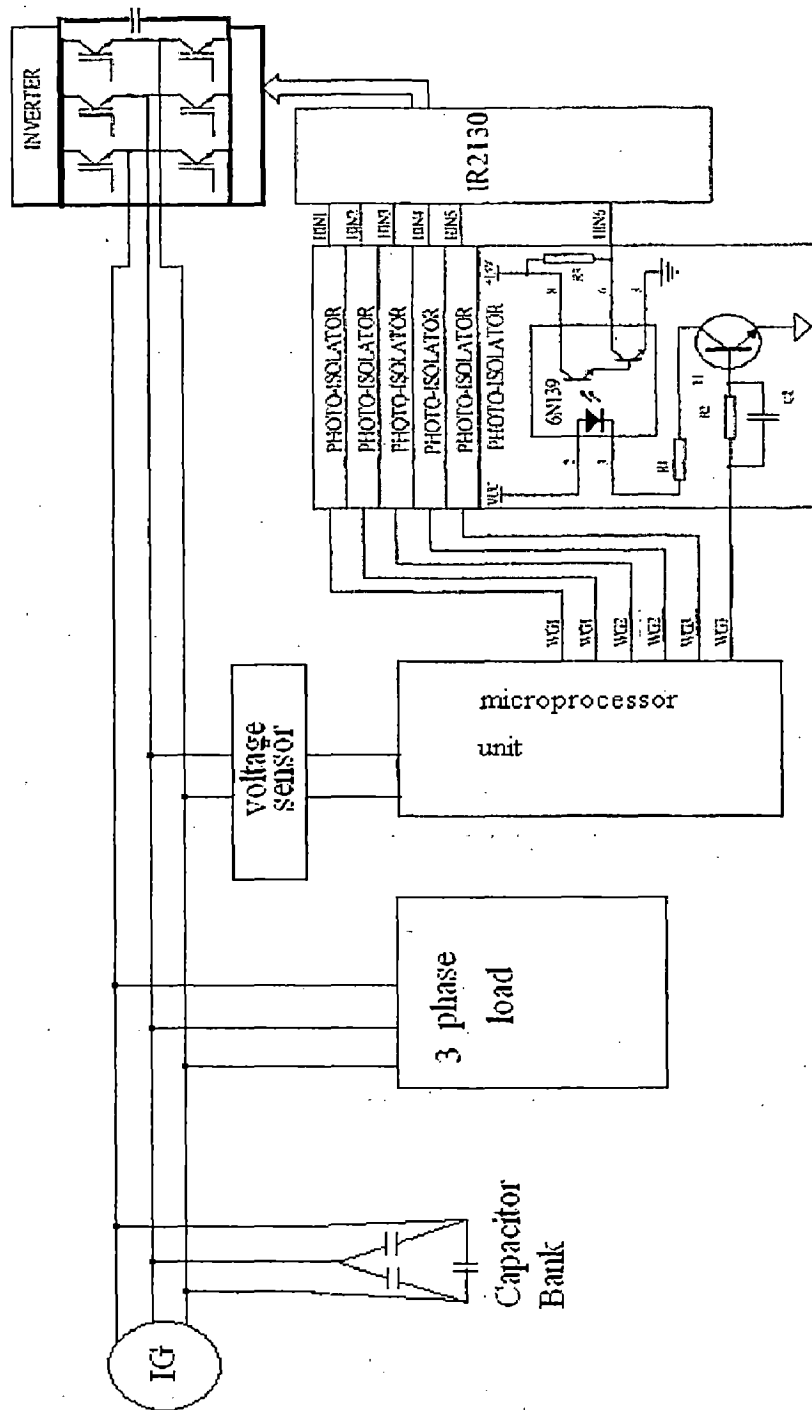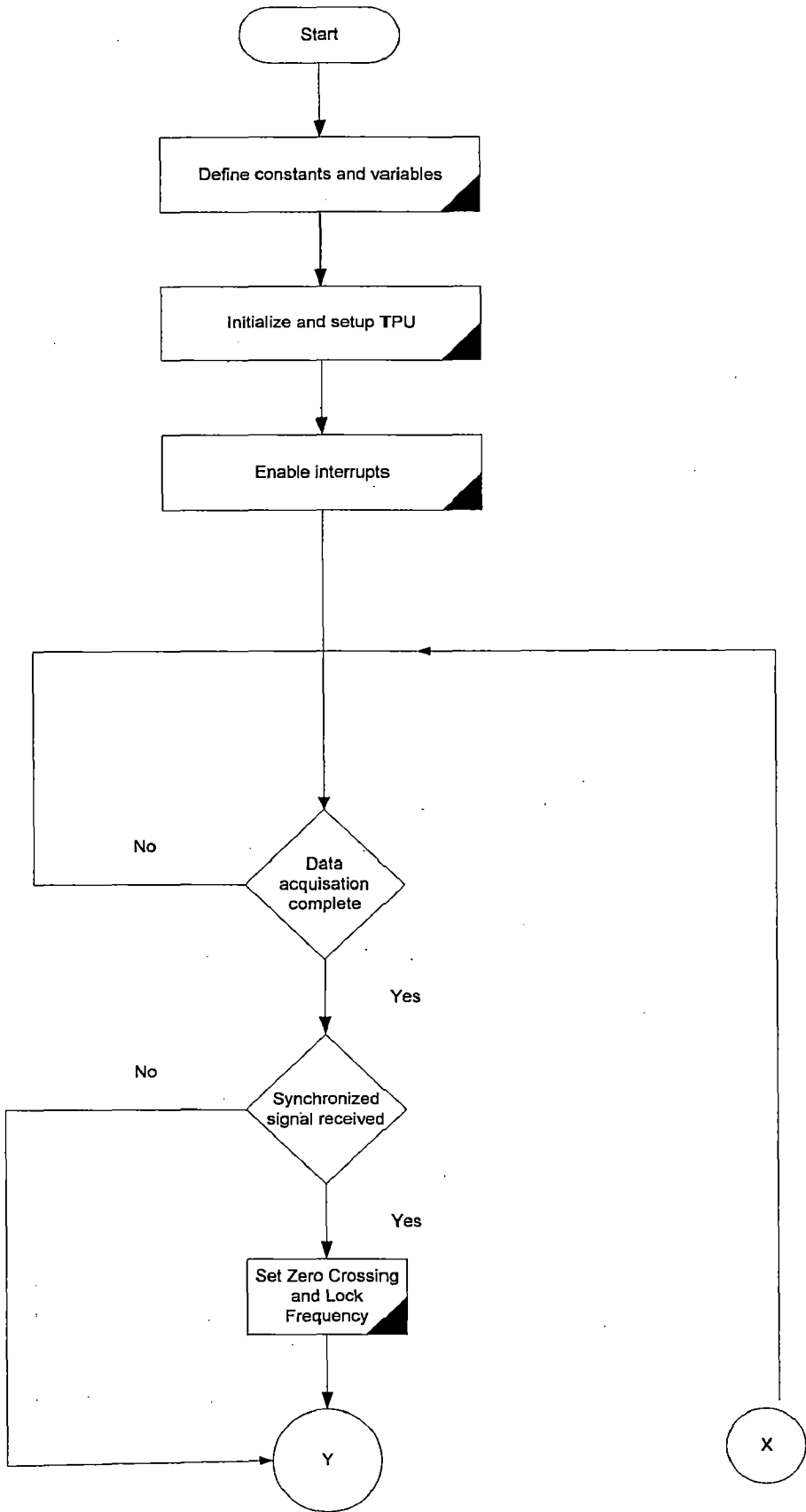
Fig. 6.1: Microprocessor Based Control of Induction Generator [23].

```
                        ┌───────────┐
                        │   Start   │
                        └─────┬─────┘
                              │
                              ▼
              ┌──────────────────────────────────┐
              │   Define constants and variables  ◢│
              └────────────────┬─────────────────┘
                               │
                               ▼
              ┌──────────────────────────────────┐
              │      Initialize and setup TPU     ◢│
              └────────────────┬─────────────────┘
                               │
                               ▼
              ┌──────────────────────────────────┐
              │         Enable interrupts         ◢│
              └────────────────┬─────────────────┘
                               │
                               │
                               │
                               ▼
                            ╱─────╲
                          ╱  Data   ╲
        No ◄─────────────◄ acquisation ►
                          ╲ complete ╱
                            ╲─────╱
                               │ Yes
                               ▼
                            ╱──────╲
                          ╱Synchronized╲
        No ◄─────────────◄signal received►
                          ╲           ╱
                            ╲──────╱
                               │ Yes
                               ▼
                      ┌─────────────────┐
                      │ Set Zero Crossing│
                      │    and Lock     ◢│
                      │   Frequency     │
                      └────────┬────────┘
                               │
                               ▼
                            ( Y )                    ( X )
```
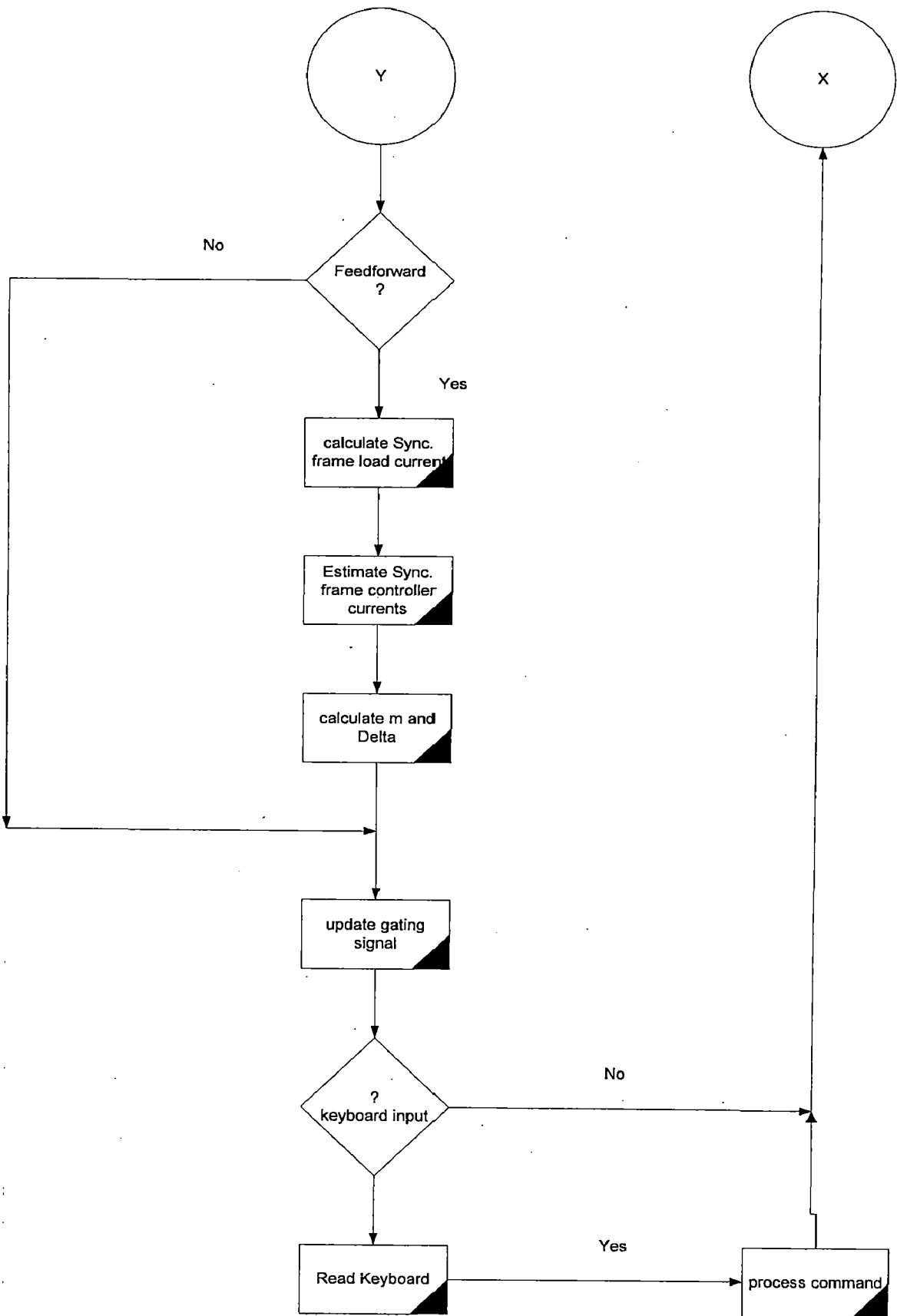
41

Fig 6.2: Flowchart for calculating firing angle

SIMULATION OF INDUCTION GENERATOR BY DIRECT VECTOR CONTROL (DVC) SCHEME

7.1 INTRODUCTION

Simulink is a subprogram in the MATLAB environment. It uses a graphical user interface and enables a system to be simulated by block diagrams and equations. The DSP block set is used to run the Butterworth filter. Shown in figure 7.1 is a typical block diagram of direct vector control scheme of induction generator. The system contains all the equation Necessary for an induction machine as described in modeling of induction generator. Subsystem 1 in figure 7.1 is the controller for the model: it changes based on which model running. Subsystem 2 is he three phase inverter block, which changes the reference voltages from the controller to the phase voltages through a PWM converter. Subsystem 3 is the induction machine block, which contain all of the necessary equation for an induction machine. The block takes in the phase voltages and calculates speed, currents, fluxes, and developed torque. Subsystem 4 takes the outputs of the model where the matrices are sent to the MATLAB workspaces as the value listed. The time index tout is also output to the workspace. Subsystem 5 is a filtering block that filters both the input voltage and output currents with an eight order low-pass Butterworth filter.

Inputs for simulink-based vector control scheme

Repeating sequence	Applies to all of the block diagrams and is the reference torque that the machine is trying to follow
J	This is the inertia on the shaft, usually 0.05
kW	The value is the constant to determine rotational losses in the machine running. $T_l=K_w\omega^2$
Freqt	This value is the frequency that the PWM operates at, usually at 2000 Hz
V_{dc}	This is the value of DC bus. Usually 300V.
Tstop	This value is how long the simulation runs, usually 10s.
fc*	All these values are used to control the filtering in the

	output, controllers and the machine. Lower filtering values can create smoother signals, but could also create instabilities in the system.

Various blocks of simulation of induction machine are shown in Fig. 7.1.ain blocks are :

(i.)   DVC stator torque with torque feedback

(ii.)   H Bridge inverter

(iii.)   Induction machine

(i) DVC stator torque with torque feedback

The direct vector controller is shown in Fig. 7.2 change of reference frame quantity (voltage and current) into synchronous frame is shown in Fig 7.3.. Then flux is calculated in flux calculator as shown in Fig. 7.4 with the help of voltage, current and speed. Sine and cosine of angle between voltage and current calculated in next block as given in Fig. 7.5. In the torque controller Fig 7.6. torque , q axis current , d axis current and flux error signal compared and give to the PID controller the output of the torque controller is V_{ds}^* and V_{qs}^*. Now the two phase quantity convert into three phase abc terms. The other components of Fig. 7.2 are given in Fig. 7.7, 7.8and 7.9.

(ii) H Bridge Inverter

The input of the inverter fig 7.10 is reference voltages output of the controller. The output of the H Bridge is inputted to induction machine block.

(iii) Induction Machine

This is shown in Figure 7.11 constitutes necessary equation (42)-(48) to represent induction machine characteristics. The main block inside the induction machine block are listed below

(i.)   Fig 7.12: 3 to 2 phase

(ii.)   Fig 7.13 : Integrator

(iii.)   Fig 7.14 : Rotation

(iv.)   Fig 7.15 : Induction machine

(v.)   Fig 7.21 : Currents

(vi.)   Fig 7.22 : Torque generator

44
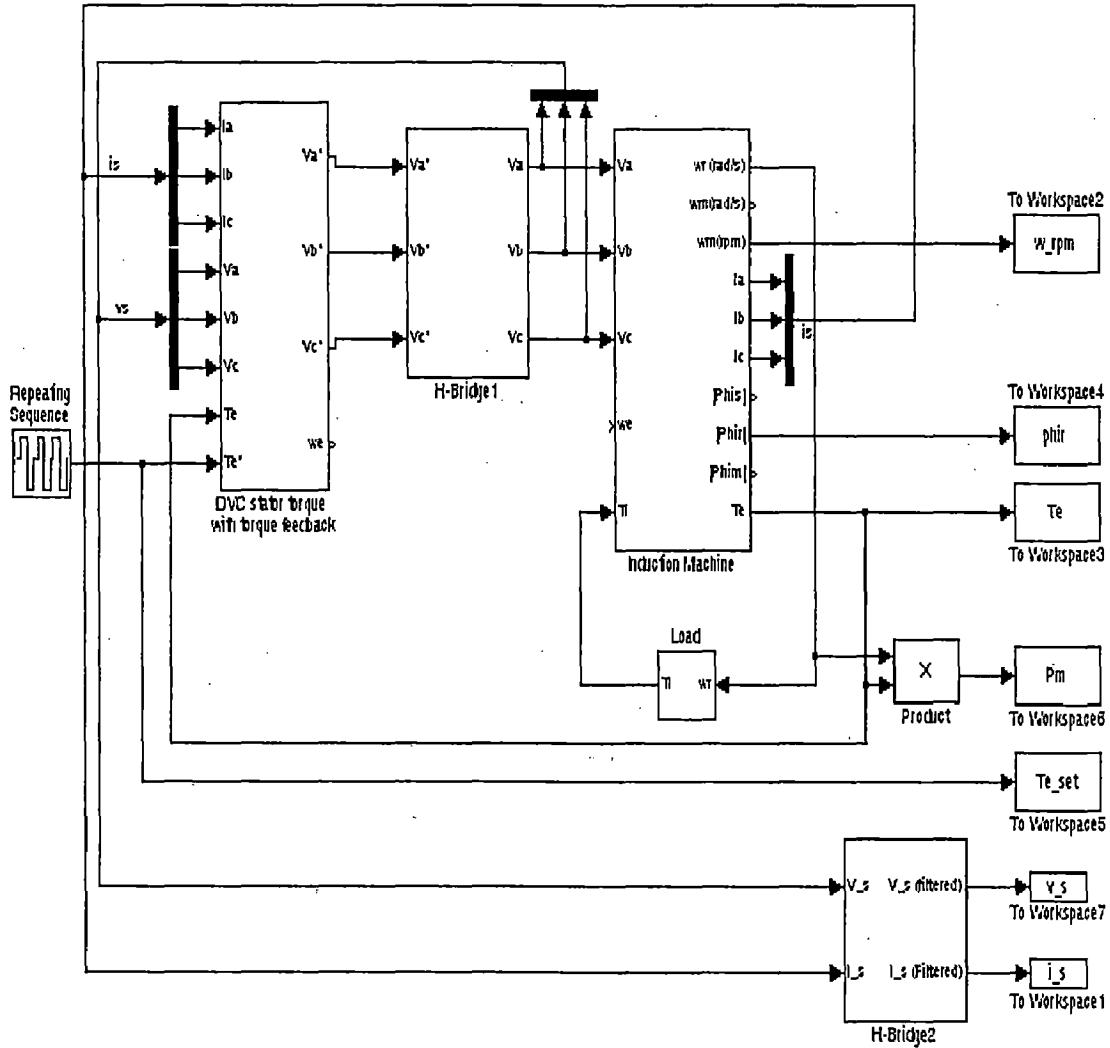
Fig. 7.1: Direct vector control of Induction Machine
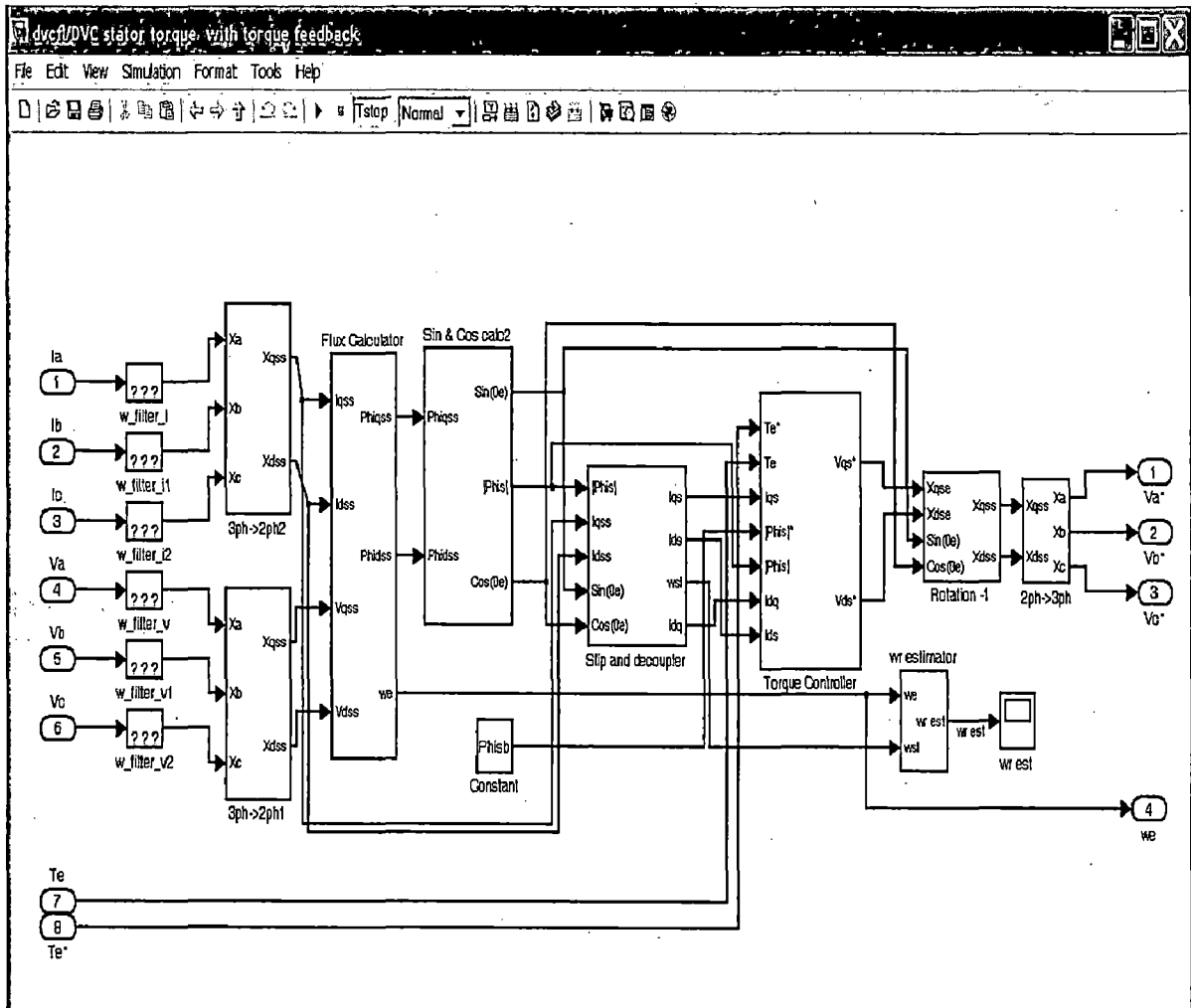
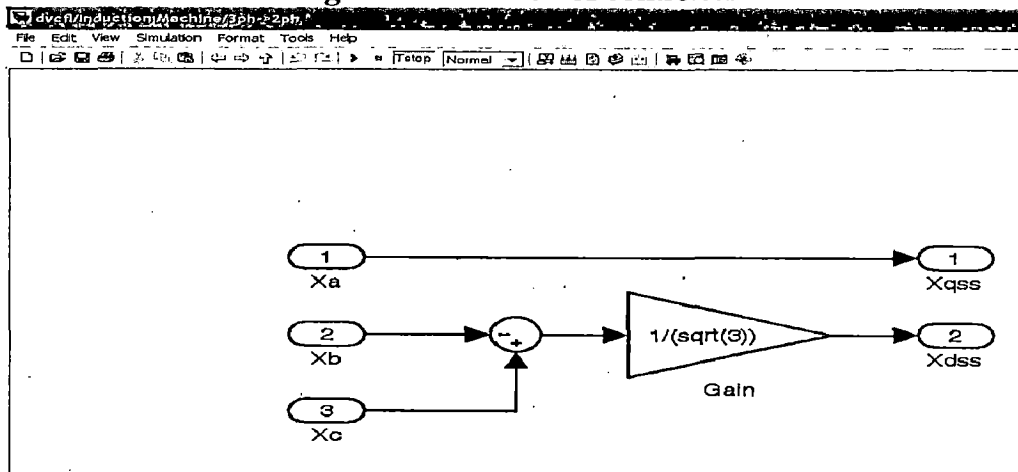**Fig 7.2:** Simulation of controller

Fig 7.3: ABC to Synchronous frame conversion
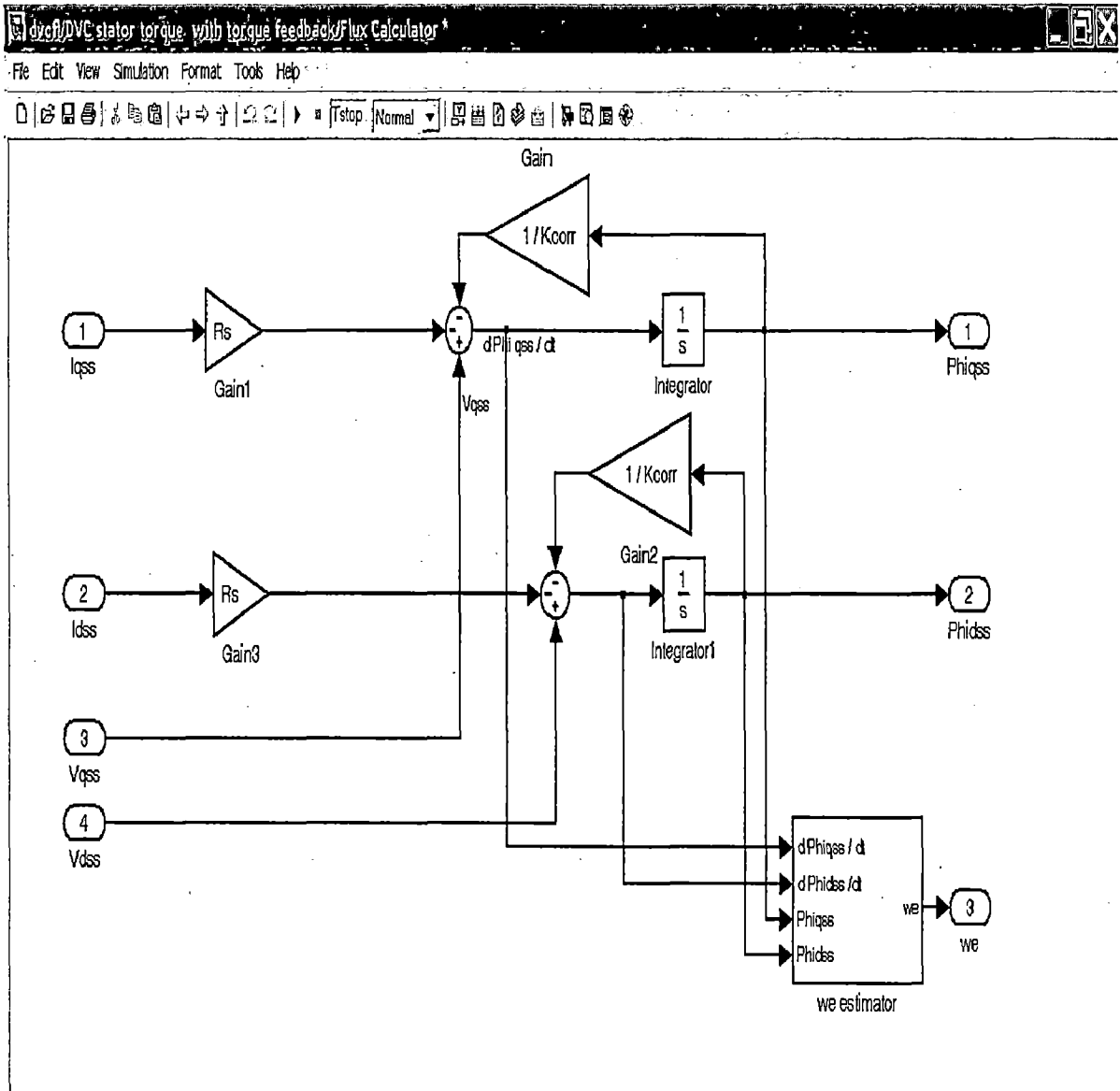
46

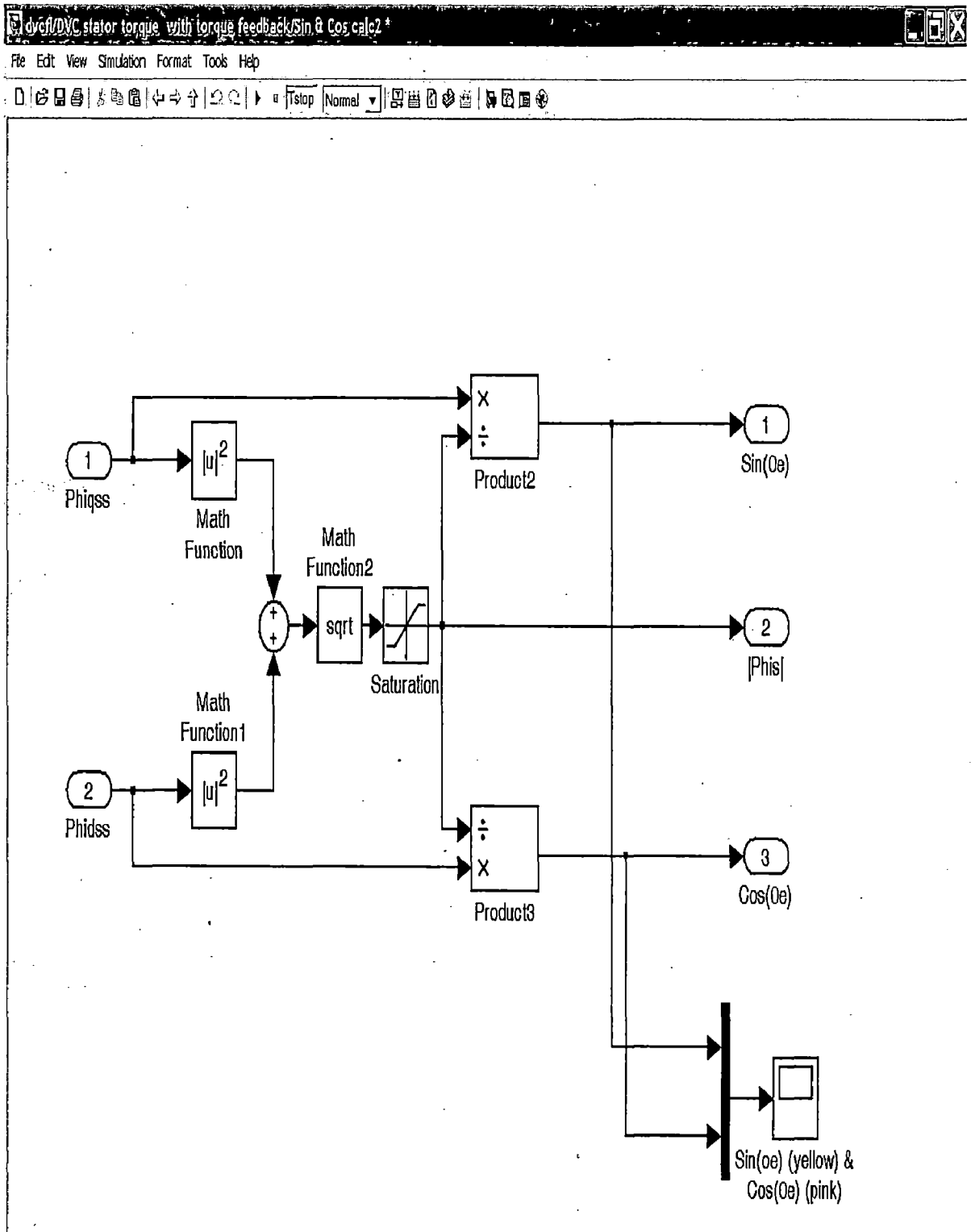**Fig 7.4:** Flux calculator

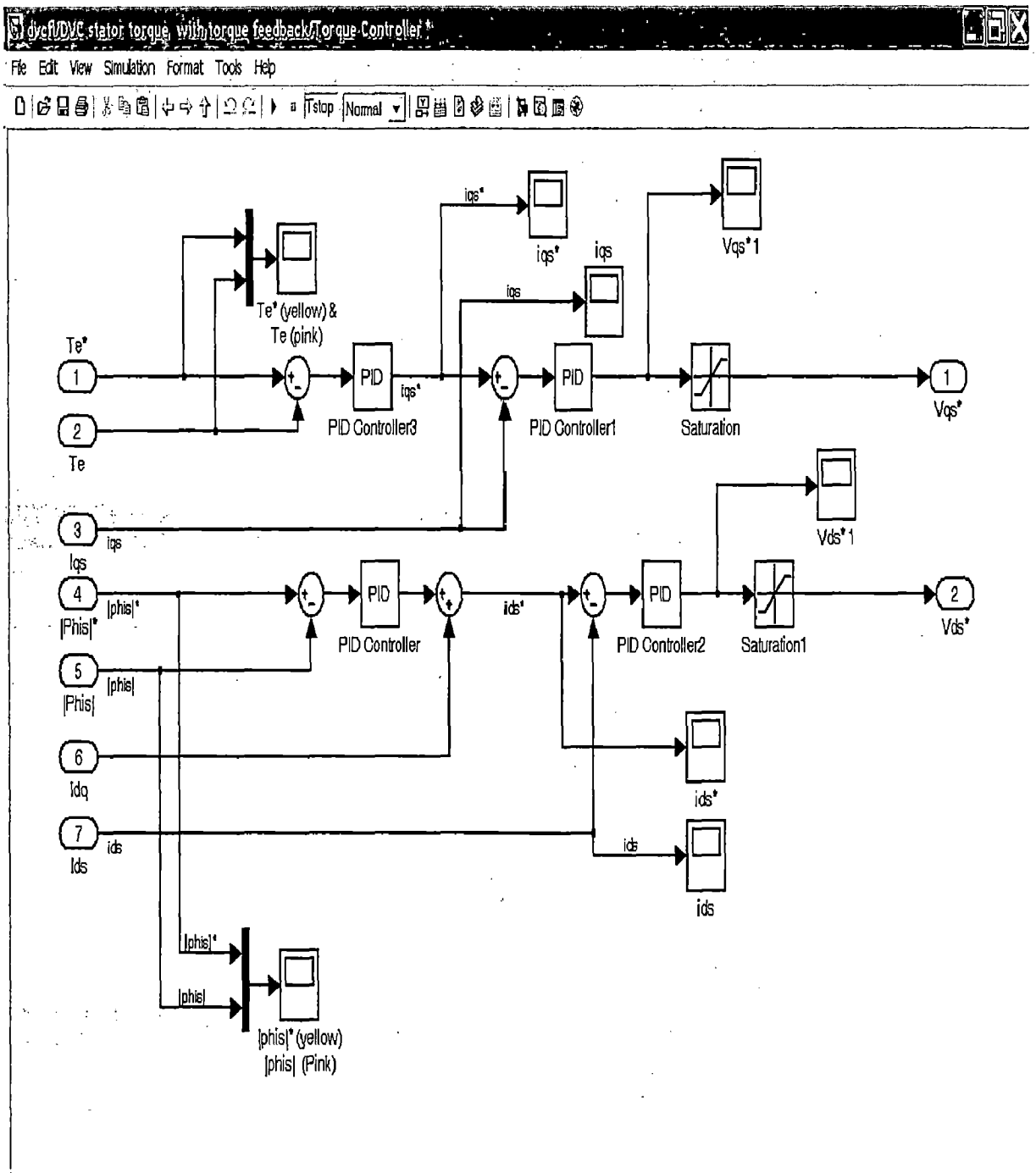**Fig 7.5:** sin and cos calculator

Fig 7.6: Torque controller
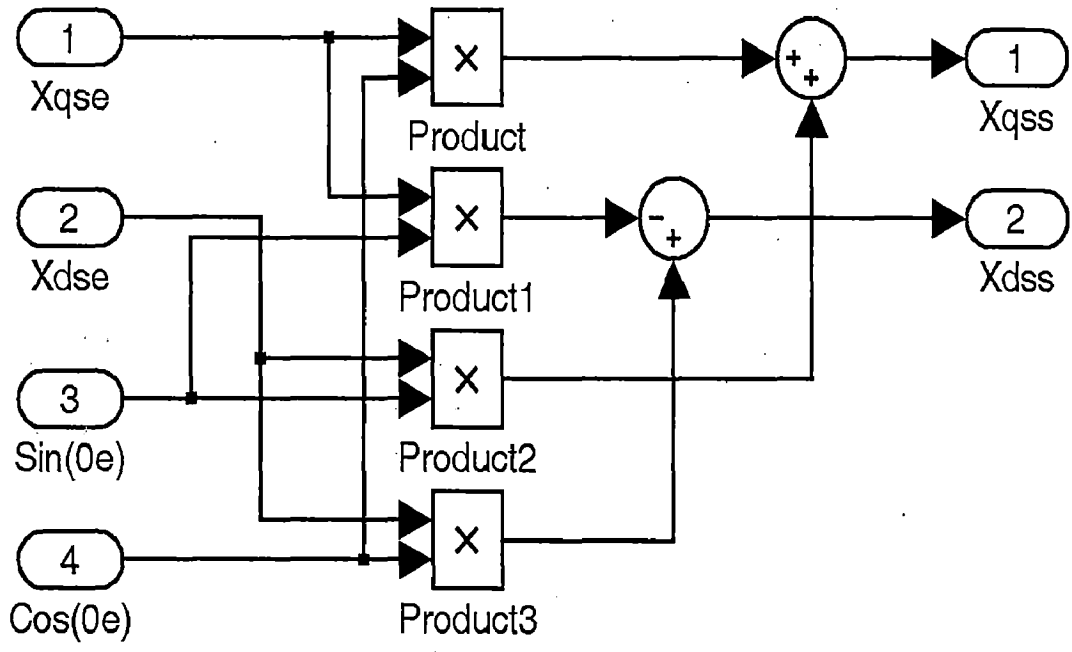
Fig 7.7: Rotation
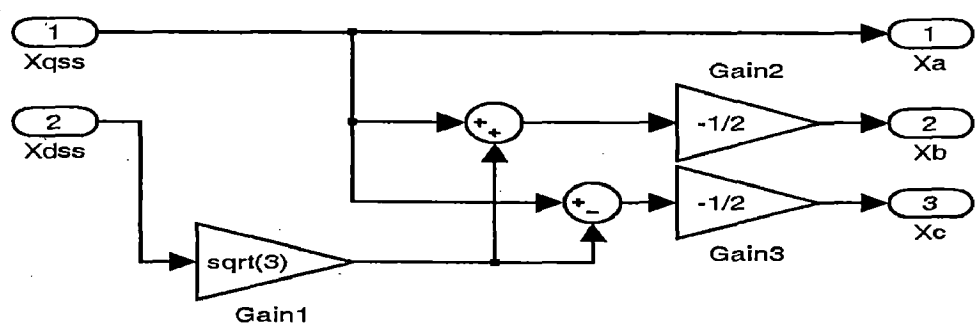
Fig 7.8: synchronous to abc reference frame
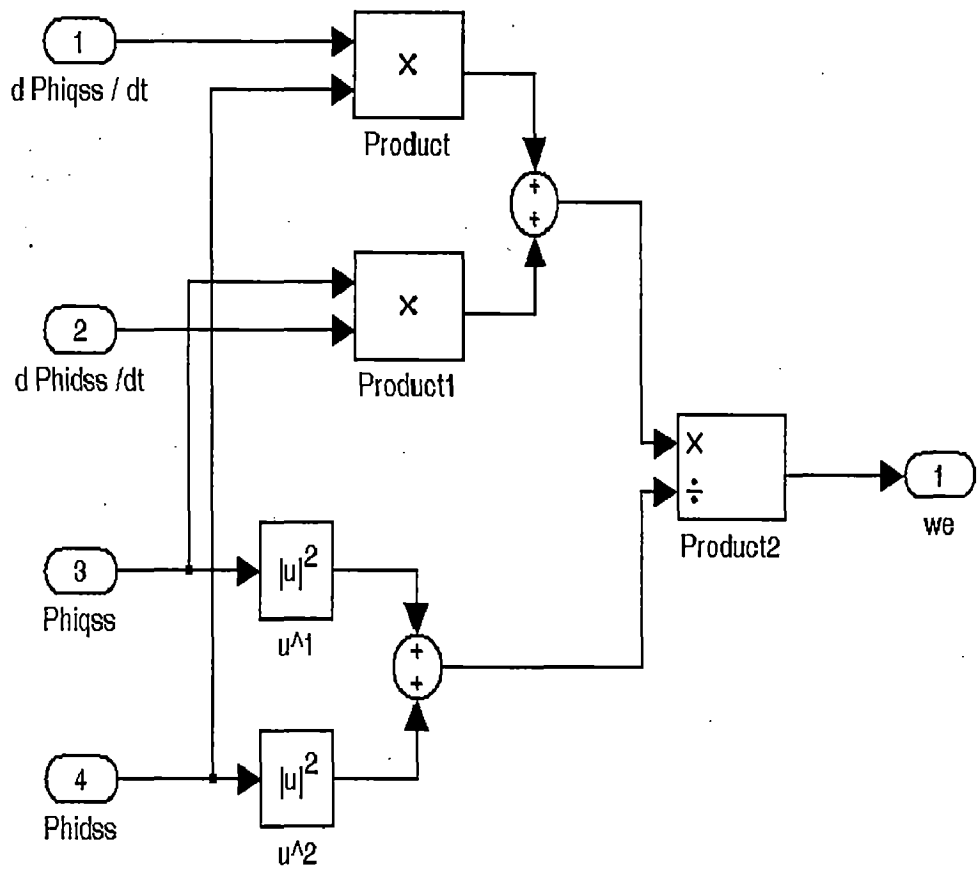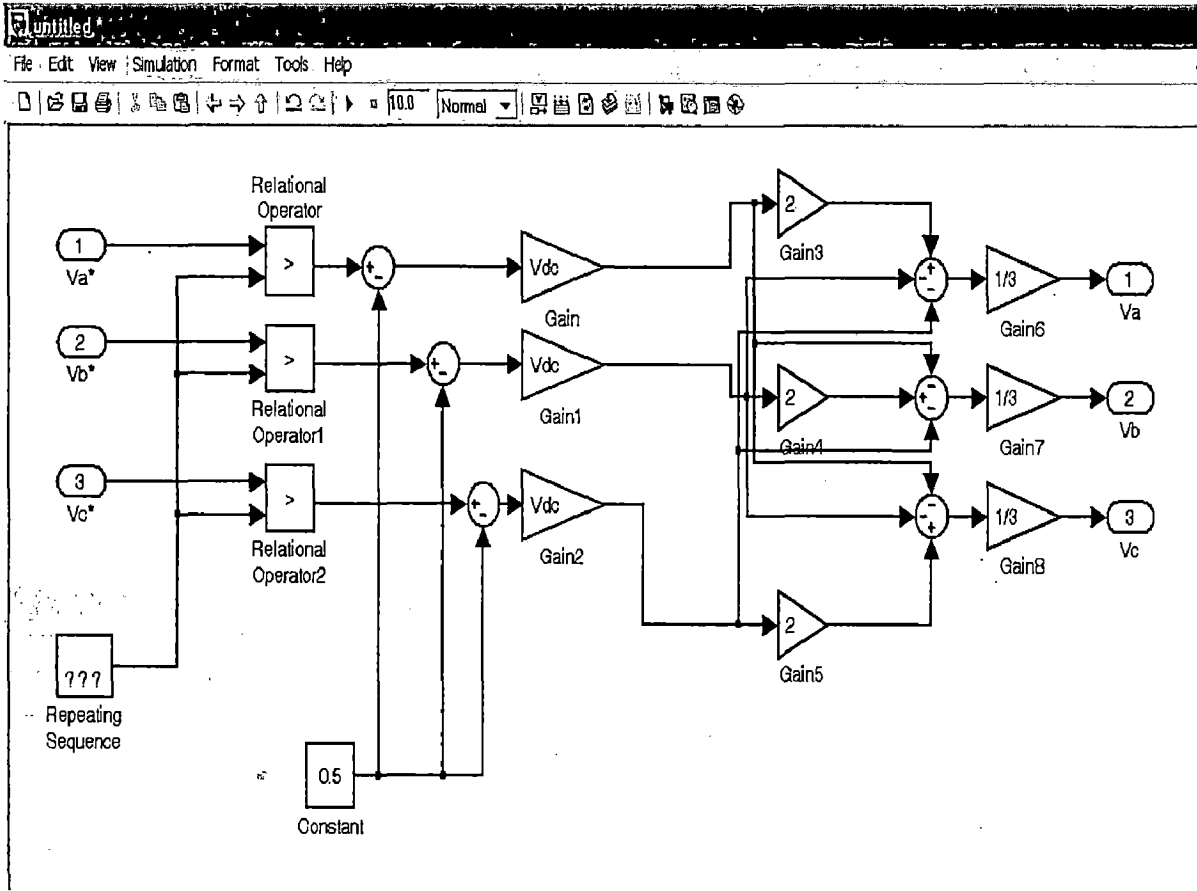
50

Fig 7.9: W_e estimator
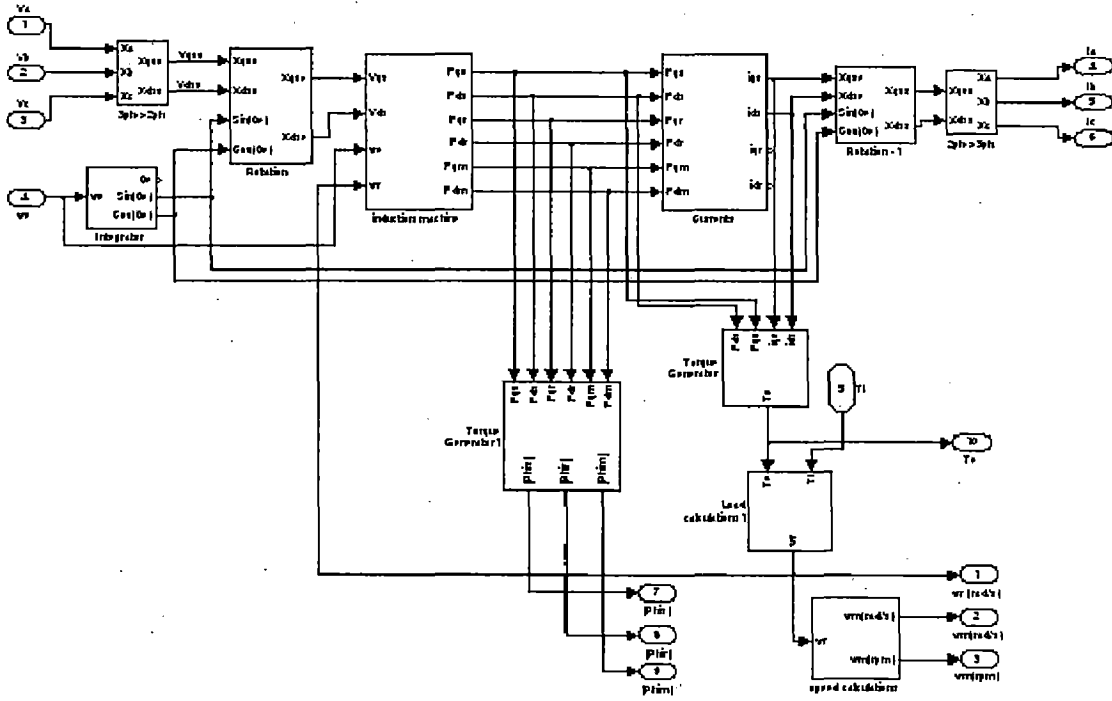
Fig 7.10: H Bridge

Fig 7.11: Induction Machine with rotation
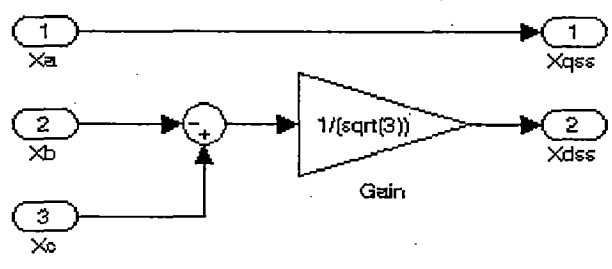
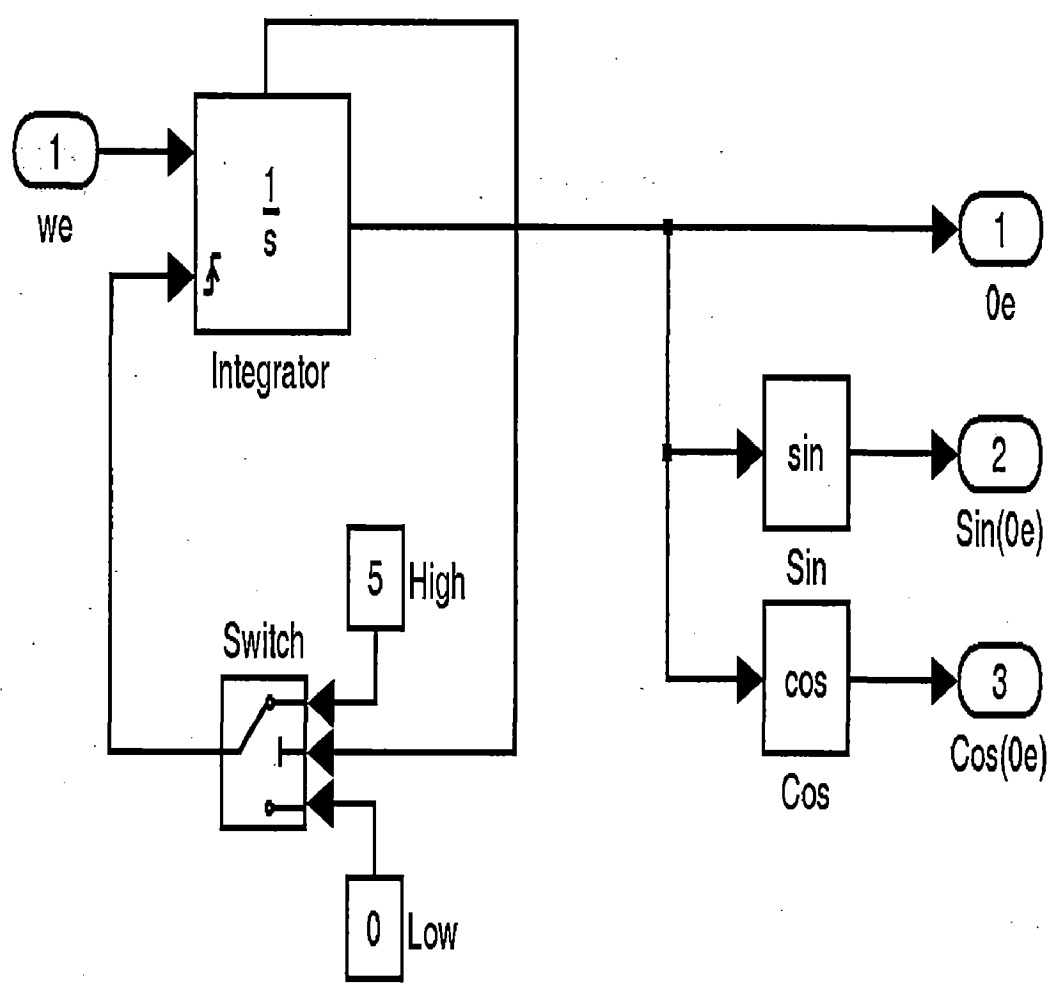

Fig 7.12: 3 to 2 phase conversion
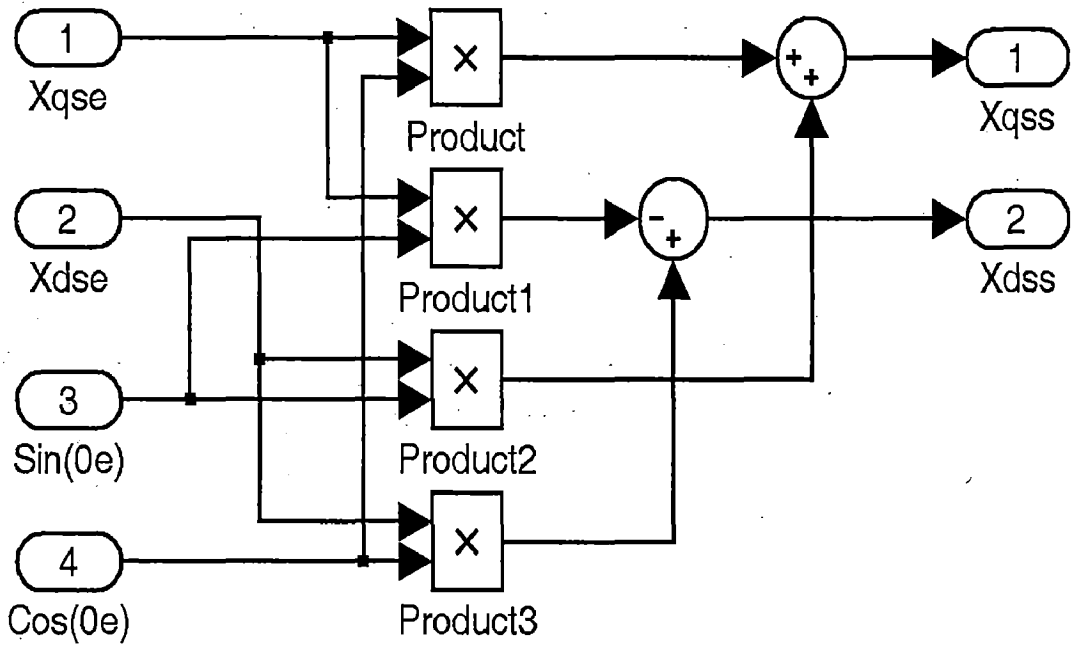
53

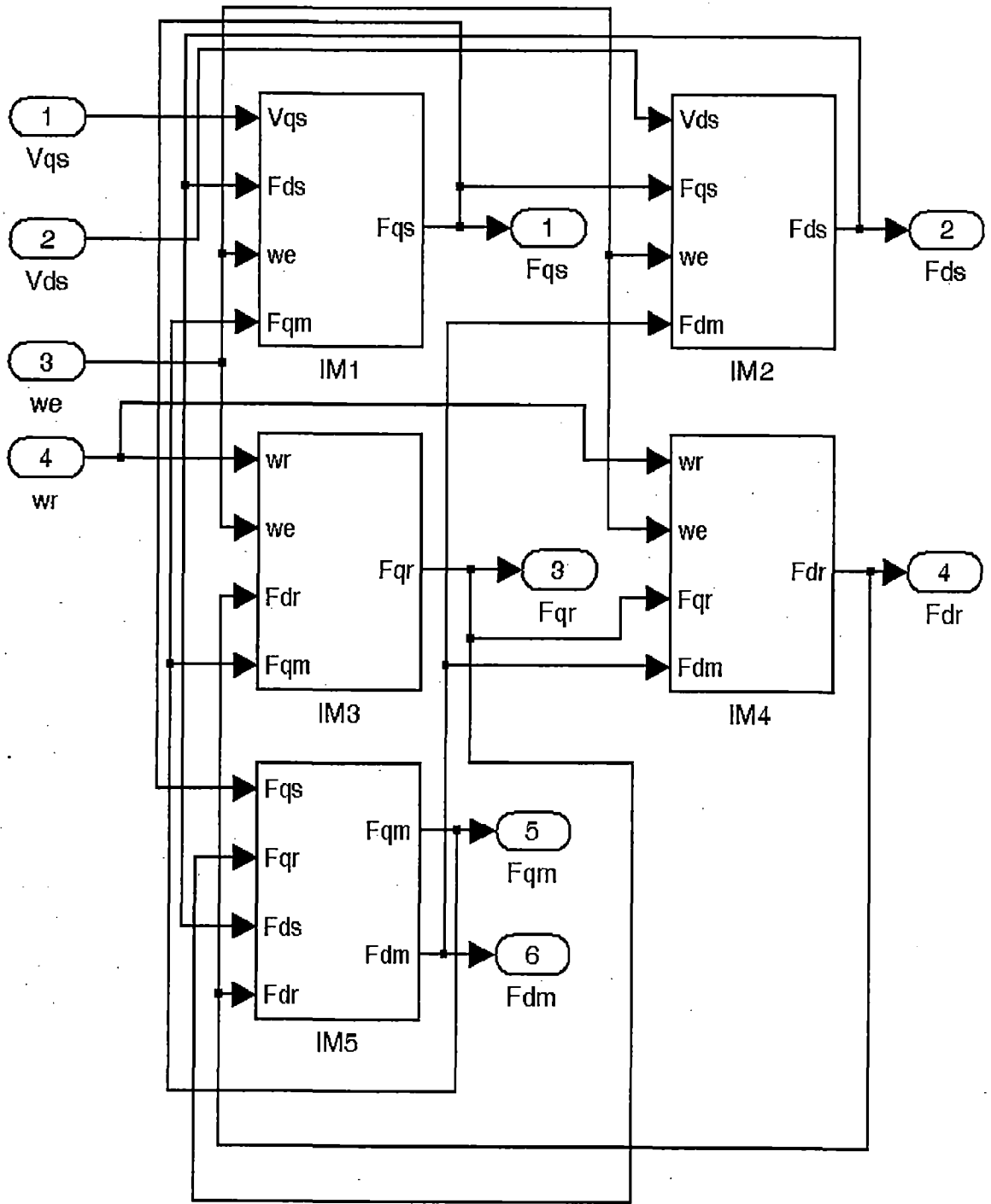**Fig 7.13:** Integrator

Fig 7.14: Rotation

Fig 7.15: Simulation of induction machine

56
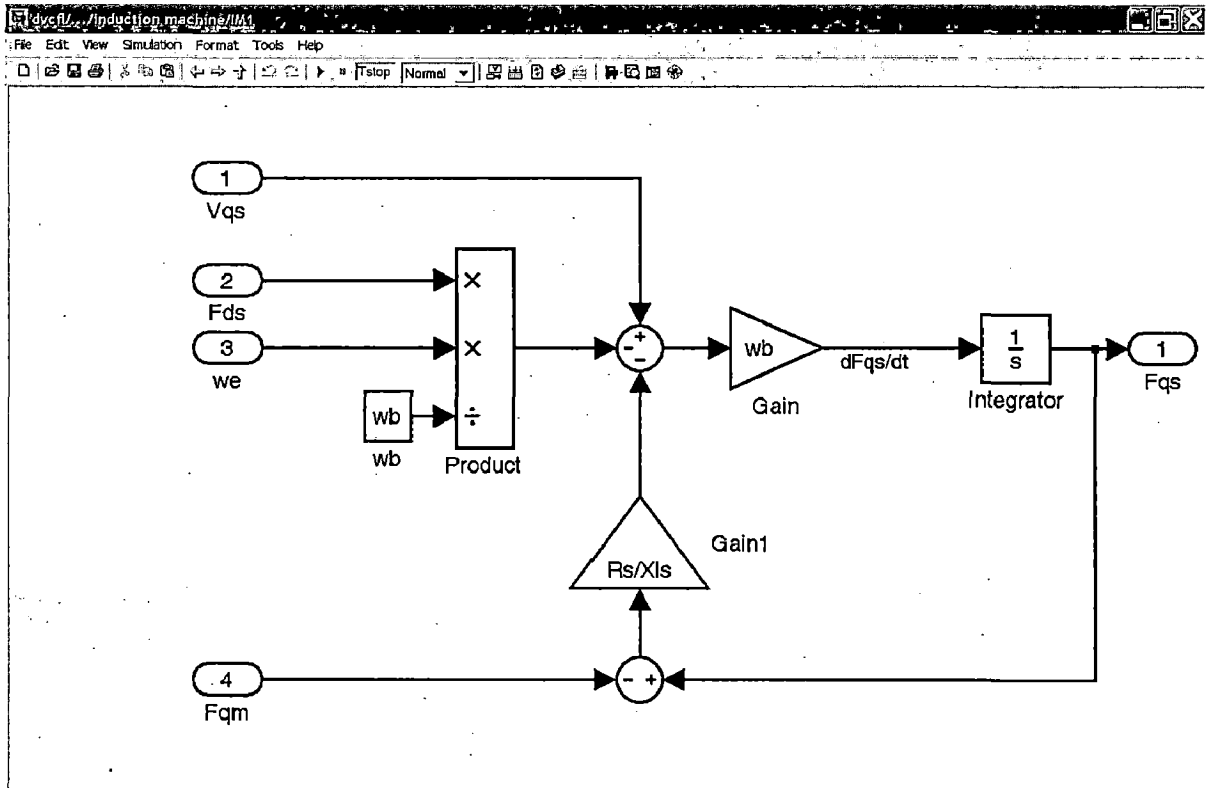
Fig 7.16:   IM1
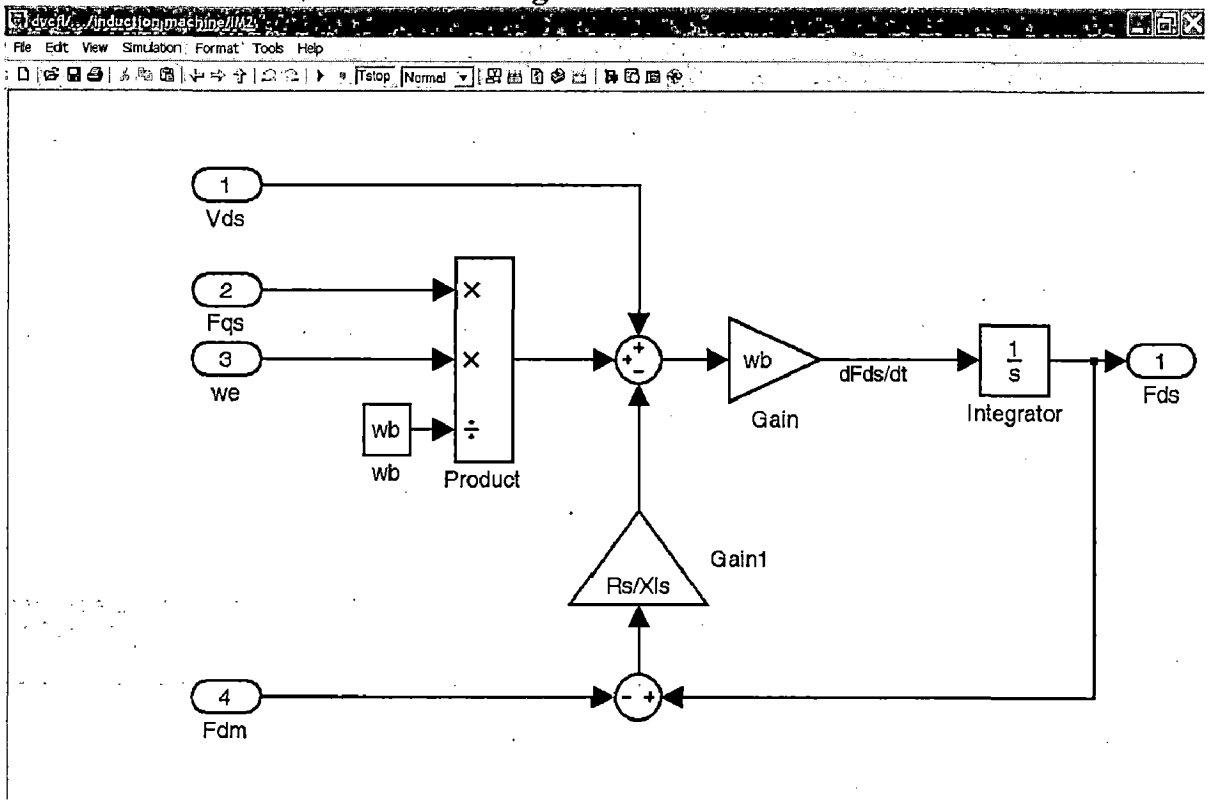
Fig 7.17: IM2
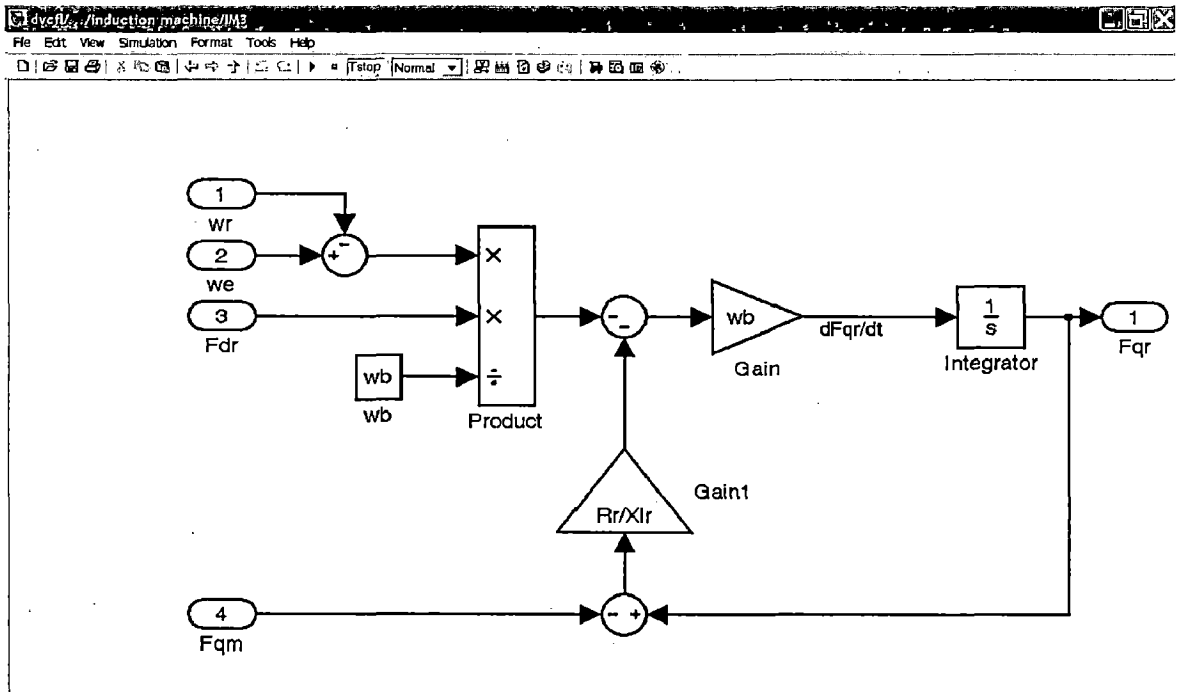
Fig 7.18: IM3

Fig 7.19: IM4

58
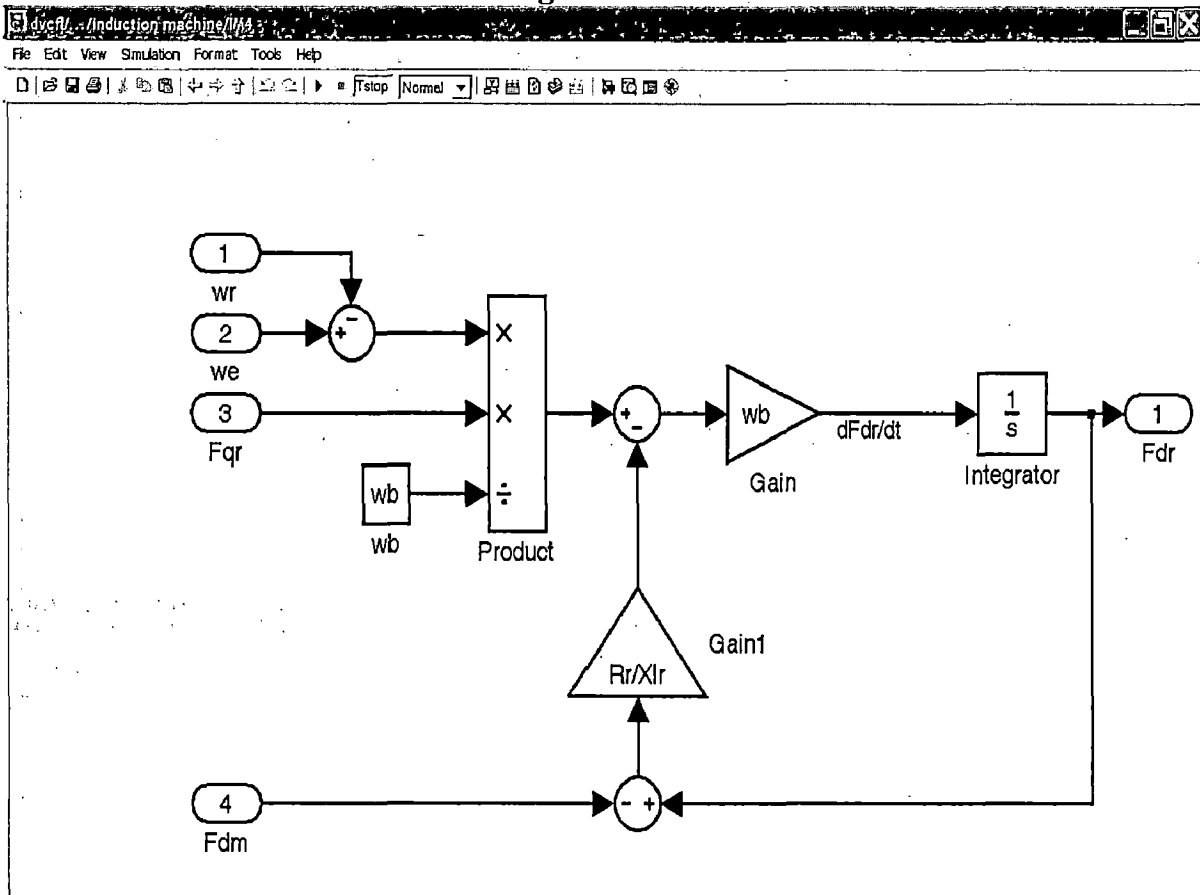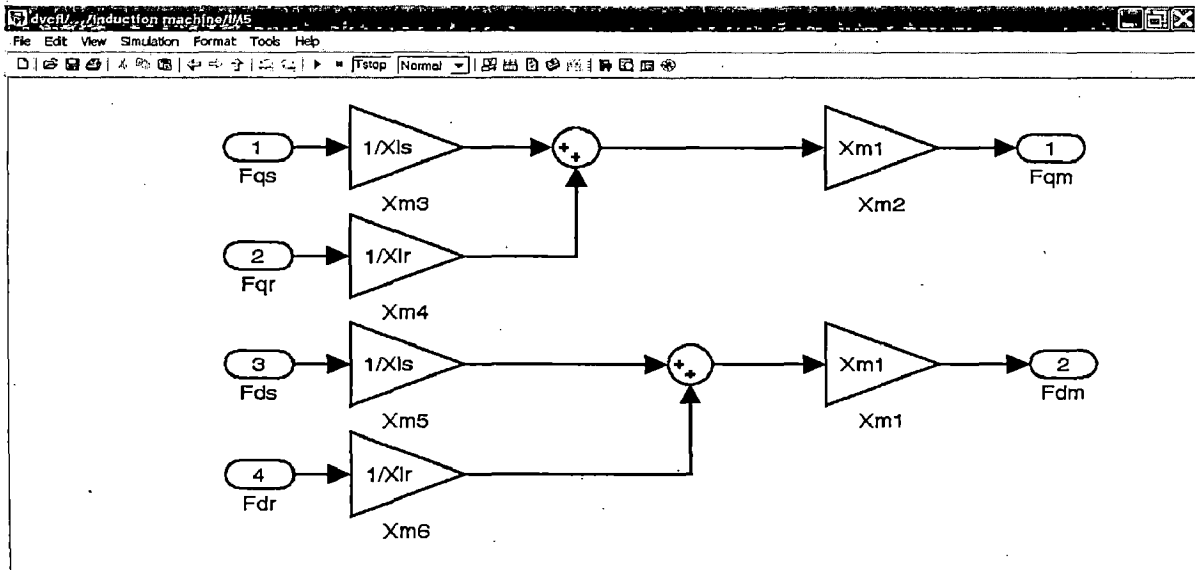
Fig 7.20: IM5

Fig 7.21: Currents

59

Fqs
1

Fds
2

Fqr
3

Fdr
4

Fqm
5

Fdm
6

1/wb
Gain

|u|²
u^2

sqrt
sqrt1

1
|Phis|

sqrt
sqrt2

2
|Phir|

sqrt
sqrt3

3
|Phim|

Fig 7.22: Torque generator

1
wr

Kw
Kw

×
Product

×
Product1

1
TI

Sign
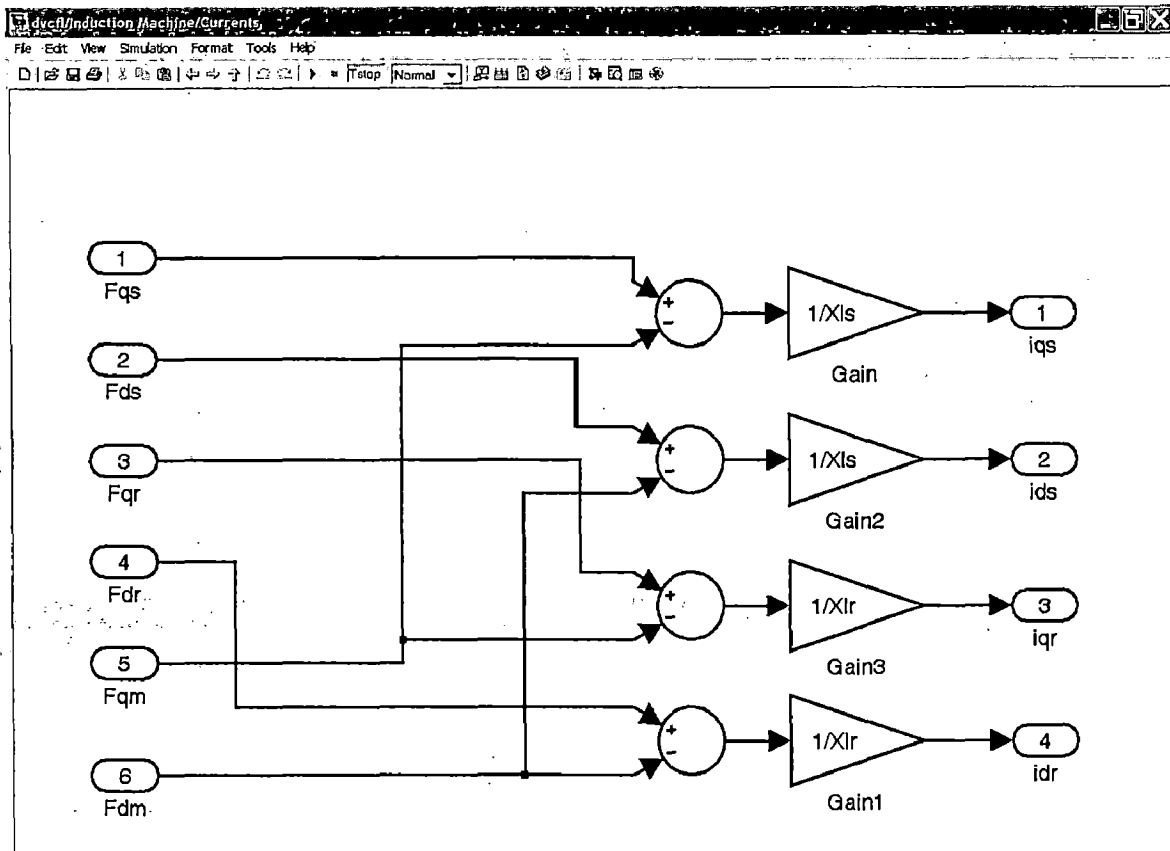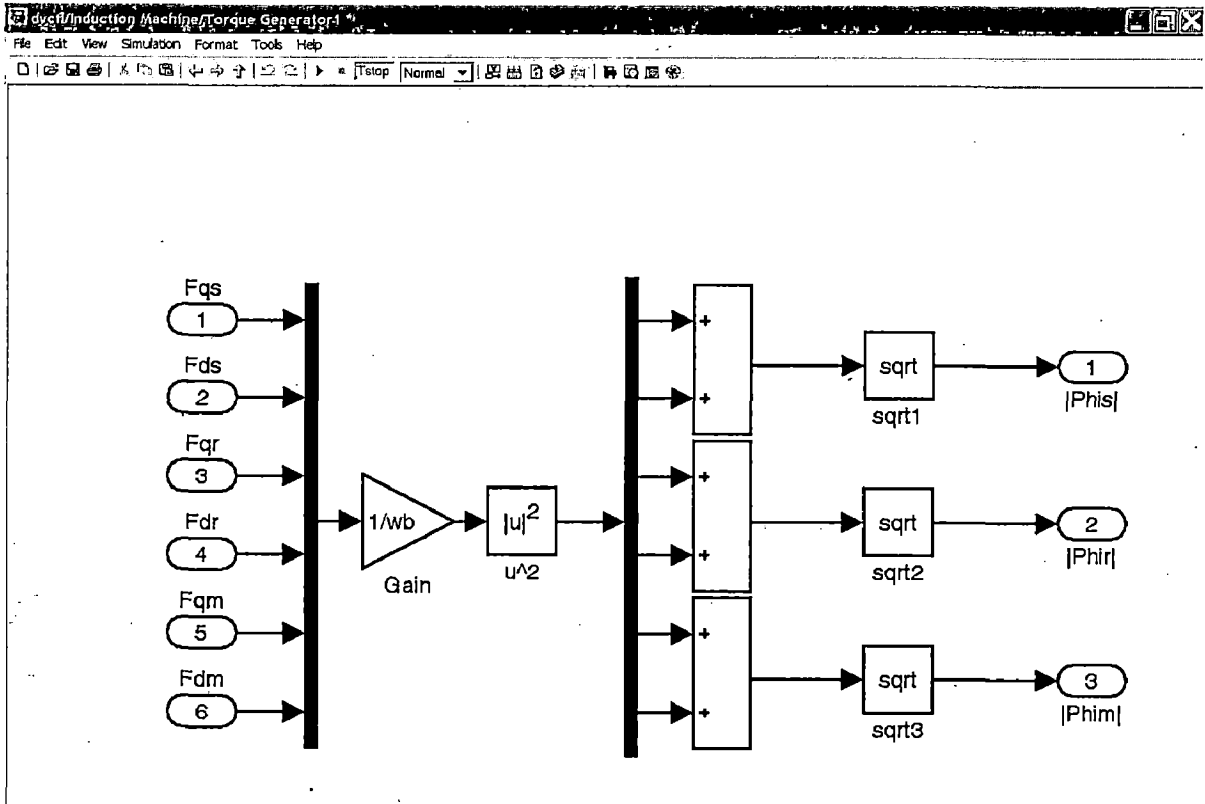
Fig 7.23: load
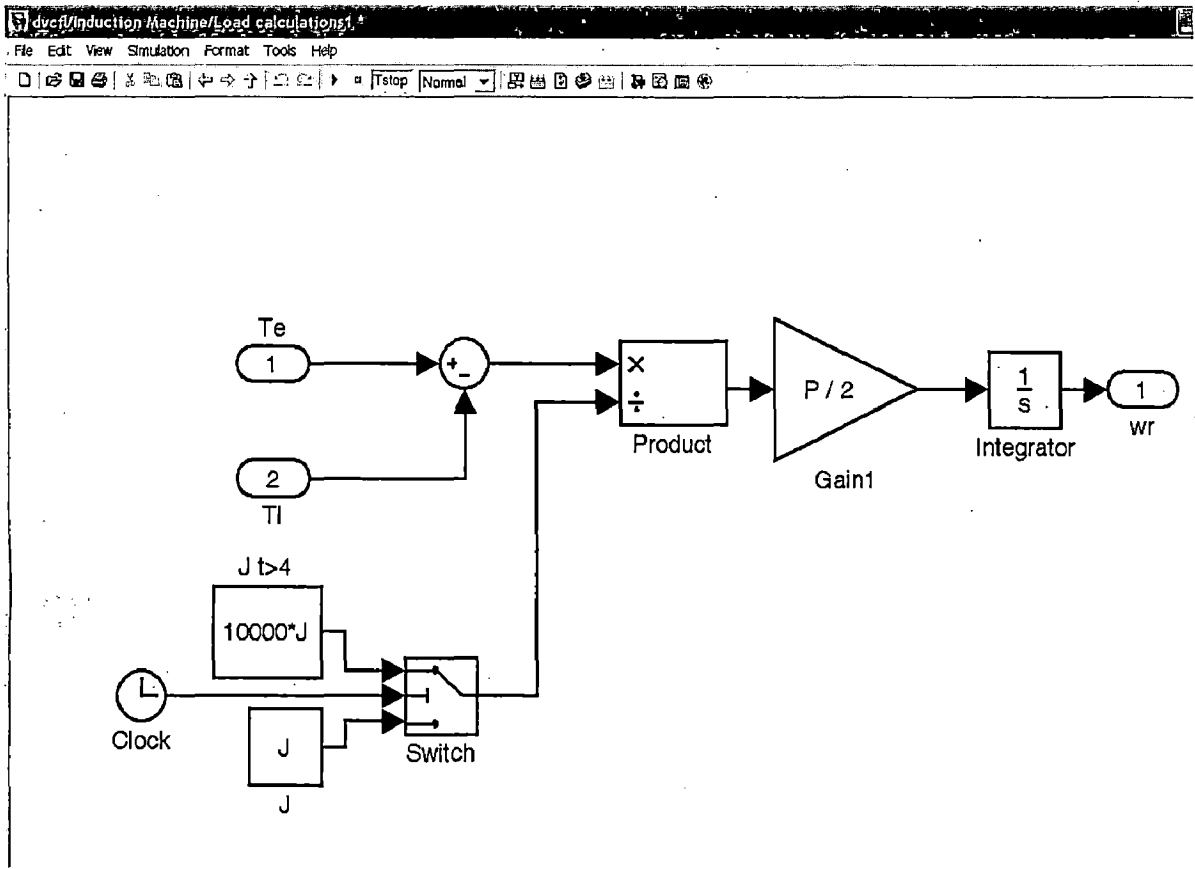
Fig 7.24: Load calculation

Fig 7.25: Speed controller

61

Fig 7.26: Rotation
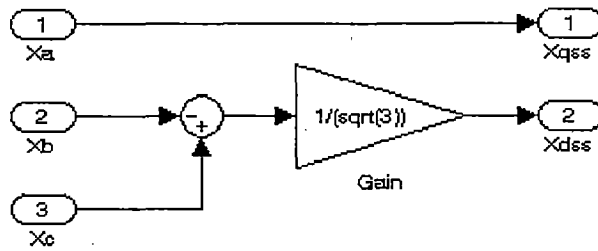
Fig 7.27: Synchronous to ABC frame conversion

RESULT AND CONCLUSION

8.1 INTRODUCTION

Many important and interesting aspects of an isolated stand-alone induction generator have been discussed and presented in this Dissertation. The study comprises theoretical analysis, simulation results related to induction generators. The modelling and characteristics of induction machines in general has also been presented to provide an overall perspective of induction generators. For an isolated induction generator the maximum power available in the wind and hydro power might not be utilised by a constant electrical load connected to the induction generator. If an isolated stand-alone induction generator is supplying a constant load then the operating points of the output power and output torque of the wind turbine will be adjusted as per the operati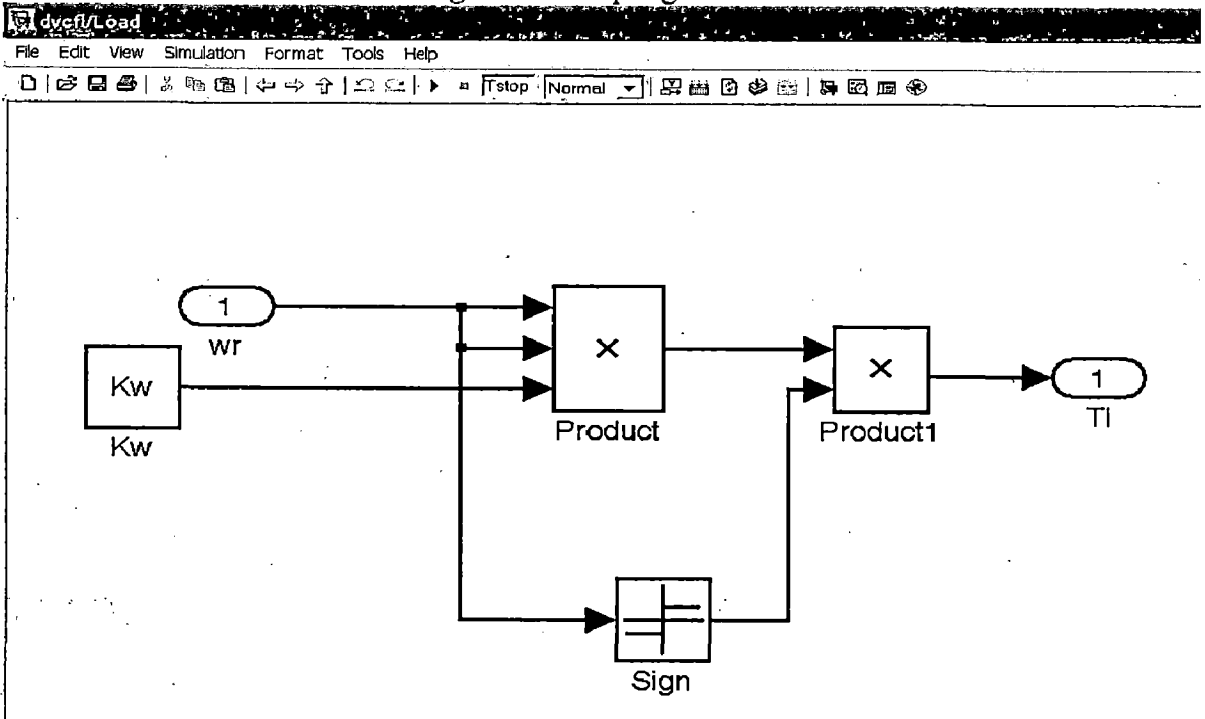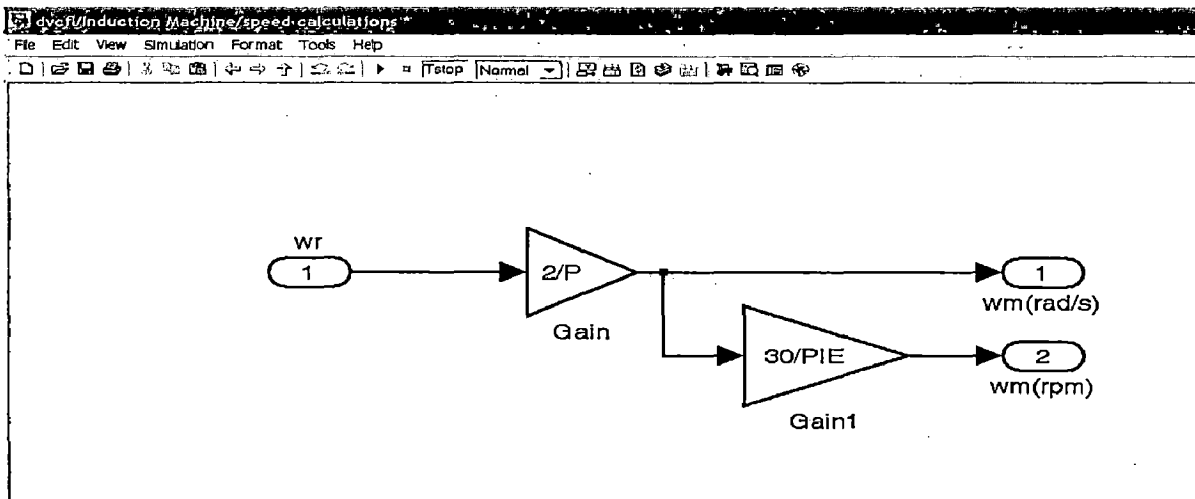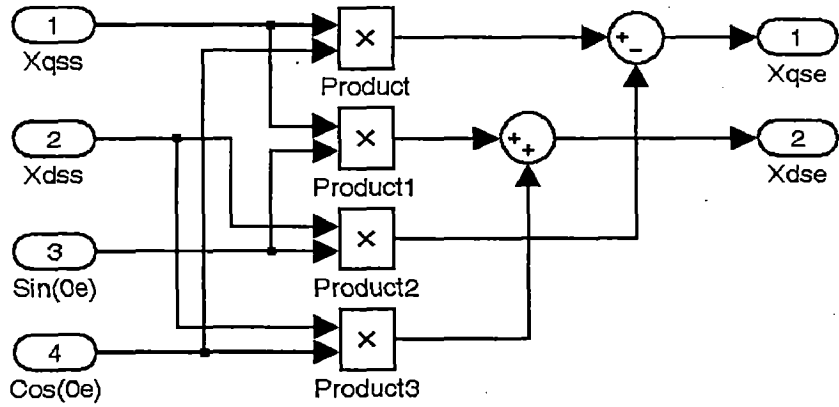on of the induction generator The literature related to isolated induction generators is reviewed in Chapter 2. This has involved clarifying the strengths and limitations of the previous works and highlighted the advantages of the research covered in this Dissertation. The three-axes to two-axes transformation presented in Chapter 5 is applicable for any balanced three-phase system. It has been discussed that the three-axes to two-axes transformation simplifies the calculation of rms current, rms voltage, active power and power factor in a three-phase system.

Only one set of measurements taken at a single instant of time is required when using the method described to obtain rms current, rms voltage, active power and power factor. Furthermore from measurements taken at two consecutive instants in time the frequency of the three-phase AC power supply can be evaluated. For the same stator terminal voltage of an induction machine the magnitude of the electromagnetic torque in the generating region is higher than the electromagnetic torque in the motoring region. The reason for the difference in electromagnetic torques is that during motoring all the electrical losses in the induction machine are supplied by an external electrical power source and the electromagnetic torque is the output of the system. However, in the generating region the electromagnetic torque is equivalent to the external mechanical input torque and all the electrical power losses in the induction machine are indirectly

supplied by the external mechanical power source and the terminal voltage is the output of the system. Hence to overcome all the internal power losses in the induction machine and have the same terminal voltage. In direct control with stator flux, both of the DVC stator models get the electrical speed directly from the currents and voltages in the machine. The controller imposes the restraint that the stator flux in the machine is aligned with the ds-axis. Since the torque produced by the machine is proportional to the current I_{qs}, this current is used to control the torque development by the machine. This is the best controller in terms of response, especially considering that there is no feedback from the torque being developed by the machine. As can be seen from the figures, from time 0 s to 6 s, the machine is in motoring mode, and from 6 s to 10, the motor is generating power due to a positive speed and a negative torque.

The feedback model assumes that there is a torque sensor on the shaft and therefore the I_{qs} is based on the difference between the reference torque and the actual torque, commanded through a PI controller. Adding this feedback does not make the controller act that much better, as the model without the feedback is very good at following the reference torque. Fig 8.1 shows Torque response for direct vector control. Fig 8.2 shows dc voltage response. Fig 8.3 shows reference voltage. Fig 8.4 shows i_{ds}* response. Fig. 8.5 shows f_{qs} response. Fig 8.6 f_{qs}* response. Fig 8.7 shows phis* (blue) and phis (green). Fig 8.8 W_e est speed response. Fig. 8.9 shows step response. Fig 8.10 shows i_{ds} response.

Suggestion for future work

Some of the topics recommended for future work are:

(i.)   Implementation of vector control to regulate the output voltage and frequency of an isolated stand-alone induction generator and compare with the simulation results.

(ii.)   Implementation of the vector control technique for an isolated induction generator with variable rotor parameters. As the contribution of rotor leakage inductance is small compared to the total rotor inductance the focus is mainly in the updating of the rotor resistance variation. This variation in rotor resistance can also be explored and extended to include variation of rotor resistance due to the operating temperature of the rotor conductors.
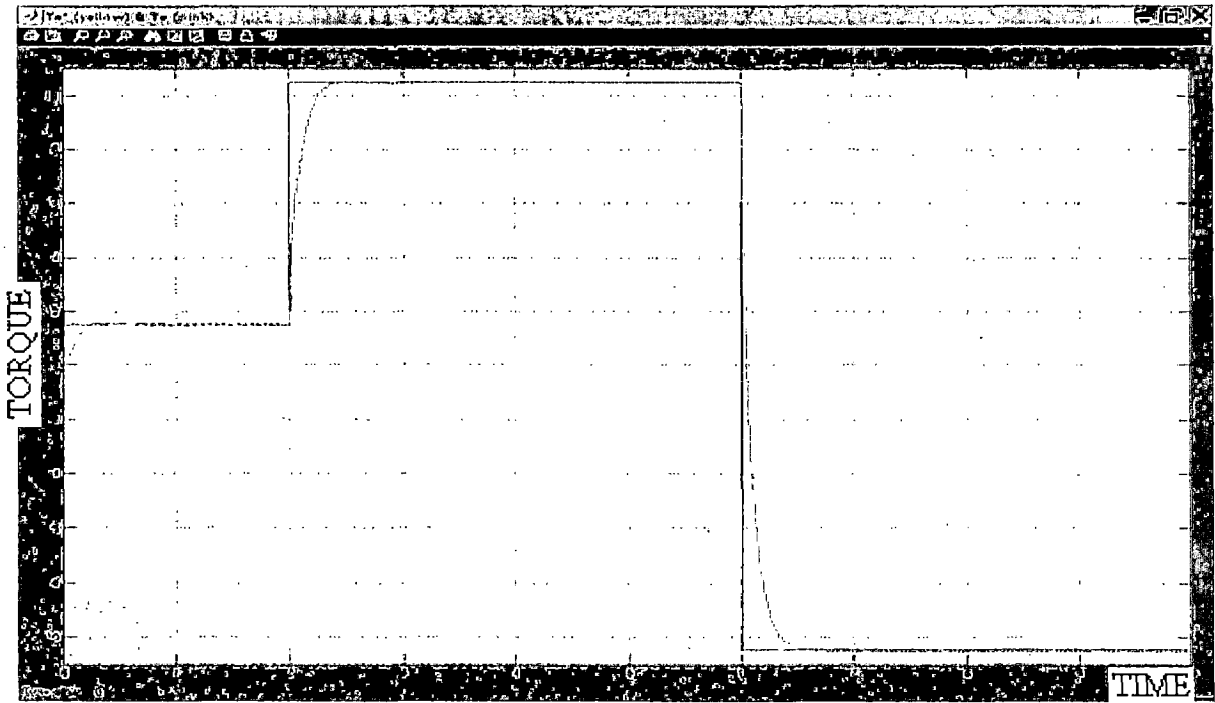
Fig 8.1: Torque response for direct vector control
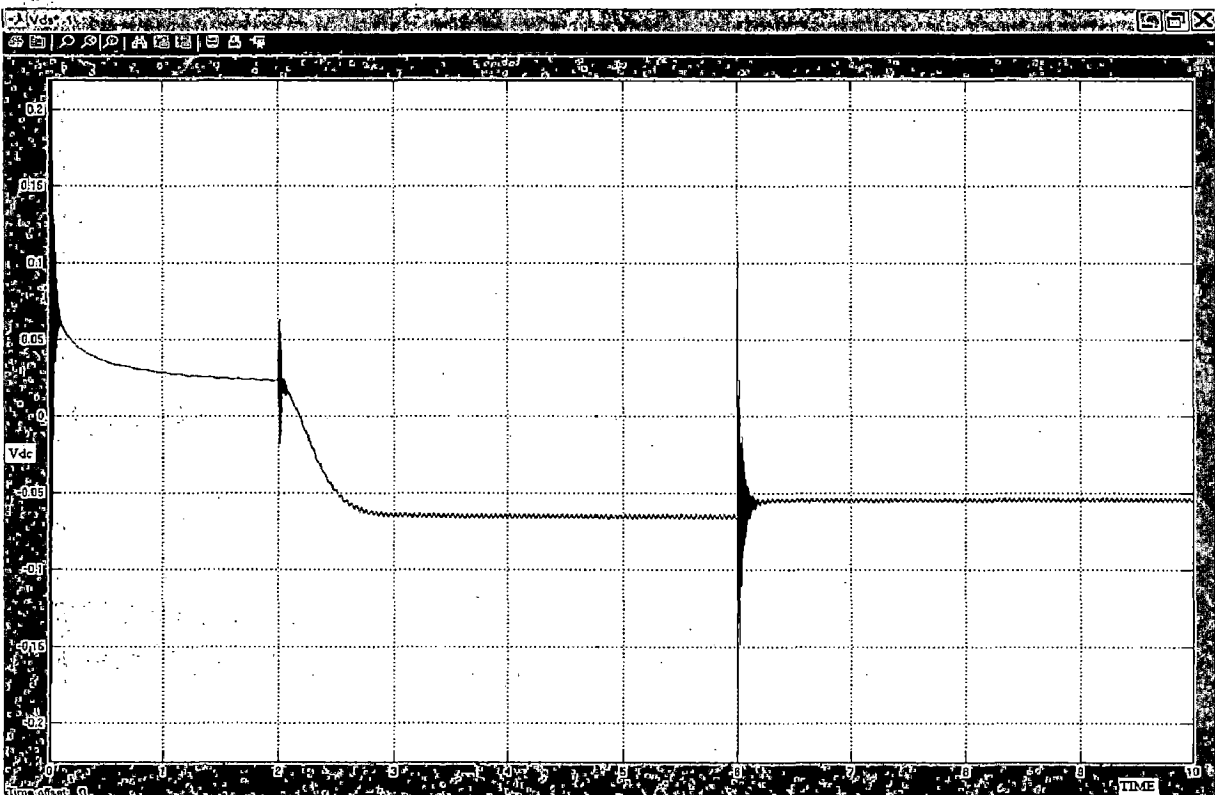
Fig 8.2: V_{dc} response

65
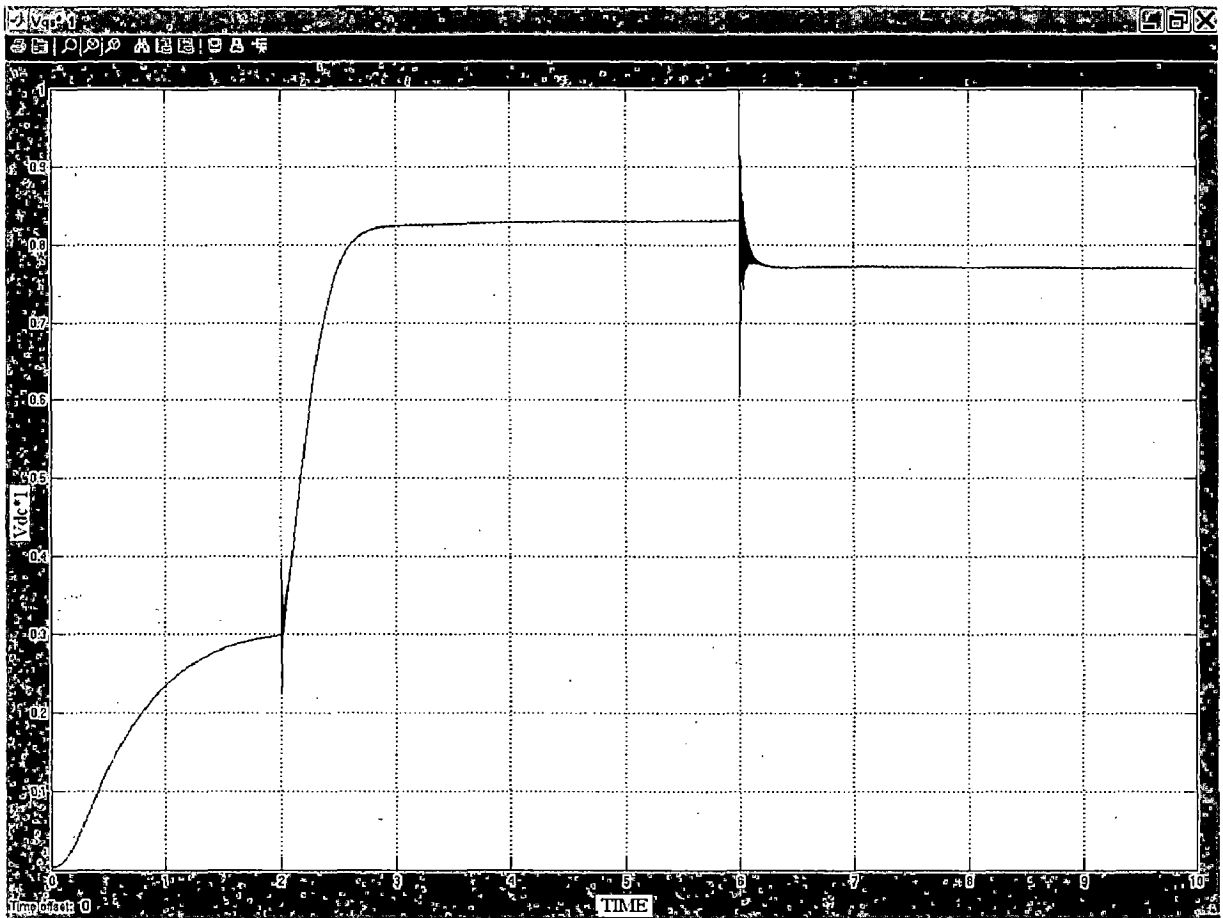
Fig 8.3: Vdc*1 response
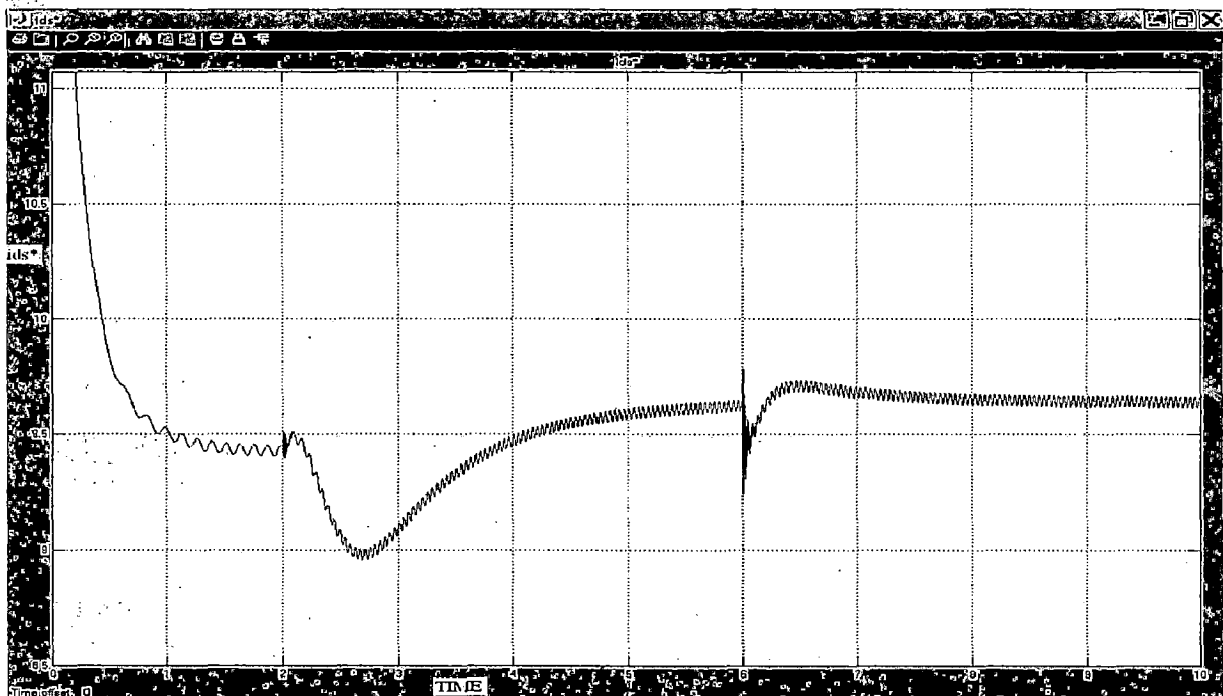
Fig 8.4: i_{ds}* response

66
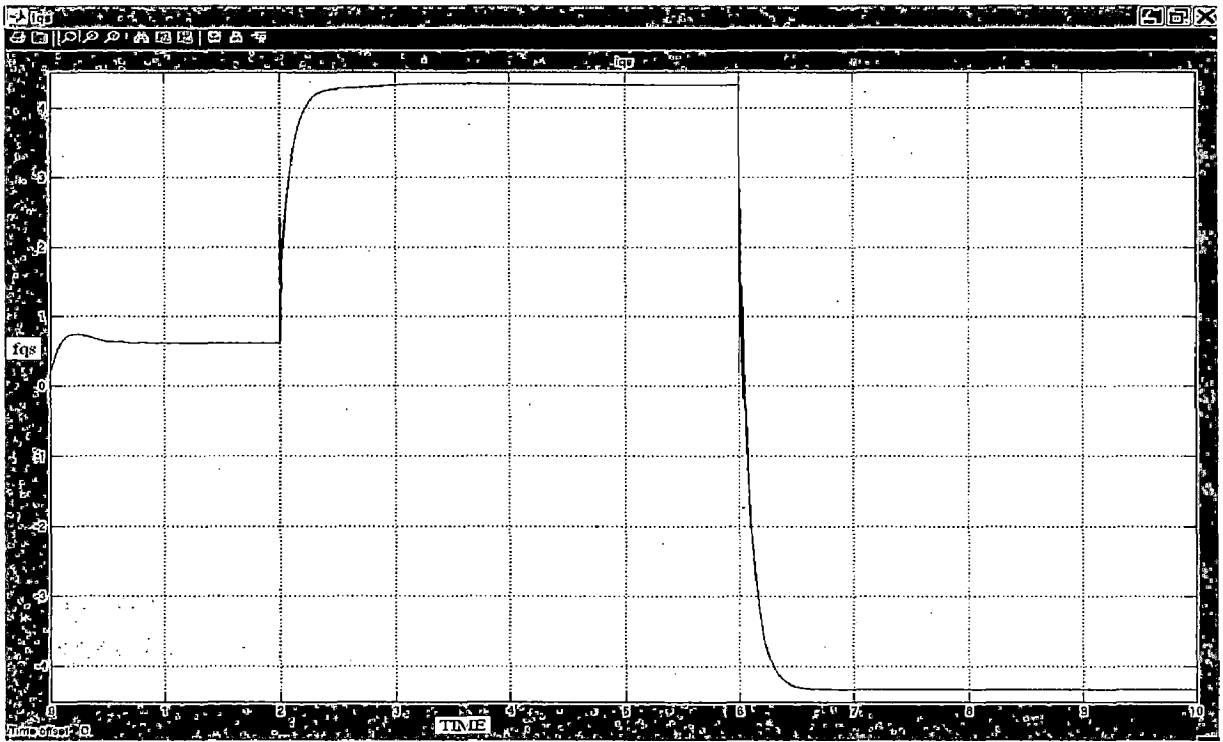
Fig 8.5: f_{qs} response

Fig 8.6: $f_{qs}*$ response

67
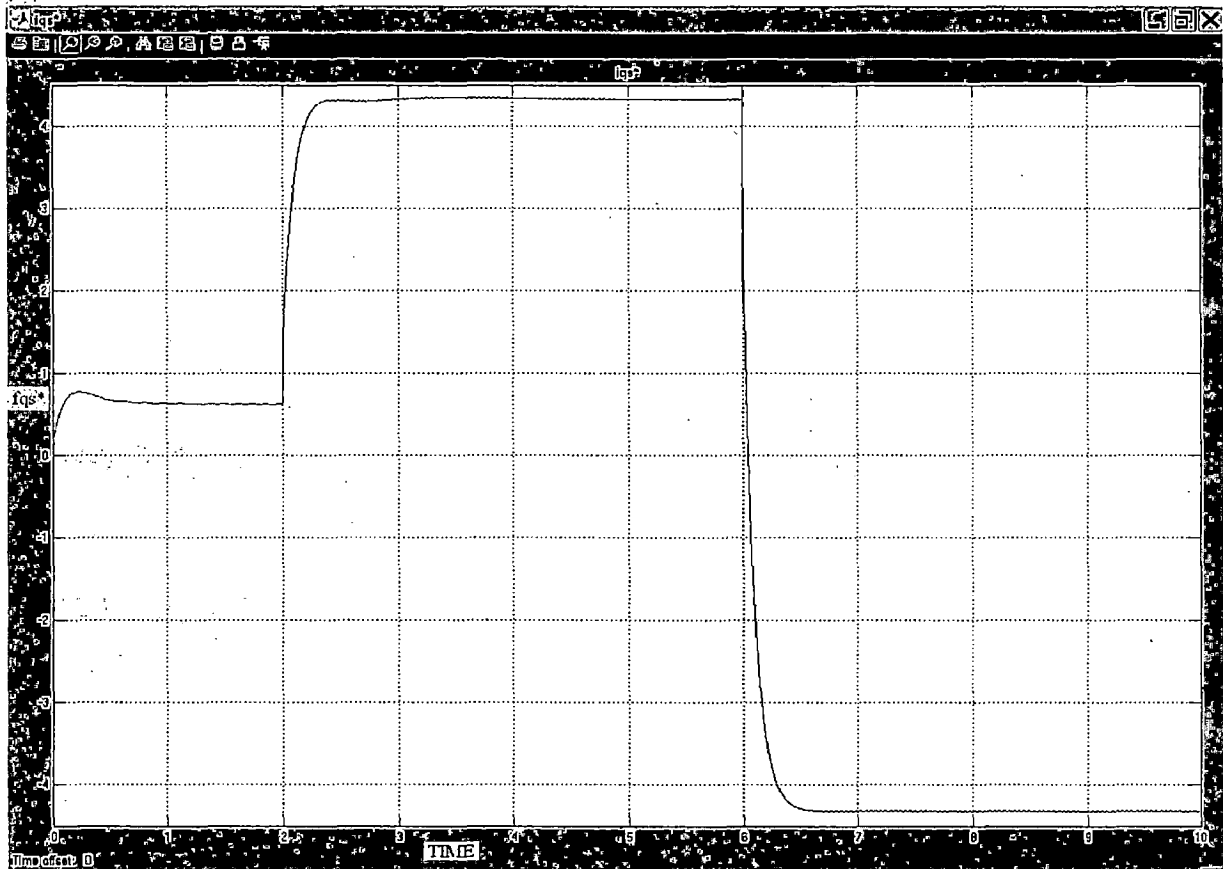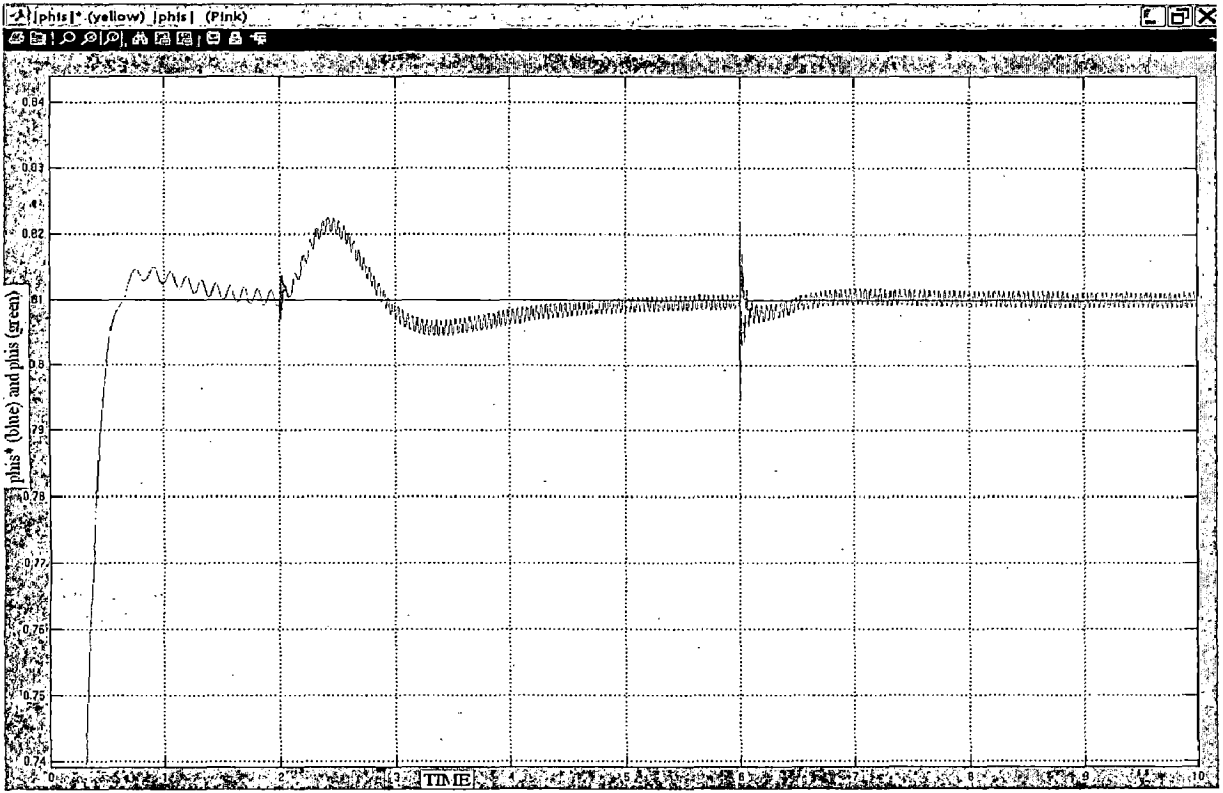
Fig 8.7: phis* (blue) and phis (green)

Fig 8.8: W$_e$ est

68
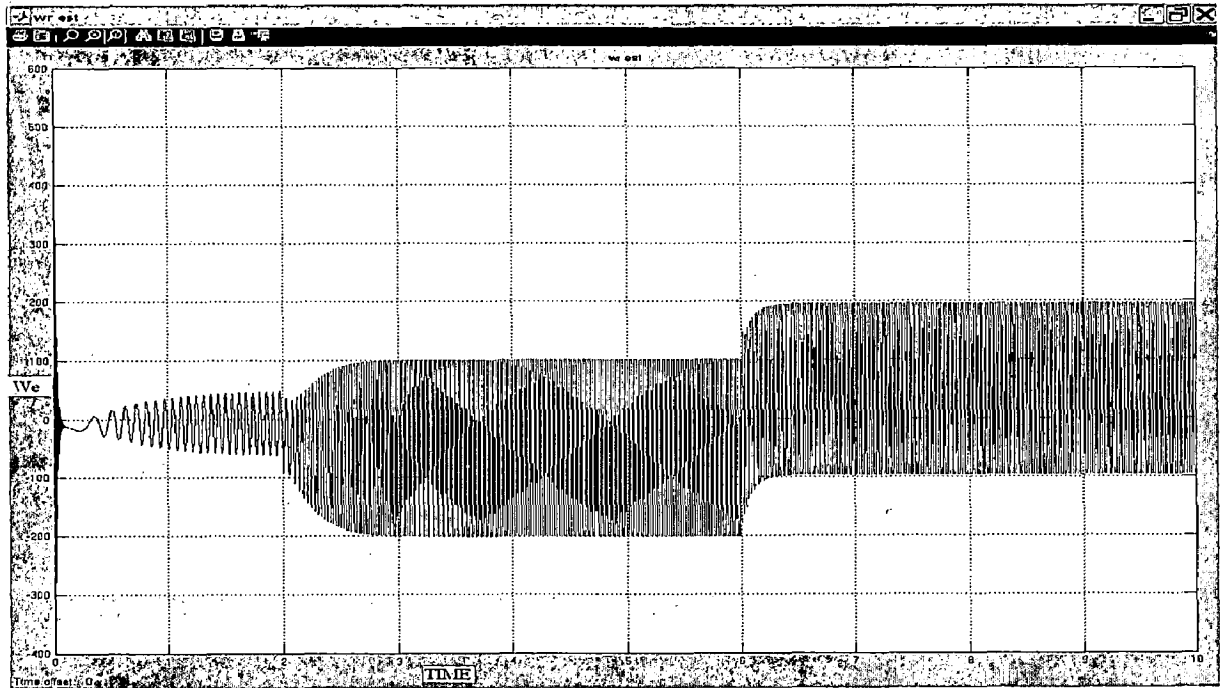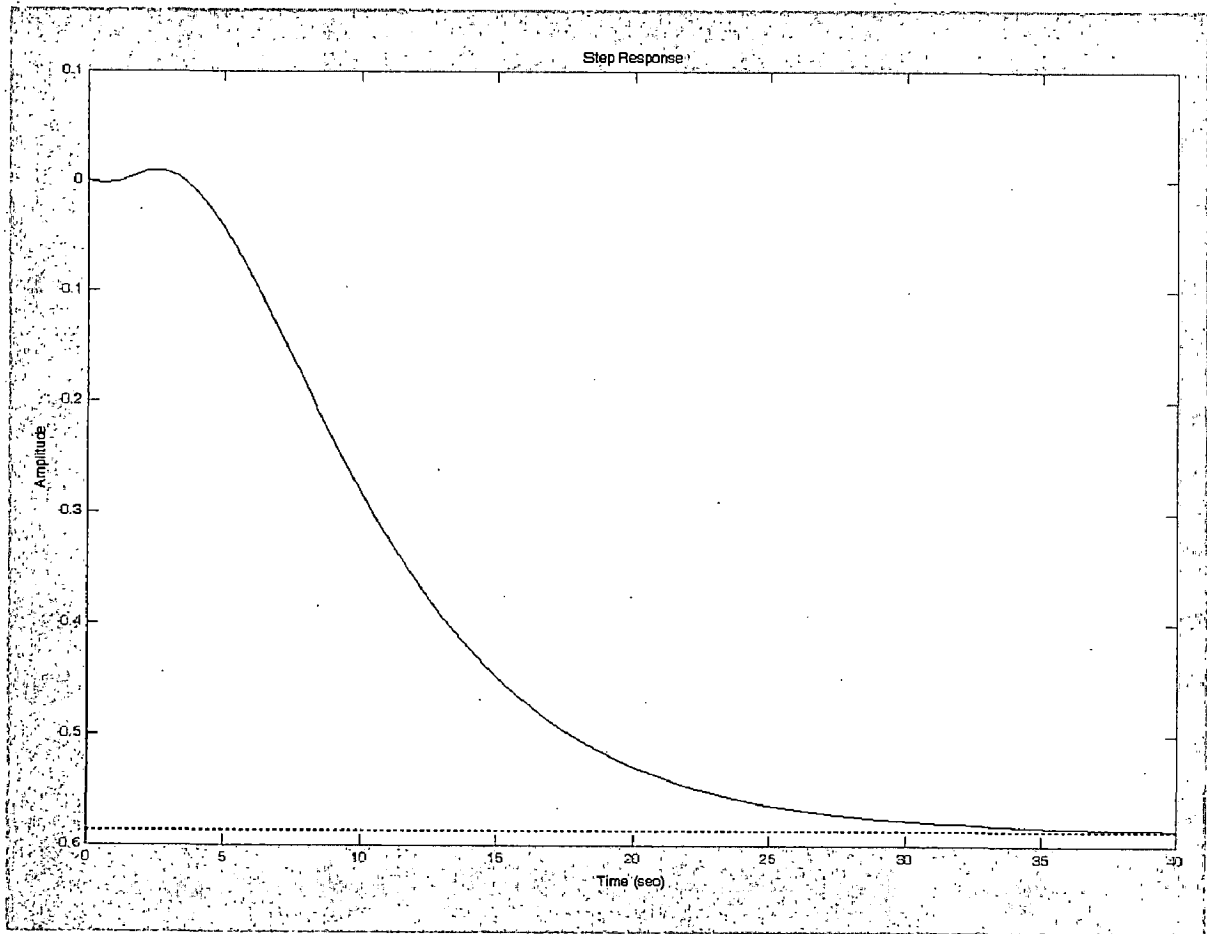
Fig 8.9: step response
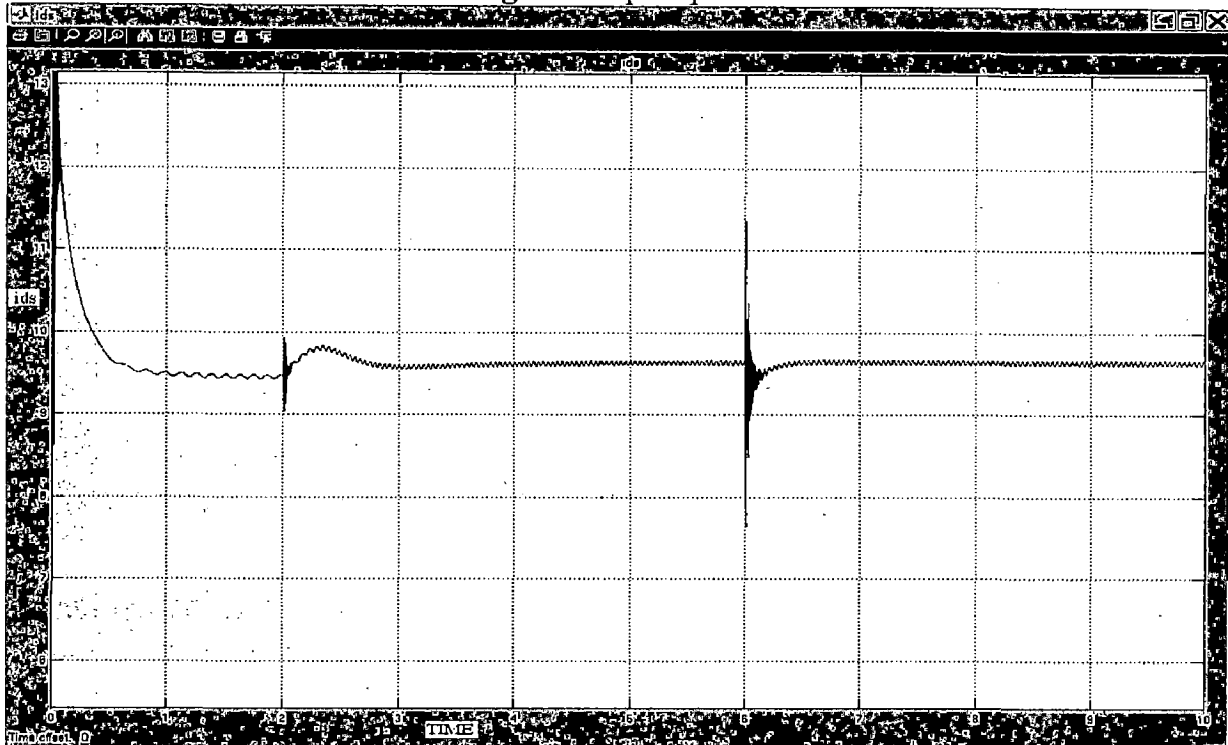
Fig 8.10: i_{ds} response

69

REFERENCES

[1]   Olorunfemi Ojo, Gan Dong, Sensor less Control of Induction Motor Using Natural Variables with Loss Minimisation, Proc IEEE APEC 2005 Annual Meeting, Austin,TX, pp. 451-457, 2005.

[2]   Dawit Seyoum and Muhammad F[]azlur Rahman, The Dynamic Characteristics of an Isolated Stand-alone Induction Generator Driven by a Wind Turbine, IEEE Transactions on Industry Applications, vol. 25, no. 4, pp. 936-941, July/August 2003.

[3]   Olorunfemi Ojo, Dynamic and System Bifurcation in Autonomous Induction Generators, IEEE Transactions Industry Appliactions, Vol 31, pp. 918-924, July/August 1995.

[4]   D. Seyoum, M. F. Rahman, and Grantham, Inverter supplied voltage control system for an isolated induction generator driven by a wind turbine, Pro IEEE IAS 2003 Annual Meeting, Salt Lake City, pp 568-576, 2003.

[5]   D. W. Novotny, D. J. Gritter, and G. H. Studtmann, Self Excitation in Inverter Driven Induction Machines.. IEEE Trans. Power Apparatus and Systems Appliactions, Vol PAS-96, pp. 1117-1125, July/August 1977.

[6]   R. Bansal, Three-Phase Stand-alone Induction Generators: An Overview, IEEE Trans. Energy Conversion, Vol. 2, pp. 292-299, June 2005.

[7]   Yanhong Xue, Shaotang Chen, Instability Issues for Control System in Induction Generator,.Pro IEEE IAS 2001 Annual Meeting , Chicago, pp 110-117, 2001.

[8]   Shashank Wekhande, Vivek Agarwal, .A Simple Wind Driven Self Excited Induction Generator with Regulated Output Voltage, IEEE Telecommunications Energy Conference, 1999 pp. 364-369, 1999.

[9]   S. N. Bhadra, K. V. Ratnam, and A. Manjunath, Study of voltage build up in a stand-alone, variable speed induction generator/ static inverter

system with dc side capacitor,. Pro 1996 International Conference on Power Electronics Drives and Systems, Vol 2, pp. 964-970, 1996.

[10] Shashank Wekhande, Vivek Agarwal, A Variable Speed Constant Voltage Controller for Stand-alone Induction Generator with Minimum Control Requirements, IEEE Pro PEDS .99, Hong Kong, pp. 98-103, 1999.

[11] H. Al-Bahrani, N. H. Malik, Steady State Analysis and Performance Characteristics of a Three-Phase Induction Generator Self Excited With a Single Capacitor. IEEE Transactions Energy Conversion, vol 5, no 4, pp. 725-732, 1990

[12] G. V. Jayaramaiah and B. G. Fernandes, Analysis of Voltage Regulator for a 3- Φ Stand-alone Inducton Generator Using Current Controlled Voltage Source Inverter, Pro IEEE IPEMC 2004 Annual Meeting, vol 3, pp 1404-1408, 2004.

[13] Lahcene Ouazene and George McPherson, Analysis of the Isolated Induction Generator, IEEE Transactions on Power Apparatus and Systems, vol. PAS-102, no. 8, pp. 2793-2798, July/August 1983.

[14] S. S. Murthy, O. P. Malik and A. K. Tandon, Analysis of Stand-alone Induction Generators, Proc IEE, Part C, no 6, pp. 260-265, 1982.

[15] J. A. A. Melkebeek, Magnetizing-Field Saturation and Dynamic Behaviour of Induction Machines, Proc IEE, Part B, vol 130, no 1, pp. 1-10, 1983.

[16] J. A. A. Melkebeek and D. W. Novotny, Steady- State Modeling of Regeneration and Self-Excitation in Induction Machines, IEEE Transactions on Power Apparatus and Systems, vol. PAS-102, no. 8, pp. 2725-2733, July/August 1983.

[17] Olorunfemi Ojo and Gan Dong, Efficiency Optimizing Control of Induction Motor Using Natural Variables, Proc IEEE APEC 2004 Annual Meeting, Anaheim, CA, pp.1622-1627, 2004.

[18]   Fuminobu Naito and Kenichi Abe, Control of Stand-alone Induction Generators, Proc IEEE PES 2002 Annual Meeting, vol 3, pp.2368-2372, 2002.

[19]   Olorunfemi Ojo, Minimum Air gap Flux Requirement for Self-Excitation Stand- Alone Induction Generators, IEEE Transactions on Energy Conversion, vol. 10, no. 3, pp. 484-492, September 1995.

[20]   S. S. Murthy, Nagamani and K. V. Satyanarayana, Studies on the Use of Induction Motors as Stand-alone Induction Generators, IEEE Transactions on Energy Conversion, vol. 3, no. 4, pp. 842-848, December 1988.

[21]   D. Seyoum, Grantham and F. Rahman, An Insight Into the Dynamics of Loaded and Free Running Isolated Stand-alone Induction Generators, International Conference on Power Electronics, Machines and Drives, 2002, pp. 580-585, 2002.

[22]   T. F. Chan, Capacitance Requirements of a Three-Phase Induction Generator Stand-alone With a Single Capacitance and Supplying a Single-Phase Load, IEEE Transactions on Energy Conversion, vol. 17, no. 1, pp. 90.94, March 2002.

[23]   S. R. Silva and R. O. Lyra, .PWM Converter Excitation of Induction Generators, Power Electronics and Applications, 1993, vol. 8, pp. 174-178, 1993.

[24]   Olorunfemi Ojo and Innocent Ewean Davidson, PWM-VSI Inverter-Assisted Stand-Alone Dual Stator Winding Induction Generator, IEEE Transactions on Industry Applications, Vol. 36, NO. 6, November/December 2000

[25]   Yang Ye, Mehrad Kazerani, Victor H. Quintana, Current Source Converter Based STATCOM: Modeling and Control, IEEE Transactions on Power Delivery, Vol. 20, no 2, April 2002

[26]   Ziyad M. Salameh, Margaret A. Casacca, and William A.Lynch, A Mathematical Model for Lead-Acid Batteries, IEEE Transactions on Energy Conversions, Vol. 7, no 1, March 1992.

[27]   Olorunfemi Ojo, Innocent E. Davidson, . A Dual Stator Winding Induction Generator with a Four Switch Inverter-Battery scheme For Control. 39th Annual PESC, 2000, vol 1, pp. 230-234, 2000.

[28]   E. Muljadi and T. A. Lipo, Series Compensated PWM Inverter with Battery supply applied to an isolated induction generator," IEEE Transactions on Industry Applications, Vol 30, Issue 4, pp. 1073-1082, July/August 1994.

[29]   Bimal K. Bose, modern Power Electronics And AC Drives , prentice hall India 2002

[30]   P. C. Krause, Analysis of electrical machinery, Wiley Interscienes 2004

[31]   Simoes and Farret, Renewable energy systems design and analysis with Induction Generator, CRC press 2004

[32]   Ziyad salameh and sunway wang, "Microprocessor control of double output induction generator" IEEE transaction on energy conversion, vol. 4. No. 2, June 1989.

[33]   R. J. Lee, P. Pillay and R. G. Harley, "DQ reference frame for simulation of induction motor", Electric power system Research, vol. 8,1984

[34]   N. kumaresan, N. Ammasaigounden and M. Subbiah, certain control strategies for three-phase semi-converters for the operation of stand-alone Induction Generators. IEEE ICIT'02 Bangkok, Thailand 2002

INITIALIZATION FILE

```
%%  Consts.m File                                          %%
%%  Created 4/25/07                                        %%
     Current_Revision = '5.89'                             %%
     % Rev = Rev + .01                                     %%
%%  Last Revised 10/01/03                                  %%
%%  This file is supposed to be used with the induction machine models %%
%%  and initializes all of the constants that are used in the model   %%
%%  Speed Parameters                                       %%
PIE = 3.1415926535;    %%  Const PIE                       %%
freqb = 50;            %%  Base frequency for machine in  hz      %%
wb = 2 * PIE * freqb;  %%  Base frequency for machine = 2 * PIE * FREQB%%
wrbrpm = 1800;         %%  Base wr in rpm                  %%
%%  Resistance Parameters                                  %%
Rs = 0.5814;           %%  Stator Resistance in ohm        %%
Rr = 0.4165;           %%  Rotor Resistance in ohm         %%
%%  Inductance Parameters                                  %%
%%  Including flux linkage values                          %%
Lls = 3.48e-3;         %%  Stator Inductance in Henry      %%
Llr = 4.15e-3;         %%  Rotor Inductance in Henry       %%
Lm = 82.23e-3;         %%  Magnetizing inductance in Henry       %%
Lr = Lm + Llr;         %%  Rotor Inductance including leakage in Henry %%
Ls = Lm + Lls;         %%  Stator Inductance including leakage in Henry%%
Xls = Lls * wb;        %%  Stator flux linkage in H-rad    %%
Xlr = Llr * wb;        %%  Rotor Flux linkage in H-rad     %%
Xm = Lm * wb;          %%  Magnetizing flux linkage in H-rad     %%
Xm1 = 1 / ((1 / Xm) + (1 / Xls) + (1 / Xlr));           %%
           %%  Xm1 used in induction machine equations     %%
alpha = Llr * Ls + Lls * Lm;                    %%
           %%  Alpha is used in the stator DVC model       %%
%%  Machine Specifications and ratings                     %%
P = 4;                 %%  4 Poles                         %%
Vamp = 220 * sqrt(2);  %%  Reference Voltage 200Vrms             %%
Phirb = 0.8;           %%  Rated rotor flux = 0.8 Wb       %%
Phisb = 0.81;          %%  Rated stator flux = 0.81 Wb     %%
           %%  Rated Current = 18 A                        %%
           %%  Ids rated = 9 A                             %%
           %%  Iqs rated = 15 A                            %%
           %%  rated frequency slip = 2.62 Hz              %%
%%  Load specifications                                    %%
J = 0.05;              %%  Moment of intertia for spinning machine   %%
Kw = 0.00047502;       %%  Load torque when proportional to w^2      %%
Tl = 40;               %%  Constant load torque                %%
```

```
                                    %%
%% PWM specifications                              %%
freqt = 2e3;          %% Triangle Frequency for PWM comparison    %%
Vprad = 0.82529;        %% No idea what this is....?              %%
sloper = 90;          %% This has to do with the max slope in V/Hz  %%
Vdc = 300;            %% This is the voltage on the DC bus        %%
%% Simulation Parameters                            %%
Tstop = 10;           %% Amount of time to simulate to          %%
t_J_large = 4;         %% After this time in torque simulations the  %%
              %% intertia on the rotor will be increased, so %%
              %% that the machine can be run in generating  %%
              %% mode. After this time, the speed won't    %%
              %% change that much.              %%
step = 1 / (24 * freqt);%% Step Size for simulation            %%
              %% A good value for this is 24 * triangle freq %%
sim_steps = 32;        %% Output simulation steps              %%
%% Filtering Parameters                            %%
fci_dvc = 1000;        %% Frequency for current filtering (DVC) in Hz %%
fci_ivc = 5000;        %% Frequency for current filtering (IVC) in Hz %%
fci = 1000;           %% Frequency for current filtering in output  %%
fcv_dvc = 1000;        %% Frequency for filtering voltage (DVC) in Hz %%
fcv = 1000;           %% Frequency for filtering voltage in output  %%
fct = 150;            %% Frequency for filtering Torque in Hz     %%
fwrest = 100;         %% Frequency for filtering estimated rotor speed%%
w_filter_i_dvc = 2 * PIE * fci_dvc;            %%
              %% Current filtering in rad/s (DVC)      %%
w_filter_i_ivc = 2 * PIE * fci_ivc;            %%
              %% Current filtering in rad/s (IVC)      %%
w_filter_i = 2 * PIE * fci;                  %%
              %% Current filtering in rad/s (output)    %%
w_filter_v_dvc = 2 * PIE * fcv_dvc;            %%
              %% Voltage filtering in rad/s (DVC)      %%
w_filter_v = 2 * PIE * fcv;                  %%
              %% Voltage filtering in rad/s (Output)    %%
w_filter_t = 2 * PIE * fct;                  %%
              %% Torque filtering in rad/s          %%
w_filter_wrest = 2 * PIE * fwrest;            %%
              %% Estimated rotor speed filtering in rad/s %%
%% DVC Rotor parameters for speed controller          %%
Tr = Llr / Rr;        %% Value used for DVC equations         %%
dvcproIqs = 0.01;       %% proportional part for Iqs controller    %%
dvcintIqs = 10;        %% intergral part for Iqs controller      %%
dvcproIds = 0.01;       %% proportional part ofr Ids controller    %%
dvcintIds = 0.10;       %% integral part for Ids controller      %%
dvcproP = 40.0;        %% proportional part for flux controller    %%
dvcintP = .05;        %% integral part for flux controller      %%
```

%%
dvcproW = 0.02;   %% Proportional part for speed controller   %%
dvcintW = 3.0;   %% integral part for speed controller   %%
%% DVC Rotor parameters for torque controller with no feedback   %%
dvcproIqstorfeed = 0.09;%% proportional part for Iqs controller   %%
dvcintIqstorfeed = 30.0;%% intergral part for Iqs controller   %%
dvcproIdstorfeed = 0.01;%% proportional part ofr Ids controller   %%
dvcintIdstorfeed = 10; %% integral part for Ids controller   %%
dvcproTtorfeed = 0.022; %% proportional part for flux controller   %%
dvcintTtorfeed = 0;   %% integral part for flux controller   %%
%% DVC Rotor parameters for torque controller with torque feedback   %%
dvcproIqstor = 0.05;   %% proportional part for Iqs controller   %%
dvcintIqstor = 10;   %% intergral part for Iqs controller   %%
                       %%
dvcproIdstor = 0.01;   %% proportional part ofr Ids controller   %%
dvcintIdstor = 10;   %% integral part for Ids controller   %%
                       %%
dvcproTtor = 0.25;   %% proportional part for flux controller   %%
dvcintTtor = 2.5;   %% integral part for flux controller   %%
%% DVC Stator parameters for torque controller with feedback   %%
Ts = Lls / Rs;   %% Value used for DVC equations   %%
fc = 0.0001 ;   %% Corner Frequency for LPF (integrator)   %%
            %% Machine will only run at 10x this speed   %%
Kcorr = 1 / (2 * PIE * fc);   %%
            %% Value used to implement LPF = RC   %%
dvcproIqss = 0.1;   %% proportional part for Iqs controller   %%
dvcintIqss = 10.;   %% intergral part for Iqs controller   %%
dvcproIdss = 0.08;   %% proportional part for Ids controller   %%
dvcintIdss = 10.0;   %% integral part for Ids controller   %%
dvcproPs = 20;   %% proportional part for flux controller   %%
dvcintPs = 100.0;   %% integral part for flux controller   %%
dvcproTs = 0.1;   %% Proportional part for torque controller   %%
dvcintTs = 5.0;   %% Integral Part for torque contorller   %%
%% DVC Stator parameters for torque controller with no feedback   %%
dvcproIqssfeed = 0.1; %% proportional part for Iqs controller   %%
dvcintIqssfeed = 10.; %% intergral part for Iqs controller   %%
dvcproIdssfeed = 0.05; %% proportional part for Ids controller   %%
dvcintIdssfeed = 10.0; %% integral part for Ids controller   %%
dvcproPsfeed = 20;   %% proportional part for flux controller   %%
dvcintPsfeed = 100.0; %% integral part for flux controller
%% IVC parameters for speed controller   %%
ivcproIqs = 0.1;   %% proportional part for Iqs controller   %%
ivcintIqs = 0.009;   %% intergral part for Iqs controller   %%
ivcproIds = 0.2;   %% proportinal part for Ids controller   %%
ivcintIds = 0.09;   %% integral part for Ids controller   %%
ivcproW = 2.4;   %% proportional part for speed controller   %%

```
ivcintW = 0.7;        %% integral part for speed controller      %%
%% IVC parameters for torque controller with feedback           %%
ivcproIqstor = 0.1;   %% proportional part for Iqs controller    %%
ivcintIqstor = 10;    %% intergral part for Iqs controller       %%
ivcproIdstor = 0.1;   %% proportinal part for Ids controller     %%
ivcintIdstor = 0.6;   %% integral part for Ids controller        %%
ivcproTtor = 0.5;     %% proportinal part for Ids controller     %%
ivcintTtor = 10.0;    %% integral part for Ids controller
%% IVC parameters for torque controller w/out feedback          %%
ivcproIqstorfeed = 0.01;%% proportional part for Iqs controller  %%
ivcintIqstorfeed = 20; %% intergral part for Iqs controller      %%
ivcproIdstorfeed = 0.1; %% proportional part for Ids controller  %%
ivcintIdstorfeed = 0.6; %% integral part for Ids controller      %%
ivcproTtorfeed = 0.5;  %% proportional part for Ids controller   %%
ivcintTtorfeed = 10.0; %% integral part for Ids controller
'Constants have been initialized'
```

LIST OF PUBLICATION

1. Rishi Raj Meena, S.N. Singh, "Microprocessor Based Voltage control of Induction Generator", Paper Poster presented in "*38 Mid Term Symposium on Emerging trends in instrumentation and process automation*", Vadodra, 7-8 April 2007.

2. Rishi Raj Meena, S.N. Singh, "Modelling and Simulation of Induction Generator", abstract accepted in the "*International conference on Modelling and simulation*", Coimbatore Institute of Technology, Coimbatore, 27-29 August, 2007.